TNO Built Environment and Geosciences

Princetonlaan 6
P.O. Box 80015
3508 TA Utrecht
The Netherlands

www.tno.nl

T +31 30 256 42 56
F +31 30 256 44 75
info-BenO@tno.nl

TNO report

TNO-034-UT-2010-01364

Central Offshore Platform and Vlieland Basin Mapping and modelling - Area 2E

Date	July 2010
Author(s)	N. Witmans S. van Gessel J.H. ten Veen
No. of copies	5
Number of pages	37
Number of appendices	9
Customer	Ministry of Economic Affairs
Projectname	NCP-2E
Projectnumber	034.22624

Conclusions and management summary

To serve future and current operators in the oil industry and governmental and non-governmental organisations a comprehensive subsurface model of the Dutch offshore is being created. The Netherlands Continental Shelf area is divided into seven sub-areas that represent more or less structural entities during Late Jurassic to Early Cretaceous time. In this report the results of sub-area NCP-2E, including the Central Offshore Platform, Noord-Holland Platform, Texel-IJsselmeer High and part of the Vlieland Basin, are described.

The structural framework of the area is outlined by major fault zones that delimit the Texel-IJsselmeer High and the Vlieland Basin and outline the transition with the Central Offshore Platform. Fault-associated salt structures (walls and domes) predominently occur on the north-western part of the Central Offshore Platform. Different phases of fault activation and reactivation have played a crucial role in the creation of hydrocarbon traps, which are mainly located in the Rotliegend. Zechstein salt is providing an excellent seal.

The main source rocks for gas are the coal measures of the Limburg Group. Next to proven Rotliegend reservoirs and to a lesser extend Zechstein reservoirs in the platform areas, the Triassic, Upper-Jurassic to Lower Cretaceous in the Vlieland Basin may offer other hydrocarbon opportunities.

Contents

1 Introduction

1.1 Mapping of the deep subsurface of the Netherlands offshore (NCP-2 project)

The detailed mapping of seven offshore areas on the Netherlands Continental Shelf was initiated in late 2005 and will be finalised in 2010. It builds on and goes one step beyond the previous regional mapping of the Netherlands onshore and offshore. In 2004 the publication of the Geological Atlas of the Subsurface of the Netherlands – *onshore* rounded off the onshore regional mapping project and a 'quick and dirty' offshore mapping (NCP-1 project) was completed in 2006 (viz. http://www.nlog.nl; Duin et al. 2006).

The main aim of the detailed mapping of seven sub-areas is to present a more comprehensive model of the subsurface to future and current operators in the oil industry and to governmental and non-governmental organisations for, amongst other things, the spatial planning of the Dutch subsurface. The deliverables include:
3D geological framework (depth and thickness grids)
Rock and fluid parameters (petrophysical parameters)
3D burial histories
Petroleum system analysis
All deliverables, such as maps, grids and graphs, can be downloaded at the http://www.nlog.nl site. When applicable, regular updates will be made available on the site.
The petroleum systems analysis will be reported separately (Verweij et. al, 2010, report nr. TNO-034-UT-2010-01298/A

1.2 Definition of mapping areas.

Based on consultation with the exploration departments of the oil companies operating in the Netherlands it was decided to divide the offshore area into seven sub-areas (fig. 1.1). These areas represent more or less structural entities at the Late Jurassic to Early Cretaceous times (fig. 1.2). The detailed mapping project started with sub-area NCP-2A: Terschelling Basin and the southern part of the Dutch Central Graben and was continued with area 2E, which comprises the Central Offshore Platform, Vlieland Basin, the northwestern part of the Texel IJsselmeer High and the offshore extension of the Noord-Holland Platform. Detailed mapping
The detailed mapping was focussed on the assessment of the present-day stratigraphic and structural framework of the sedimentary fill of the area as well as on the properties of rocks and fluids it contains, such as reservoir porosities, pressures, salinities, source rock maturity, characteristics of oil and gas. Special attention was paid to provide new porosity data for the main reservoir units in the Upper Rotliegend Group. This report concerns the present-day setting and characteristics of the study area.

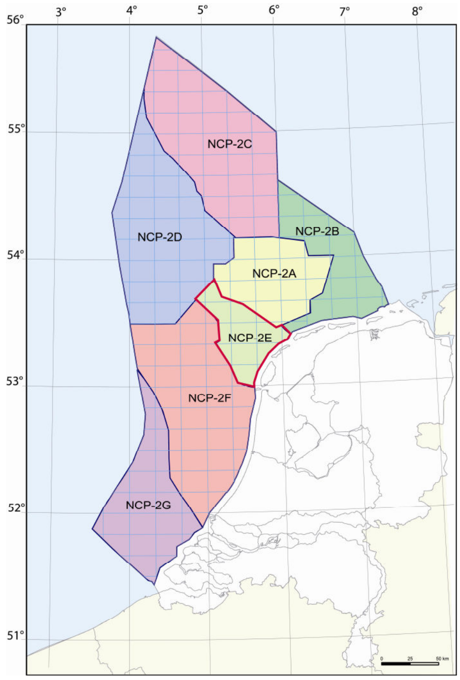

Figure 1.1 NCP-2 areas; Location of the project area NCP-2A: Terschelling Basin and the southern part of the Dutch Central Graben

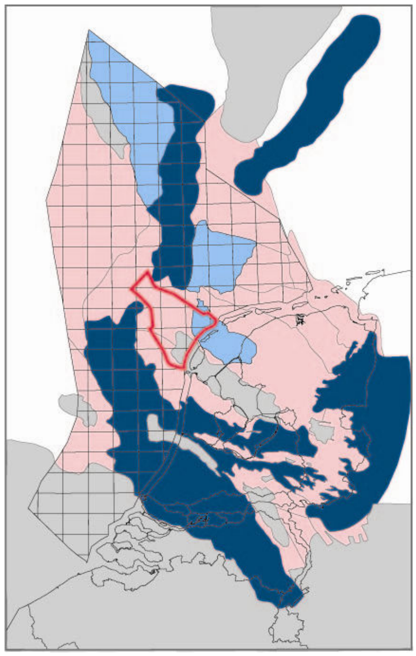

Figure 1.2 Structural setting at Late Jurassic-Early Cretaceous.
Grey: highs, Pink: platforms, Dark blue: basins with Lower Jurassic, Light blue: basins without Lower Jurassic

2 Database

Most data used in the project are publicly released seismic and borehole data that were acquired by various oil companies. In addition we used published information and research results and laboratory analyses from previous in-house studies. Also reports from third parties on wells or regional studies were consulted

2.1 Stratigraphic data/Dino database

The basic information for the mapping project was derived from the released data of 48 boreholes available in the DINO database (see annex 5.1). The selection criteria for these boreholes include: the presence of a specific stratigraphic interval of interest, the presence of complete stratigraphic intervals, the total depth of the borehole, geographic spacing, the presence of hydrocarbons, the availability of a representative set of well logs, the availability of cores in stratigraphic intervals of interest. At the start of the project stratigraphic information of the different boreholes in the DINO database varied both in quality and in detail of the stratigraphic subdivision (Group, Formation, Member).

2.2 Seismic data

The available regional seismic framework for the entire offshore area was used as the groundwork for the detailed mapping using released 3D seismic surveys (in two areas 2D surveys were used in the project, viz. annex 5.2) . The inlines of most surveys have an E-W orientation and intersect the dominant geological structures at high angles. The quality of the seismic signal is generally good to fair from the ground surface to the Top Zechstein horizon, enabling a reliable interpretation for this interval. Below the Zechstein Group the quality of the signal is mostly too poor to allow a reliable regional interpolation. Mapping the deeper levels depended on available well data (see also 2.1.4).

In general, every 10th inline and every 25th xline was interpreted for each seismic survey. In structurally less complicated areas a wider spaced grid consisting of every 20th inline and every 50th xline, was sufficient to map the surfaces within confidence levels.

2.3 Borehole data

2.3.1 Well logs

The available well logs for the 48 selected wells include gamma-ray, sonic and sometimes also neutron-density logs.

2.3.2 Cores and cuttings

In 33 wells within the area core measurements were available for petrophysical analyses. If necessary we used additional measurements on cores from wells bordering the area (TNO report 2007). Furthermore, cuttings of 3 wells were analysed for biostratigraphic studies in the Tertiary and Upper Cretaceous.

2.4 Information from literature

Apart from the references listed under chapter 5, consultancy reports and reports from operators concerning the wells or the study area were used for reference. These reports contain information about the geological and stratigraphic subdivision, biostratigraphy, core descriptions and analyses, geochemical data, pressure and temperature data.

3 Approach

Lithostratigraphic (re)-interpretation of well logs, the incorporation of the lithostratigraphic information into the seismic interpretation, time-to-depth conversion of the seismic velocity and the construction of depth and thickness maps of the eight major lithostratigraphic units constitute the basic methods used in the mapping process. Additional units of importance for the petroleum system were identified by lithostratigraphic well correlation (reservoir and source rock units). Biostratigraphic analyses were applied to improve the lithostratigraphic sub-division of Tertiary and Upper Cretacous strata. Petrophysical analysis provided new porosity and permeability data for the Upper Rotliegend reservoir units.
The hydrodynamic analysis, which is reported in Verweij et al. (TNO report 034-UT-2010-01298/A) resulted in the characterisation of the pressure and fluid flow system, and maturity analysis on samples increased the quantitative knowledge on the present-day source rock maturities.1D, 2D and 3D basin modelling of the entire study area was used to highlight the relation between the 3D burial history of the basin and the history of important components of the petroleum system, such as the temperature and maturation history of its source rocks, timing of hydrocarbon generation.

3.1 Construction 3D geological model

3.1.1 Well log correlation

The gamma-ray, sonic and, if available also the neutron-density, logs were combined into a digital composite well log for each of the 48 selected wells. The composite logs of all 48 wells were loaded into the Petrel programme and lithostratigraphically (re-) interpreted on member level. The construction of 9 cross sections, some on group level allowed a detailed lithostratigraphic interpretation. Additional cross-sections were set up with a good spatial distribution to create a more regional view. The interpretation of the composite well logs resulted in a more detailed lithostratigraphic subdivision of the area. The new detailed stratigraphic information at well locations was incorporated in the interpretation of the seismic data. The thicknesses of the main reservoir units that were identified at well level were implemented in the grids of the 3D-depth model.

3.1.2 Seismic interpretation

The stratigraphic interpretation of the 3D seismic surveys was focussed on identification of the lower boundaries of the Upper North Sea Group, Lower North Sea Group, Chalk Group, Rijnland Group, Schieland Group, (the Altena Group is not present in this area), Upper and Lower Germanic Trias groups and the Zechstein Group. No separate reservoir units were seismically interpreted due to their limited thickness and/or distribution.

For constructing the structural model the interpretation was focussed on identifying the major faults i.e. faults with large (vertical) offsets and faults that are important for the definition of the structural elements. The faults were labelled according to the lithostratigraphic groups which they offset, because such information is a prerequisite for the construction of the 3D model. The interpreted faults are stored a Fault Database (FDB), on which queries can be performed such that faults can be analysed and grouped according to several age, geographic or dimensional criteria. The lithostratigraphic interpretations of wells were converted to the time domain using available check shot data, and used to support the seismic interpretation.

3.1.3 3D time model

For the 3D-modeling and the time-depth conversion the program Petrel, version 2007, was used. The horizon and fault interpretations formed the base to construct the 3D-time model. The fault interpretations were converted to fault pillars, which were edited to fit the fault planes into the horizon interpretations.

The study area is characterised by numerous salt structures in the northwestern part. The faults above and below those structures are decoupled, leading to two independent fault systems. In the Petrel fault modeling module, modeled fault planes run throughout the entire model, which consequently can lead to crossing fault planes. Petrel uses the fault pillars to construct the 3D time model, which is the main input for the time-depth conversion, in which those crossing faults are not allowed. Therefore, one model was constructed for the faults displacing the base Zechstein and a second model with the faults not displacing the Zechstein as a result of salt movement. A complication in this work flow is that at many places the salt is completely absent. At those places several faults displace not only the Zechstein, but also the Triassic deposits. For this reason a third model was constructed with for faults displacing the Triassic sediments.

Time-depth conversion

The interpreted seismic data were converted from time to depth using a slightly modified version of the seismic velocity model of Van Dalfsen, e*t al*. (2007). This model consists of V_0-grids and a constant k for all groups except for the Zechstein, for which a V_{int}-grid was created based on borehole information from the entire Dutch on- and offshore. There are no velocity data available for the salt intrusions and therefore a constant halite velocity of 4450 m/s was assumed.

The depth surface at base Zechstein often showed a velocity pull-up under salt domes. These anomalies were clipped in the depth model, honouring the adjacent faults, resulting in a corrected base Zechstein and underlying formations. All depth surfaces were re-calculated to time grids. This procedure will be standard for all mapped areas, including the already published time grids for are 2A.

The nine depth surfaces corresponding to the bases of the major stratigraphic (sub-)groups were fitted together and, if needed slightly edited, to form the 3D-depth model. Finally the reservoir units which were derived from the wells were incorporated in the model.

3.2 Assessment rock and fluid properties and conditions

3.2.1 Petrophysical analysis

In the study area the analysis of petrophysical parameters focussed on the Upper and Lower Slochteren Sandstone of the Upper Rotliegend Group. Porosity and permeability data were derived from core data and well log data (report 2008-U-R0605B). Seventeen wells – of which most has core data – were selected (Table 3.2.1).

Table 3.2.1 Reservoir intervals in the analysed wells

Well	ROSLU				ROSLL			
	m, MD		m, TVDss		m, MD		m, TVDss	
L04-07					3832.92	3894.11	3761.67	3822.20
L07-01	3644.00	3705.00	3617.53	3678.37	3796.00	3871.34	3769.06	3844.03
L07-04	3912.00	3982.00	3879.29	3949.22	4097.52	4177.00	4064.61	4144.04
L07-06	3876.00	3954.75	3841.72	3920.27	4062.26	4130.00	4027.62	4095.15
L08-01-S1	3952.53	4018.52	3925.02	3990.96	4139.99	4213.00	4112.38	4185.33
L08-P-01	4084.93	4145.93	4019.27	4070.97	4278.00	4346.00	4181.77	4239.84
L08-P-03					4858.50	4934.00	4530.67	4602.33
L10-01	3851.50	3958.50	3818.69	3925.66	4003.00	4089.00	3970.14	4056.11
L10-10	3778.50	3885.00	3739.23	3845.32	3927.00	4017.50	3887.16	3977.32
L10-A-01	3804.00	3948.00	3643.07	3781.05	3994.00	4073.00	3825.17	3900.97
L10-D-01-S1	3594.00	3735.00	3561.18	3702.01	3774.50	3857.00	3741.47	3823.87
L11B-A-01	3524.00	3604.00	3494.26	3574.25	3696.00	3758.00	3666.23	3728.22
L12-03	2912.00	2996.00	2884.49	2968.26	3068.30	3120.30	3040.433	3092.38
L12-05	3260.00	3279.00	3220.06	3239.04	3430.00	3438.00	3389.92	3397.91
L14-A-01	3212.00	3336.44	3180.68	3305.07	3364.00	3422.00	3332.67	3390.67
L15-01	2865.00	2989.00	2832.02	2956.00	3090.00	3099.00	3056.99	3065.99
M10-02	2787.00	2904.00	2677.52	2792.16				

The petrophysical analysis itself was executed in the program Interactive Petrophysics (IP). The composite logs and the petrophysical results (clay volume, porosity, saturation and permeability) were exported as curves and loaded into Petrel for property modeling. Interpretation of the gamma-ray logs was applied to assess the net-to-gross ratio of the reservoir units. A cutoff of 50% of the clay volume and a porosity cut-off 5% were applied.
Permeability data is calculated from the available core data. In other cases the permeability was calculated from the log porosity.
The results can be found in Annex G. The report can be downloaded from the nlog site.

3.3 Construction 2D maps and cross-sections

The depth and thickness surfaces in Petrel are converted to 2D grids and imported into ArcGIS. Maps of the nine major stratigraphic units (Upper North Sea, Middle and Lower North Sea, Chalk, Rijnland, and Schieland groups, Upper and Lower Germanic Trias subgroups and the Zechstein Group) are presented here. Additionally, the depth and thickness maps of the Upper Rotliegend Group were constructed from well data. The reservoir units of the Lower Detfurth Sandstone and Lower Volpriehausen Sandstone members as well as the Upper and Lower Slochteren Sandstone Members were integrated in the 3D-model and are shown in the three cross sections. All maps and cross sections are provided in PDF format for presentation purposes (Annex B, C, F). Ascii-gridfiles (ZMAP- and ARCGIS-format) of the surfaces and ZMAP lines files of the faults can be downloaded from the nlog site. A composite model of the time horizons in NCP-2A, 2B and 2E is also available.

The reservoir units of the Lower Detfurth Sandstone and Lower Volpriehausen Sandstone members as well as the Upper and Lower Slochteren Sandstone members were integrated in the 3D-model and are shown in the three cross sections.

These structural cross sections of the major stratigraphic units (2 NE-SW and 1 W-E direction) are generated from the 3D model (Annex F). The cross sections are provided in PDF-format only.

4 Present-day 'setting'

4.1 Geological framework

The dominant features of the present-day structural and geological framework are of Mesozoic origin: the Central Offshore Platform, the Noord-Holland Platform, which both were affected by Mid- and Late Jurassic uplift and subsequent erosion. The Vlieland Basin in the northeast has Upper Jurassic deposits overlain by Lower Cretaceous sediments. In the southeastern part of the study area the Texel-IJsselmeer High presents itself as a high up until the Late Jurassic Kimmerian phase. After this the high was covered by Cretaceous and Tertiary sediments with thicknesses comparable to the other structural elements.

The Cenozoic sedimentary fill of the Southern North Sea Basin covers the Mesozoic structural elements that rest on the Southern Permian Basin which in turn overlies the Variscan Basin. The associated tectono-stratigraphic sequences are separated by four major phases of tectonic activity and erosion (Annex F), namely the Saalian, Tubantian, Mid-Kimmerian and Subhercynian/Laramide tectonic phases.

4.1.1 Structural framework

The structural framework of the area is outlined by major boundary fault zones that delimit the Texel-IJsselmeer High and the Vlieland Basin and outline the transition with the Central Offshore Platform. Fault-associated salt structures (walls and domes) predominantly occur on the Central Offshore Platform.

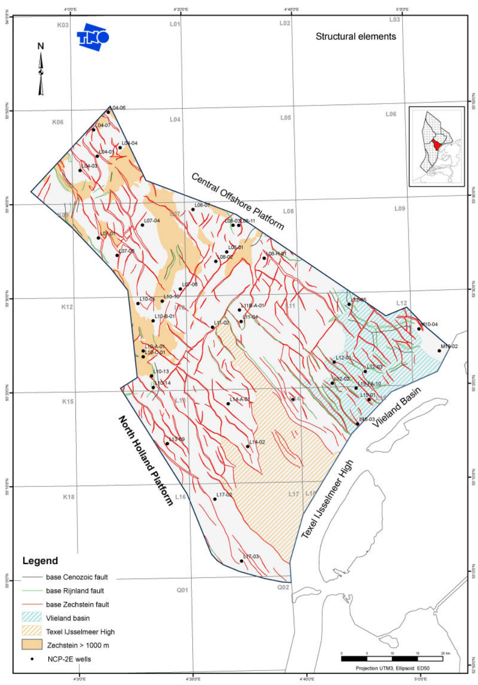

Figure 4.1.1 Main structural elements (see also Annex D)

The major boundary fault zones that are interpreted from seismic data include (Annex E, Figure 4.1.1) a NW-SE trending boundary fault zone between Texel-IJsselmeer High and the Vlieland Basin.

a NW-SE trending boundary fault zone between Texel-IJsselmeer High and the North Holland Platform.

a NE-SW trending boundary fault zone between Texel-IJsselmeer High and the Central Offshore Platform.

Next to these, throughout the area a large number of shorter, NNE- to N-trending faults show an oblique interrelationship with the NW-SE-trending faults; together these fault groups define oblique rift geometries.

Faults
A total of 404 interpreted faults are stored in the FDB and are grouped according their activity during one or more of the three major (post Saalian) phases of tectonic activity and erosion, namely the, Tubantian, Mid-Kimmerian and Subhercynian/Laramide tectonic phases. Fault groups are listed in Table 4.1.1 and explained in Figure 4.1.2.

Table 4.1.1 Fault groups

<table>
<tr><th colspan="2">Subgroup</th><th>Base unit</th><th>Top unit</th><th>Remark</th></tr>
<tr><td colspan="2">1) Tubantian</td><td>PreZE or RO or ZE</td><td>ZE</td><td>Faults that terminate upward in ZE salt (where salt is thick). Might also include reactivated faults from the Saalian tectonic phase[1]</td></tr>
<tr><td rowspan="3">Post Zechstein faults</td><td>2) Pre Subhercynian/ Laramide (soft- + unlinked faults)</td><td>ZE or RB</td><td>KN or CK</td><td>(Normal) faults that detach in ZE (or RB) or RN salt and active during the Kimmerian phases and that may have experienced inversion.</td></tr>
<tr><td>3) Hard-linked faults Tubantian - subRecent</td><td>PreZE or RO or ZE</td><td>All units above ZE</td><td>Faults originating below salt (as group 1) but also affecting youngest units (where salt is thin or absent) and show multiple reactivation.</td></tr>
<tr><td>4) Post Laramide</td><td>CK</td><td>NU or N</td><td>Faults after inversion, predominantly affecting Noordzee Group and Cretaceous, un- or poorly related to salt tectonics</td></tr>
</table>

[1] note that stratigraphy below the Zechstein Group was not interpreted, but that numerous faults cross-cut Carboniferous and Permian (Upper Rotliegend Group) units.

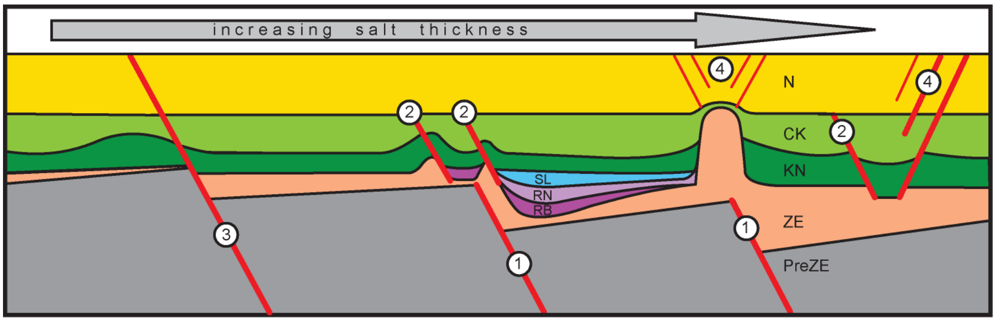

Figure 4.1.2 Identified fault groups of Area 2E (as listed in Table 4.1.1) and their relation with salt thickness. Stratigraphic abbreviations (from old to young): PreZE = pre Zechstein Group, ZE = Zechstein Group, RB = Lower Triassic, RN = Upper Triassic, SL – Upper Jurassic (Lower Jurassic is missing in Area 2E), KN = Lower Cretaceous, CK = Upper Creatceous, N = Tertiary.

Group 1 – Tubantian faults
Description

This group includes faults that originated in pre Zechstein or Zechstein time and show differences in thickness distribution of the Zechstein anhydrite and salt. Faults terminate upward in the Zechstein salt. The faults occur throughout the entire area and represent long and branching NW-SE trending fault zone delimiting tilt-block (half)graben basins below the Zechstein salt. At the TIJH and the COP the NW-SE faults show a en-echelon arrangement with NNW-trending faults that together form small pull-apart type basins (oblique rifts) where Zechstein deposits are thickly preserved. In the Vlieland Basin such oblique rifts are absent. Instead, here the NE-SW faults, together with NE-trending faults form an orthogonal fault pattern. Both types of cross-cut relations exist. The NE-SW-trending faults also demarcate the transition with the Central Offshore Platform.

In the absence of recognisable fault offsets above the Zechstein formation (e.g. Rotliegend) it is assumed that main fault activity was contemporaneous with Zechstein deposition, i.e. during the Tubantian tectonic phase 1 (Geluk, 1999). Reactivation features associated with these faults are not observed.

Frequency (length classified)	**Mean length / sector**	**Equal area stereoplot**
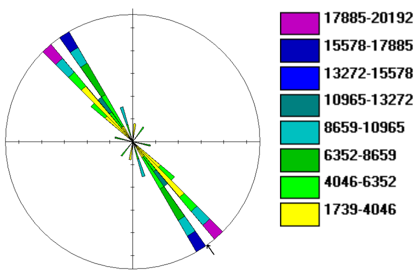 n = 312	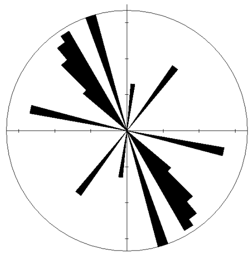 Mean strike: 156-336 Max. length: 7979,12 m	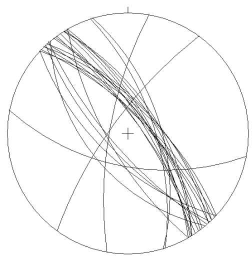

Figure 4.1.3. Group 1 fault statistics

Group 2 - Pre Subhercynian/ Laramide faults

Faults belonging to this group occur throughout the entire area, are relatively short and predominantly NW-SE trending. Especially in the NW part of the area some NE-SW trending faults follow the grain of the major salt walls All faults are bracketed between the Zechstein Group and the Noordzee Group. They affect and cut the Triassic Jurassic and Cretaceous stratigraphy and and therefore may have experienced a long period of activity and reactivation from Triassic till Cretaceous time. The larger faults of this group detach in the Zechstein salt that acted as a major decollement. Mostly, these faults are located above or in close vicinity of subsalt faults and are referred to as soft-linked faults. If no correlation exists, faults are inferred to be unlinked. Some smaller faults terminate in Lower Triassic Röt salt. Where associated with folds and pop-up structures these faults may have been reactivated as (minor) reverse slip faults sense.

Frequency (length classified)	Mean length / sector	Equal area stereoplot
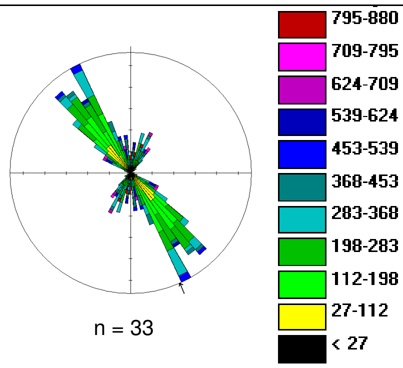 n = 33	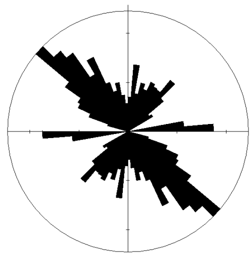 Mean strike: 102-182 Max. length: 7434,2 m	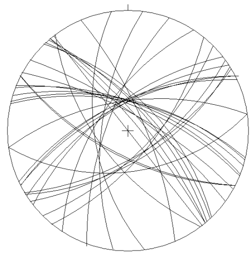

Figure 4.1.4. Group 2 fault statistics

.

Group 3 - Tubantian – subRecent hard-linked faults

Faults in this group originate in pre-Zechstein or Zechstein time and relate to pronounced differences in thickness distribution of Zechstein anhydrite and salt. Faults cut most of the units above the Zechstein Group and may even affect the Noordzee Group.These faults constitute a broad NW-SE trending fault zone at the transition between the Texel IJsselmeer High and the Vlieland Basin. In the latter structure the distribution of Triassic and Upper Jurassic units is influenced by these faults. Longest faults follow this NW-SE trend. Some shorter NE-SW-trending fault segments delineate the northernmost extension of the Texel IJsselmeer High and form the transition with the Central Offshore Platform. In the absence of recognizable fault offsets below the Zechstein formation (e.g. Rotliegend) it is assumed that main fault activity was contemporaneous with Zechstein deposition, i.e. during the Tubantian tectonic phases 1 (and maybe 2). Later reactivation occurred during Triassic and Jurassic (Kimmerian) rifting phases and a small number of faults are utilized during inversion.

Frequency (length classified)	Mean length / sector	Equal area stereoplot
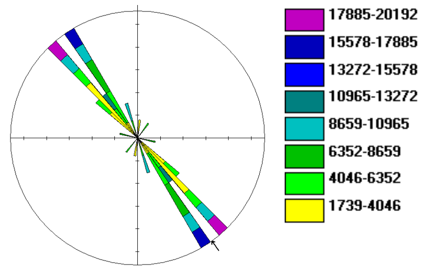 n = 25	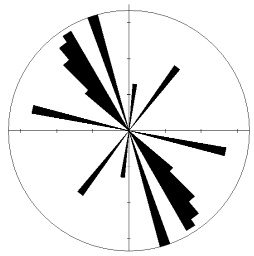 Mean strike: 144- 324 Max. length: 7834,9 m	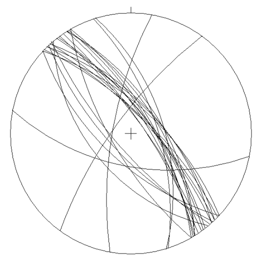

Figure 4.1.5. Group 3 fault statistics

Group 4 - Post Laramide faults

This group includes faults that almost exclusively occur in association with salt domes, but which are not affected by Subhercynian inversion tectonics. The relatively short faults are rather randomly distributed and most of them detach on the Cretaceous-Tertiary unconformity or terminate in the Upper Cretaceaous Chalk Group. A large number of smaller NE-SW trending conjugate normal faults within the Lower North Sea Group (not interpreted) belong to this group as well. These particular faults detach on the Mid-Miocene Unconformity and are not associated with salt domes.

Frequency (length classified)	Mean length / sector	Equal area stereoplot
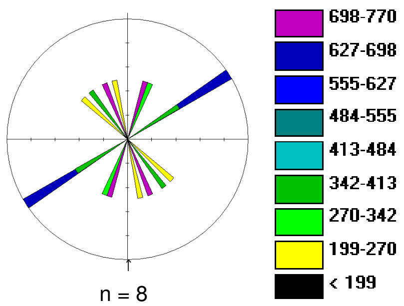 n = 8	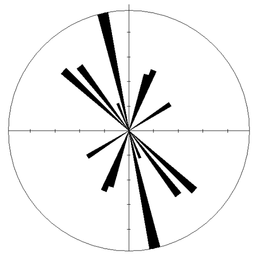 Mean strike: 180-360 Max. length: 4187,9 m	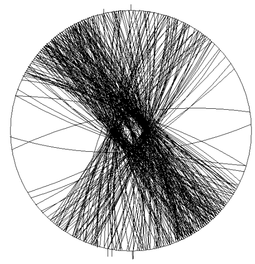

Figure 4.1.6. Group 4 fault statistics

Interpretation and Age

The Zechstein salt acts as a major detachment zone because of its great thickness and visco-plastic behaviour and often separates sub-salt fault systems (Group 1) from the faults in the overburden (soft-linked fault systems). Instead, Group 3 represents deep reaching (hard-linked) basin boundary faults that occur mainly were on either side of the fault is thin or absence. It is likely that the Group 3 faults are already established in the Early Permian and rejuvenated later. Thickness changes in the Zechtstein Z1 Formation are related to formation of tilt-block (half) grabens during the Tubantian 1 tectonic phase (Geluk, 1999). This might be due to erosion of fault blocks that are uplifted during Tubantian 1 tilt-block faulting. These blocks are covered by the Zechstein Upper Claystone Member and fault activity can thus be confined to the Late Permian period. Complete absence/removal of the Zechstein Group can also be related to the Hardegsen Unconformity that represents a younger Early Triassic erosion phase. Post Zechstein tectonic activity is driven by basement faulting and salt deformation and resulted in new formation of (Group 2) faults in the Zechstein overburden or reactivation of the Group 3 faults. Reactivation of Group 1 faults and formation of new faults below base Zechstein is probable during the post-Zechstein tectonic phases, although evidence is absent.

The NW-SE to NNW-SSE-trending faults of Group 2 represent soft- and unlinked faults that were initiated as dip slip normal (or oblique) faults during the early Kimmerian ~E-W extensional phase (Late Triassic) that split up the Southern Permian Basin. Mid-Kimmerian (Middle - Late Jurassic) thermal uplift of the Central North Sea Dome and related rifting led to removal of the Lower Jurassic sequence. Subsequently, contemporaneous activity of NW-SE and NE-SW oblique slip faults during the Late Kimmerian phases (Late Jurassic) can be explained by a trans-tensional stress field (Wong, 2007).

Fault offsets recognised in the post-Zechstein sequence are mainly related to active salt deformation during the Cenozoic. The close relationship between fault intersections in the basement and geometry of salt structures (Remmelts, 1996) suggests a genetic link. From Early Triassic onward, mobilization of Zechstein salt triggered by basement faulting was the main driving mechanism for generation of fault-block tilting and soft-linked faulting in the post Zechstein cover. These subsidiary faults delineate the salt domes and walls in the northwestern sector. The occurrence of scattered unlinked faults in the post Zechstein units can be regarded subordinate to salt flow and -withdrawal. Minor reverse faults in the overburden occur in the northwestern part of the area and are associated with 7-10 km scale open folds. Reactivation as minor reverse faults occurred during the Subhercynian phase (Late Cretaceous) in a transpressional stress field (tectonic inversion). The compressive stresses acting on the sub salt basement led to tectonic inversion of existing structures and enhanced salt flow.
The youngest faults in the area belong to Group 4 and are related to a youngest phase of salt flow after tectonic inversion. These salt structures remained active during the Late Tertiary until recent times. The smaller conjugate sets of NE-SW faults below the Mid Miocene Unconformity might be related to a Late Paleocene - Eocene extension phase associated with development of the North Sea Rift System (de Lugt et al., 2003; Wong et al., 2007).

Salt structures

Salt deposits occur in the Late Permian Zechstein Group and in the Triassic Röt, Muschelkalk and Keuper formations. The presence of Zechstein salts greatly influenced the post-Permian structural and sedimentary development of the area. The original estimated depositional thickness of the Zechstein Group was 650 m (ZE1 to ZE4 formations), a thickness extrapolated from wells in undisturbed areas, like Uithuizermeeden-01 (Van Adrichem Boogaert & Kouwe, 1992-1997) while its present-day thickness varies from approximately 5000 m to only a few metres in withdrawal

areas. The larger part of the area is regarded as a salt depletion area, where salt has moved away laterally and vertically into salt structures, which predominantly occur in the northwestern part of the area. Identified salt structures include salt pillows, salt walls and diapirs and salt tongues, with greatly varying dimensions (length between 5-30 km, width up to 8 km, height up to 5 km).
Timing of salt movement is related to phases of active fault movement (see also Remmelts 2006). Halokinesis started already in the Early and Middle Triassic during differentiation of the Texel Ijsselmeer High. The salt movement during the Late Triassic occurred mainly on the Central Offshore Platform where salt thickness due to positive salt flow was greatest. A subsequent major phase of salt movement took place during the Late Jurassic and resulted in piercing of many of the salt structures and furthered compartmentalisation of the Vlieland Basin. A Late Cretaceous-Early Tertiary phase of reactivation of the salt structures led to formation of salt pillows underneath most folds throughout the area.

4.1.2 Stratigraphy

The well logs of 48 selected wells were loaded into Petrel and lithostratigraphically (re-) interpreted on member level. For this purpose several correlation panels have been constructed, some on group level to facilitate detailed interpretation. Others were set up with a spatial distribution to create a more regional view. A tectono-stratigraphic chart for this specific area was constructed (Annex E, Figure 4.1.11). Furthermore, other sources such as biostratigraphy, core descriptions, consultancy reports and specific literature have been used to enhance and improve the litho- stratigraphic interpretation. The main characteristics of the stratigraphic buildup is described per stratigraphic group. Annex B and C present the depth and thickness maps of the groups.

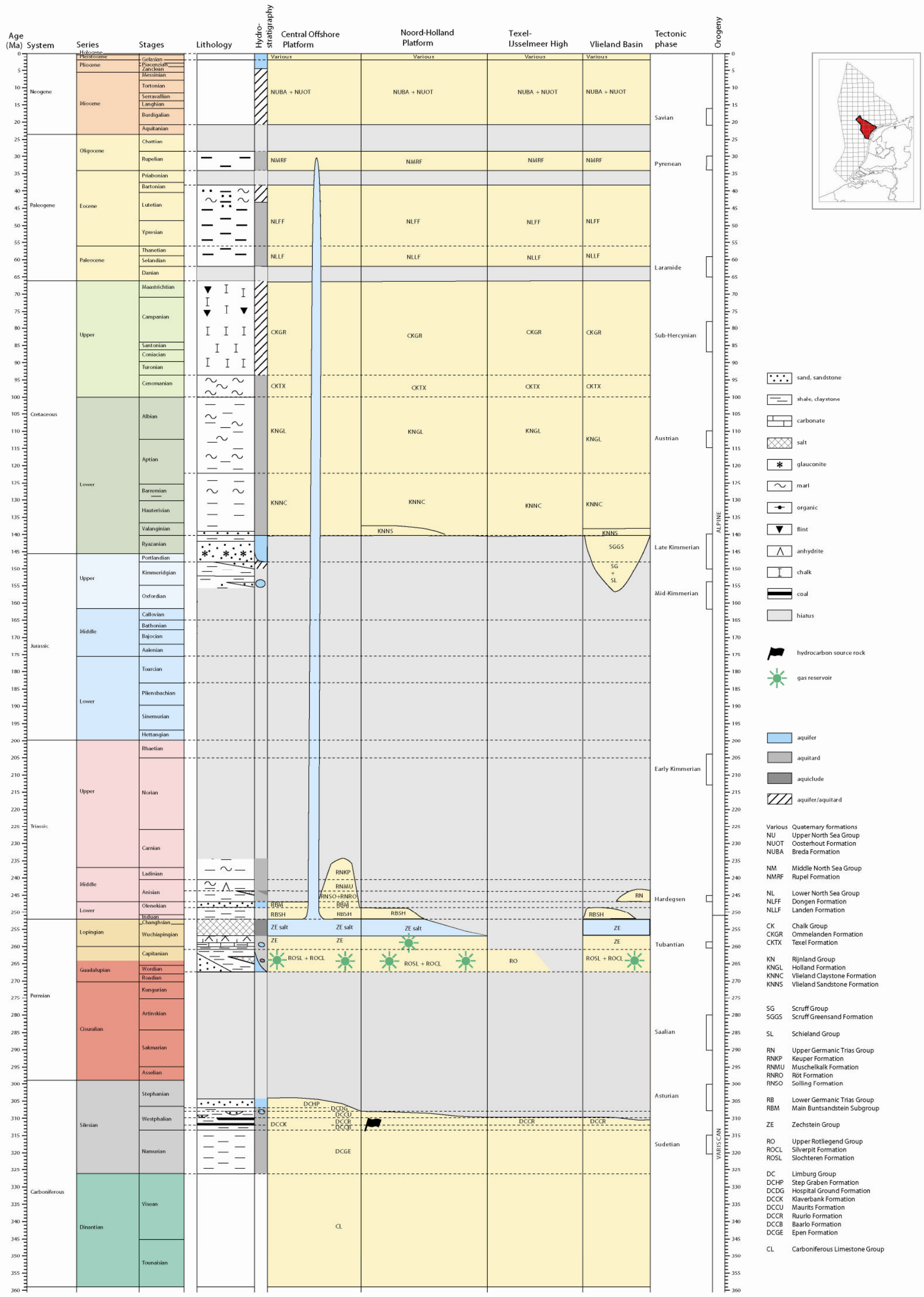

Tectono-stratigraphic chart of the Central Offshore Platform, Noord-Holland Platform, Texel-IJsselmeer High and Vlieland Basin. Time scale according to Gradstein et al. (2004).

Figure 4.1.7 Tectono-stratigraphic chart of the Dutch Central Graben and Terschelling Basin (see also Annex E).

Limburg Group

About 45 of the newly interpreted wells reached the Limburg Group. The burial depth of the top of the Limburg Group increases from SE towards NW and reaches depths between 3000 and greater than 5000 m. The base of the Limburg Group is assumed to be at depths of 6-7 km (pers. comm. H. Kombrink). Most information on the lithostratigraphy of this group was deduced from regional mapping studies.

The sediments of the Limburg Group were deposited during the Silesian in an E-W oriented flexural foreland basin. This basin formed under the influence of the northward migrating Variscan thrust front and is bounded by the London Brabant Massif to the south and the Mid North Sea – Ringkøbing-Fyn High to the north (Van Buggenum and Den Hartog Jager 2007; Ziegler 1990).

At the largest scale, the Limburg Group shows an overall regressive cycle associated with the filling of the Variscan foredeep basin. The lower part is defined by the largely marine claystones of the Geul subgroup (Namurian to Earliest Westphalian A). On top of that are the Caumer, Dinkel and Hunze subgroups which show a transition towards more continental and finally arid conditions. The Caumer subgroup (Namurian B – Westphalian C) marks the onset of peat (coal) deposition in a deltaplain / swamp environment. In this subgroup the Klaverbank Formation represents the proximal, coarser-grained fluvial and deltaic sandstones, whereas the Baarlo and Ruurlo formations comprise the more distal delta fines, including coal layers. The Maurits Formation of the Caumer subgroup represents the lacustrine and floodplain fines with prolific coal formation. The transition to more fluvial conditions during the Westphalian C/D resulted in the deposition of the sandstone dominated Dinkel subgroup (Hospital Ground Formation). Finally the conditions become arid with the occurrence of red beds in the Hunze subgroup (Step Graben Formation).

The Asturian tectonic phase (Westphalian C/D to Stephanian) resulted in differential movements. The Carboniferous deposits underwent strong uplift and subsequent erosion during the Saalian thermal uplift (Early to Middle Permian) the effect of which is displayed in the Pre-Permian subcrop map (Figure 4.1.8). In the SE the Ruurlo Fm subcrops under the overlying Upper Rotliegend and to the NW the younger deposits of the Step Graben Formation have been preserved.

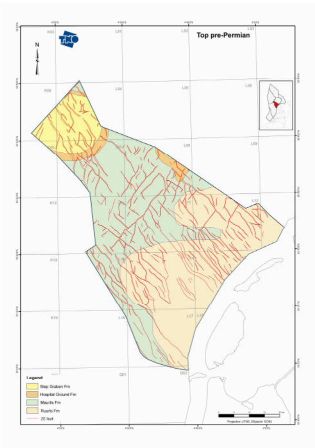

Figure 4.1.8 Top Carboniferous (based on Mijnlieff 2002)

Upper Rotliegend Group

In the mapped area the Rotliegend sandstones are the main target for hydrocarbons. Therefore most wells penetrate the Upper Rotliegend Group. The Saalian Unconformity separates the sediments of the Upper Rotliegend Group from the Limburg Group. The hiatus spans some 50 Ma in the study area.

Following the Saalian phase of uplift and erosion, clastic deposition in the Netherlands started in the latest Middle Permian and lasted until the earliest Late Permian. Sediments were deposited under arid conditions into a large E-W trending complex of continental sedimentary basins known as the Southern Permian Basin and stretching from the British Isles into Poland. The Dutch on- and offshore primarily received their sediments from the Variscan mountain belt to the south.

The Upper Rotliegend Group is subdivided into the Slochteren Formation comprising mainly fluvial and eolian sandstones and conglomerates, and the further to the north the Silverpit Formation which is composed of claystones, siltstones and evaporites deposited in a playa / lake environment. Both formations are each other’s lateral equivalent.

The study area is located in the transition zone between both formations and the deposits in the northern part mainly comprise the fine grained sediments of the Silverpit Formation with the basal sand of the Lower Slochteren Member. In the central part of the area the occurrences of the Upper and Lower Slochteren members were encountered. Along the southern margin (L17) only the sandy deposits of the Slochteren Formation are present (see Annex F).

Figure 4.1.9 shows that the thickness of the Upper Rotliegend Group increases in northwesterly direction towards the centre of the Southern Permian Basin.

The Upper Rotliegend is conformably overlain by Late Permian marine carbonates and evaporites of the Zechstein Group.

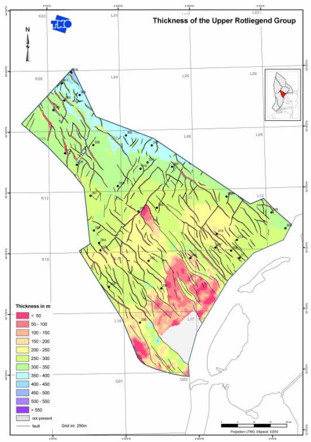

Figure 4.1.9 Thickness of the Upper Rotliegend Group

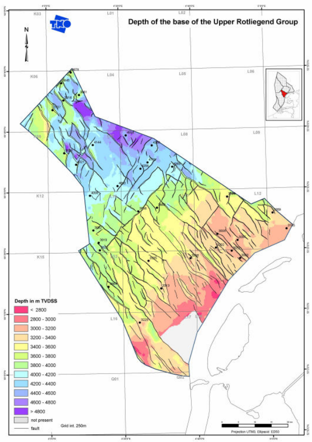

Figure 4.1.10 Depth base of the Upper Rotliegend Group

Zechstein Group

The Zechstein Group deposits result from a series of marine transgressions into the Southern Permian Basin, each transgression followed by an evaporation phase. The Zechstein Group consists of four to five evaporite cycles. The Zechstein Upper Claystone Formation covers these cycles unconformably. In the northwestern part of the mapped area only the Z1 Formation has its regular succession. Most of the Z2, Z3 and Z4 cycles have been deformed by halokinese. In the central part much of the Zechstein has been removed by later erosion. In the southeastern part, on and around the Texel-IJsselmeer High the Zechstein deposits are thin or have been completely eroded (Annex B and C).

The Z1 cycle is composed of the Kupferschiefer, a thin organic-rich shale at the base, followed by the Z1 Carbonates Member and the Werra Anhydrite. The Z2 consists of a basal carbonate followed by anhydrite and salt. Z3 and Z4 cycles aredeposited with claystone and/or carbonate at the base, followed by the deposition of anhydrite and salt and sometimes overlain by a roof anhydrite. In the northwestern part of the mapped area their internal succession is deformed by salt movements. The various members are concentrated in deformed state in the salt domes and salt walls. In between the salt structures the sequences are squeezed out. The Zechstein Upper Claystone Member is generally present between salt structures and absent above the structures.

In the northwestern area the present-day thickness is affected by salt deformation and varies from approximately 3000 m to only a few metres in withdrawal areas (Figure 4.1.11). In the area around the Texel-IJsselmeer High the thickness of the Zechstein Group is generally between 100 and 200 m. The burial depth of the base of the Zechstein Group increases from less than 3000 m in the Vlieland Basin to more than 4000 m in the northwestern part (Figure 4.1.12).

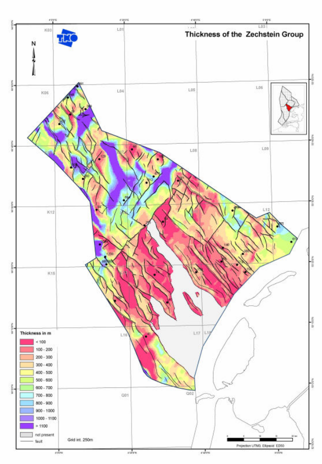

Figure 4.1.11 Thickness of the Zechstein Group

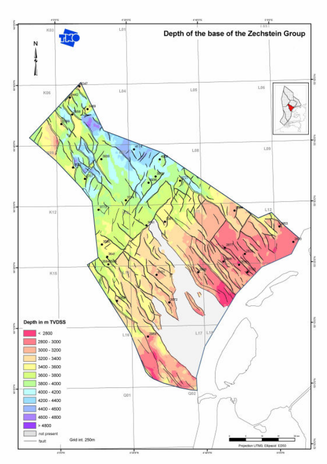

Figure 4.1.12 Depth base Zechstein Group

Lower and Upper Germanic Trias groups

After the deposition of the Zechstein Group the sedimentation of the Triassic rocks took place in a similar basinal setting but under continental conditions during Early Triassic times. The depositional environment in the mapped area is interpretated as lake to lake-margin (Geluk, 2007a). Restricted marine conditions returned during Middle and Late Triassic times.

Two major groups of sediments are recognised in the Triassic rocks: the Lower and Upper Germanic Trias groups. The boundary between these two groups is formed by the Hardegsen or base Solling Unconformity.

The Lower Germanic Trias Group (Indian to Olenekian age) is mainly a clastic succession. It consists of fine-grained siliclastic deposits with oolite intercalations in the lower part of the succession and more sandbodies alternating with claystones and siltstones in the higher parts of the succession. It is subdivided from bottom to top in the Main Claystone, the Rogenstein, the Volpriehausen, Detfurth and Hardegsen formations.

The Lower Germanic Trias Group is present in the northwestern part of the area and (as a very thin erosional remnant) in the Vlieland Basin. The most complete succession can be found in between salt structures.

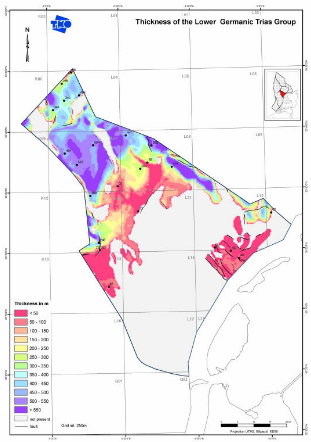

Figure 4.1.13 Thickness of the Lower Germanic Trias Group

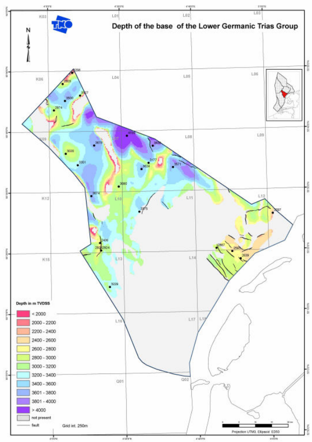

Figure 4.1.14 Depth base Lower Germanic Trias Group

The Upper Germanic Trias Group (Anisian – Norian age) consists of 4 formations: the Solling, Röt, Muschelkalk and Keuper formations. The sediments were deposited under continental to restricted marine conditions. All formations are present in the mapped area.

The Solling Formation consists of fine-grained silt- and claystones often with a thin sandstone unit at the base. The Röt Formation has at its base a halite sequence followed by silt- and claystones often with anhydrite layers.

The present-day distribution of the sediments of Muschelkalk and Keuper formations is restricted to rim-synclines in between salt domes. Erosional remnants of the

Muschelkalk Formation are also present in the Vlieland Basin. The sediments of the Muschelkalk and Keuper formations consist of halite, anhydrite, some carbonates and silt- and claystones.

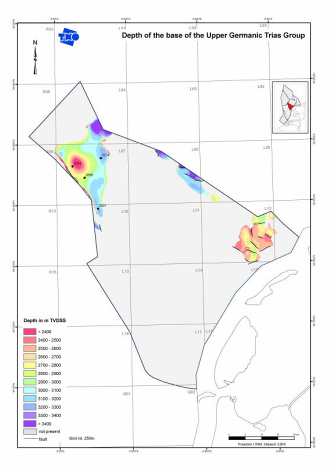

Figure 4.1.15 Thickness of the Upper Germanic Trias Group

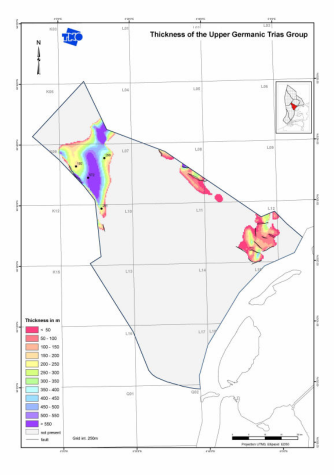

Figure 4.1.16 Depth base Upper Germanic Trias Group

Altena and Schieland groups

The present-day distribution of the Altena Group lies outside the mapped area and is discarded. The Upper Jurassic Schieland Group is only present in the Vlieland Basin. The depositional environment varies from continental to restricted marine.

After the Early Kimmerian phase the structuration of the area changed from having a position in the Southern Permian Basin into fault bounded basins and highs. Early in the Middle Jurassic the thermal Central North Sea Dome developed, resulting in the Mid-Kimmerian uplift. In the mapped area these movements caused deep erosion and complete removal of the Lower to Middle Jurassic sediments.

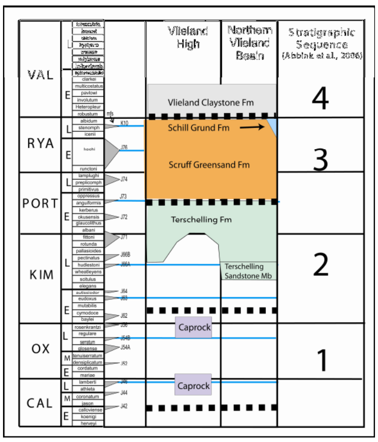

Figure 4.1.17 Tectono-stratigraphic diagram for the Schieland Group on the Vlieland High and in the northern Vlieland Basin.

The Upper Jurassic sediments were deposited in the Vlieland Basin. Biostratigraphic study (internal TNO report 2006-U-R0049/B) shows that probably all three tectono-stratigraphic sequences (viz. Abbink et al. 2006) are present in this area. The sediments of tectono-sequence 1 have been found in well L12-05 as "caprock" on a salt dome. Their age is Early-Oxfordian - Early Kimmeridgian and they can be interpretated as Rifgronden Member and Friese Front Formation. In well L12-03 and L15-03 the Terschelling Formation and the Scruff Greensand Formation have been encountered, which can be placed in respectively tectono-sequence 2 and 3. The greatest thickness of the "Upper- Jurassic" sediments in the Vlieland Basin is 178 m and the depth of the base of the Schieland Group lies in between 2400 and 2850 m.

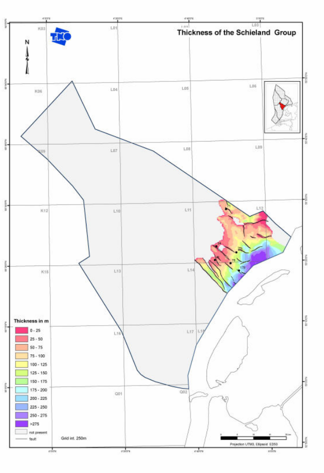

Figure 4.1.18 Thickness of the Schieland Group

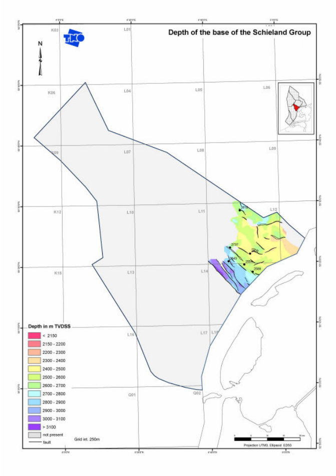

Figure 4.1.19 Depth base Schieland Group

Rijnland and Chalk groups

The Rijnland Group is deposited in the entire 2E area. The greatest depths can be found in between saltdomes and on the platform area NW of the Texel-IJsselmeer High. The greatest thicknesses occur along the flanks of salt domes and walls, indicating that the salt movements partly controlled the sedimentation.

The Chalk Group in its present-day setting shows the greatest depth and thicknesses on the former platforms, such as Central Offshore Platform, Noord-Holland Platform and even on the NW extension of the Texel-IJsselmeer High.

After the Kimmerian rifting phases a period with regional subsidence commenced. In the Early Cretaceous sedimentation took place not only in the former basins but also on platforms and highs due to global sea-level rise. This overall transgression resulted in area 2E for a large succession of mainly clay- and siltstones. During Aptian times deeper marine conditions dominated and calcareous claystones were deposited. In the Late Cretaceous the hinterland had been flooded almost completely and hardly any clastic influx occurred in the deposition of limestones and chalk.

The Vlieland Claystone Formation of the Rijnland Group comprises fine-grained sediments like clay- and siltstones. In the 2E area the top of the Vlieland Claystone is calcareous and if very pronounced, this interval can be placed in the Vlieland Marl Member. The Vlieland Claystone Formation has an average thickness of 200 m.

At the base of the sequence the Friesland Sandstone Member of the Rijnland Group has has a distribution in the Vlieland Basin and in the southern part of the 2E area on the Noord-Holland Platform. The thickness of the Friesland Sandstone Member is average 20 to 50 m. The Holland Formation is represented by the Lower and Upper Holland Marl members separated by the Middle Holland Claystone Member and can be found in the entire area.

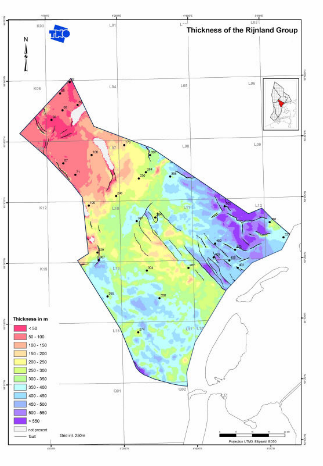

Figure 4.1.20 Thickness of the Rijnland Group

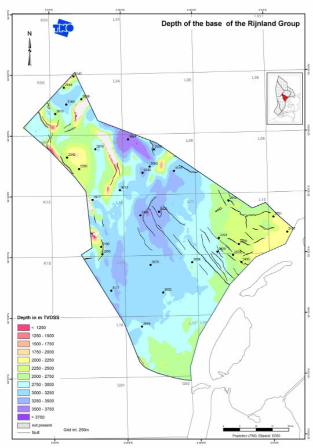

Figure 4.1.21 Depth base Rijnland Group

The Chalk Group is present with the Ekofisk, Ommelanden, Plenus and Texel formations. The deposits consist of a thick succession of carbonate rocks. The bulk of the group comprises bioclastic limestones and marly limestones. Originally, these limestones had a more chalky nature, but as a result of deep burial they were compacted strongly and became denser. Chert concretions are particularly present at the top. Chalk Group can reach thicknesses of over 1500 m in the southern part of the area. In Vlieland Basin early pulses leading to the Subhercynian erosion phase resulted in erosion and non-deposition in the Turonian and Santonian (Van der Molen , 2004). Thicknesses average from 100 to 400 m in the central part of the basin.

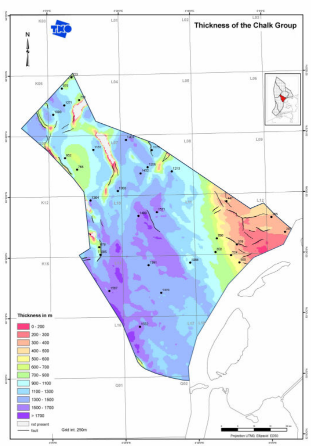

Figure 4.1.22 Thickness of the Chalk Group

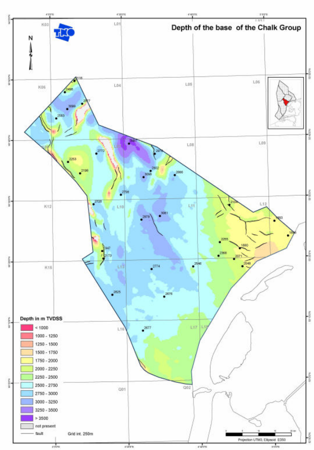

Figure 4.1.23 Depth base Chalk Group

Lower, Middle and Upper North Sea groups

The Lower, Middle and Upper North Sea groups are present in the entire area. The deposits of the Lower, Middle and Upper North Sea Group have their greatest thickness in the northwest. Salt movement greatly influenced the depositional thickness of the Lower and Middle North Sea groups, while the base of the Upper North Sea Group is only on top of the salt domes. The depth of the base of the Lower and Middle North Sea groups increases from south with depths at 800 m to the north with depths greater than 1600 m. In the rim-synclines the base can be found at depths greater than 2000 m. The Upper North Se Group shows the same variation with depths from 300 – 800 m from south to north and depths less than 350 m over salt domes.

After the Mesozoic rifting phases and the Subhercynian and Laramide inversion phases the siliclastic sediments of the Lower, Middle and Upper North Sea groups were deposited in a large rapidly subsiding epicontinental basin, the North Sea Basin, which formed after the movements of the Laramide tectonic phase by thermal relaxation, isostatic adjustment and sea level rise .In the mapped area the sediments were deposited in a marine environment. The present-day deposits of the North Sea Supergroup have been effected by salt movements.

The North Sea Super Group consists of three groups, viz. the Lower, Middle and Upper North Sea Group. The Lower North Sea Group is divided into the Landen and Dongen formations. At the base of the Dongen Formation a mixture of clay, silt and volcanic ash form the Basal Dongen tuffite. The Lower North Sea Group consists mosly of clay(-stone) with a marly deposits in the Brussels Marl Member. The Middle North Sea Group consists of clay(-stone) of the Rupel Formation. Sandy deposits prevail in the Upper North Sea Group. The overlying Quaternary deposits are incorporated in the Upper North Sea Group.

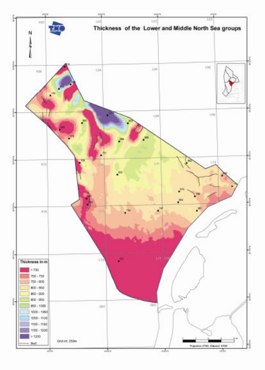

Figure 4.1.24 Thickness of the Lower and Middle North Sea groups

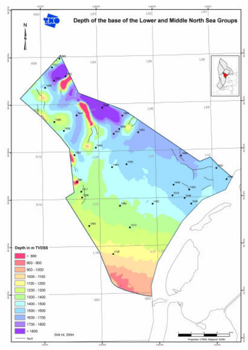

Figure 4.1.25 Depth base Lower North Sea Group

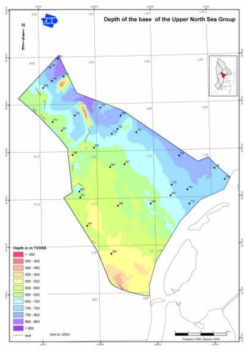

Figure 4.1.26 Depth base Upper North Sea Group

5 References

Abbink O.A., Mijnlieff H.F., Munsterman D.K. & Verreussel R.M.C.H. New stratigraphic insights in the 'Late Jurassic' of the Southern Central North Sea Graben and Terschelling Basin (Dutch Offshore) and related exploration potential. Netherlands Journal of Geosciences — Geologie en Mijnbouw, 85-3, p. 221-238.

Alblas, L.D. (2001) The petroleum industry in the Netherlands – its settings and possible future. Geol. Mijnbouw/Neth. Journ. Geosc. 80, p. 23-32.

Breunese, J.N. & Rispens, F.B. (1996) Natural gas in the Netherlands: exploration and development in historic and future perspective. In: Rondeel, H.E., Batjes, D.A.J. & Nieuwenhuijs, W.H. (eds) Geology of Gas and Oil under the Netherlands. Kluwer, Dordrecht, p. 19-30.

De Jager, J., Doyle, M.A., Grantham, P.J. & Mabillard, J.E. (1996) Hydrocarbon habitat of the West Netherlands Basin. In: Rondeel, H.E., Batjes, D.A.J. & Nieuwenhuijs, W.H. (eds) Geology of Gas and Oil under the Netherlands. Kluwer, Dordrecht, p. 191-209.

De Jager, J., 2003. Inverted basins in the Netherlands, similarities and differences. Netherlands Journal of Geosciences / Geologie en Mijnbouw 82: p. 339-349.

De Jager, J., 2007. Geological Development. In: Wong, Th.E, Batjes, D.A.J. & De Jager, J. (eds): Geology of the Netherlands. Royal Netherlands Academy of Arts and Sciences (Amsterdam): p. 5 -26.

De Jager, J. & Geluk, M.C., 2007. Petroleum Geology. In: Wong, Th.E., Batjes, D.A.J. & De Jager, J. (eds): Geology of the Netherlands. Royal Dutch Academy of Arts and Sciences (Amsterdam): p. 241 -264.

Dirkzwager. J.B., 2002. Tectonic modeling of vertical motion and its near surface expression in the Netherlands, PhD thesis, VU-Amsterdam: 156 pp.

Duin E.J.T., Doornenbal J.C., Rijkers R.H.B., Verbeek J.W.& Wong Th.E., 2006. Subsurface structure of the Netherlands - results of recent onshore and offshore mapping, Netherlands Journal of Geosciences - Geologie en Mijnbouw, 85-4, pp. 245 -276.

Frikken, H.W. (1999) Reservoir-geological aspects of productivity and connectivity of gasfields in the Netherlands. PhD thesis, Technical University Delft, 13/9/99, 91 pp.

Geluk, M.C. (1999a) Late Permian (Zechstein) rifting in the Netherlands - models and implications for petroleum geology. Petroleum Geoscience 5 (2), p. 189-199.

Geluk, M.C., 2005. Stratigraphy and tectonics of Permo-Triassic basins in the Netherlands and surrounding areas. PhD thesis, University of Utrecht: 171 pp.

Geluk, M.C., 2007a. Permian. In: Wong, Th.E., Batjes, D.A.J. & De Jager, J. (eds): Geology of the Netherlands. Royal Dutch Academy of Arts and Sciences (Amsterdam): p. 63 - 83.

Geluk, M.C., Paar, W.A. & Fokker, P.A., 2007b . Salt. In: Wong, Th.E., Batjes, D.A.J. & De Jager, J. (eds):: *Geology of the Netherlands*. Royal Dutch Academy of Arts and Science (Amsterdam): p. 283 – 294.

Gradstein, F.M., Ogg, J.G. & Smith, A.G. (eds), 2004. A geologic time scale. Cambridge University Press: 589 pp.

Herngreen, G.F.W. & Wong, Th.E., 1989. Revision of the ‘Late Jurassic’ stratigraphy of the Dutch Central Graben. Geologie en Mijnbouw 68: p. 73-105.

Herngreen, G.F.W., Smit, R. & Wong, Th.E., 1991. Stratigraphy and tectonics of the Vlieland Basin, The Netherlands. In: A.M. Spencer (ed.): Generation, accumulation and production of Europe’s hydrocarbons. Special publications EAPG no. 1, Oxford University Press (Oxford): p. 175-192.

Herngreen, G.F.W., Kouwe, W.F.P. & Wong, Th.E. , 2003. The Jurassic of the Netherlands. Geological Survey of Danmark and Greenland Bulletin 1, p. 217-229.
Netherlands Institute of Applied Geoscience TNO – National Geological Survey (2004). Geological Atlas of the Subsurface of the Netherlands – onshore, TNO – NITG, Utrecht: 101 pp.

Overeem, I., Weltje G. J., Bishop-Kay C.and Kroonenberg S. B. (2001) - The Late Cenozoic Eridanos delta system in the Southern North Sea Basin: a climate signal in sediment supply? Basin Research 13, p. 293-312.

Remmelts, G., 1996. Salt tectonics in the southern North Sea, the Netherlands. In: Rondeel, H.E., Batjes, D.A.J. & Nieuwenhuijs, W.H. (eds): Geology of gas and oil under the Netherlands. Kluwer (Dordrecht): 143-158.

Rijkers, R.H.B. & Duin, E.J.Th.,1994. Crustal observations beneath the southern North Sea and their tectonic and geological implications, Tectonophysics 240: p. 215-224.

Rijkers, R.H.B. & Geluk, M.C., 1996. Sedimentary and structural history of the Texel-IJsselmeer High, The Netherlands. In: Rondeel, H.E., Batjes, D.A.J. & Nieuwenhuis, W.H. (eds): Geology of gas and oil under the Netherlands. Kluwer (Dordrecht): p. 265-284.

Van Adrichem Boogaert, H.A. & Kouwe, W.F.P. (eds), 1993 - 1997. Stratigraphic nomenclature of the Netherlands, revision and update by RGD and NOGEPA, Mededelingen Rijks Geologische Dienst 50.

Van Dalfsen, W., Doornenbal, J.C., Dortland, S. & Gunnink, J.L. (2006). A comprehensive seismic velocity model for the Netherlands based on lithostratigraphic layers, Netherlands Journal of Geosciences / Geologie en Mijnbouw 85/4: p. 277-292.
Van der Molen, A.S., 2004. Sedimentary development, seismic stratigraphy and burial compaction of the Chalk Group in the Netherlands North Sea area, PhD thesis. University Utrecht: 175 pp.

Van Wijhe, D.H., 1987. Structural evolution of inverted basins in the Dutch offshore. Tectonophysics 137: p. 171-219.

Verweij, J.M. (2003) Fluid flow systems analysis on geological timescales in onshore and offshore Netherlands. With special reference to the Broad Fourteens Basin. Doctoral Thesis Vrije Universiteit Amsterdam, 278 pp.

Wong, Th.E., Batjes, D.A.J. & De Jager J. (eds), 2007. Geology of the Netherlands, Royal Netherlands Academy of Arts and Sciences (Amsterdam) 354 pp.

Ziegler, P.A., 1988. Evolution of the Arctic-North Atlantic and the Western Tethys, American Association of Petroleum Geologist Memoir 43: p. 164-196.
Ziegler, P.A., 1990. Geological Atlas of Western and Central Europe (2nd edition). Shell Internationale Petroleum Maatschappij B.V.; Geological Society Publishing House (Bath): 239 pp.

Internal TNO reports:

Internal TNO reports and reports by interns and trainees are made available upon request.

Abdul Fattah, R. (trainee, 2007-2008), Van Wees, J-D, Verweij, J.M., Bonte, D. 2008. Tectonic heat flow modeling for the NCP2a area of the Dutch offshore. TNO report 2008-U-R0558A

Berlinger, S. (intern 2006). Compilation of the Q50 reservoir productivity map for the Dutch Lower & Upper Slochteren play area.

Stegers, D.P.M. (intern, 2006). Sedimentary facies analysis of sequence 2 of the Upper Jurassic in the Terschelling Basin and the southern Dutch Central Graben. TNO report 2006-U-R0191/A.

TNO BenO (2005). Carboniferous palynostratigraphy of Wells M03-01 and M10-04; NCP-2a. TNO report NITG 05-130-B0905.

TNO BenO (2007). De resultaten van het palynologisch onderzoek naar het Tertiair van boring L07-06 (interval: 590-870 m) TNO report 2007-UT-R0873B

TNO BenO (2007). Biostratigraphy of the upper Chalk Group from well L8-7, offshore the Netherlands. TNO report 2007-UT-R1262A.

TNO BenO (2008) De resultaten van het dinoflagellaatcystenonderzoek naar de ouderdom van de boringen L12-05, L12-03 en L15-03 uit het noordelijk deel van het Vlieland Bekken.. TNO report 2006-U-R0049B.

TNO BenO (2008). NCP_2E Rotliegend Petrofysica. TNO report 2008-U-R0605B.

TNO BenO (2009). De resultaten van het palynologisch onderzoek naar het Tertiair van boring K10-03 (interval: 350-910 m) TNO report 034-UT-00453B

TNO BenO (2009). Terschelling Basin and southern Dutch Central Graben. Mapping and modeling – Area 2A. TNO report 034-UT-2009-01569.

TNO BenO (2010). Schill Grund High and Ameland Block. Mapping ans Modelling – Area 2B.

TNO report 034-UT-2010-01363

TNO BenO (2010. Central Offshore Platform Burial history, temperature, source rock maturity and hydrocarbon gegeration – Area NCP2E. TNO report 034-UT-2010-01298/A.

6 Appendices

6.1 List of wells

SHORT_NAME	X_UTM31	Y_UTM_31	TD	OPERATOR	END_DATE
L04-01	570877	5956460	3991	PET	31-8-1974
L04-03	567473	5953668	3830	PET	21-2-1981
L04-04	575390	5958169	3975	PET	3-2-1985
L04-05	583844	5960545	4155	NAM	30-5-1992
L04-06	573062	5965151	4335	PET	2-8-1994
L04-07	570132	5961694	4124	PET	22-11-1995
L07-01	571092	5940328	3934	PET	28-6-1971
L07-04	579792	5942872	4182	PET	23-12-1973
L07-05	572355	5932054	3886	PET	3-3-1974
L07-06	587298	5930269	4150	PET	3-8-1974
L07-08	574795	5936886	4060	PET	30-7-1975
L08-01	596436	5937585	4229	PEN	12-7-1972
L08-02	594273	5935702	4307	PEN	31-12-1973
L08-03	597701	5942833	4429	PEN	21-3-1974
L08-07	589791	5945953	4700	AMC	26-8-1985
L08-H-01	603857	5936333	4250	PEN	7-2-1986
L08-P-01	603399	5944828	4450	WIN	12-4-1992
L08-P-03	603399	5944828	5075	WIN	27-11-1995
L09-01	614266	5935405	3856,7	PHL	22-6-1973
L10-01	578922	5927393	4122	PLA	22-2-1970
L10-06	576648	5922552	4119	PLA	8-3-1972
L10-13	581601	5913123	3967,6	PLA	17-9-1973
L10-14	581938	5910832	3814	PLA	16-3-1974
L10-C-01	579955	5916888	3909	PLA	3-8-1974
L11-02	593624	5922712	3993	PLA	12-7-1974
L11-04	599285	5923844	3745	PLA	14-8-1978
L11-05	603586	5920415	3619	CHE	1-10-1978
L11-A-01	591726	5910705	3642	PLA	9-10-1984
L12-01	617692	5915850	3451	SIG	20-1-1969
L12-02	617306	5911682	3276	NAM	2-5-1976
L12-03	623808	5913999	3150	NAM	11-7-1979
L12-05	620604	5927230	3708	NAM	1-2-1988
L13-02	578536	5903211	3635	NAM	1-11-1975
L13-03	568565	5903503	3435	NAM	9-11-1976
L13-09	584713	5899735	3739	NAM	5-5-1986
L14-02	600611	5899172	3366,5	PLA	21-10-1976
L14-05	609503	5908422	3517	PLA	8-2-1985
L14-A-01	596744	5907624	3438,1	PLA	1-11-1975
L15-01	624602	5908457	3202	NAM	16-7-1978
L15-FA-101	622023	5910693	3143	NAM	30-4-1980
L16-01	579593	5881506	3695	PET	1-3-1973
L16-12	579122	5890647	3525	CON	16-12-1991

SHORT_NAME	X_UTM31	Y_UTM_31	TD	OPERATOR	END_DATE
L17-01	590107	5879293	3332	CHE	9-10-1976
L17-02	594101	5888776	3300	CHE	14-7-1979
L17-03	599384	5876567	3299,3	ARC	14-12-1988
M10-02	638409	5918069	3070	NAM	31-1-1982
M10-04	634423	5922386	3873	PLA	15-12-1988
Q02-01	600906	5857531	2817	AMC	31-7-1987
Q02-02	600752	5865596	3573	PLA	6-8-1989
Q02-03	600073	5860891	3588	PLA	19-9-1991

6.2 List of 3D seismic surveys

Block	Survey code TNO
L11,L12,M10,L14,L15	Z3NAM1988A
L09,L08	Z3NAM1988D
L04,L05	Z3NAM1990B
L13	Z3NAM1991F
L08	Z3PEN1985A
K03,K06,L01,L04,L05,K09,L07,L08,L10	Z3PET1992A
L10	Z3PLA1989C
L07,L08,L10,L11	Z3PLA1991D
L10,L11,L13,L14,L16,L17	Z3PLA1992B
L11	Z3UNC1987A
L08,L07	Z3WIN1995A

For the location of the 2D seismic lines see Appendix A

6.3 List of maps (download page)

6.4 List of figures

6.5 List of tables

7 Annexes

A. Location map seismic data and wells
B. Depth maps B1-B9
C. Thickness maps C1-C8
D. Structural elements map
E. Tectono-stratigraphic diagram
F. Cross sections F1-F3
G. Petrophysical properties (G1-G29)
H. Reservoir thickness (H1-H5)
I. Oil and gas fields

8 Signature

Utrecht, August 2010	TNO Built Environment and Geosciences
J.C. Doornenbal Head of Department	N. Witmans Author

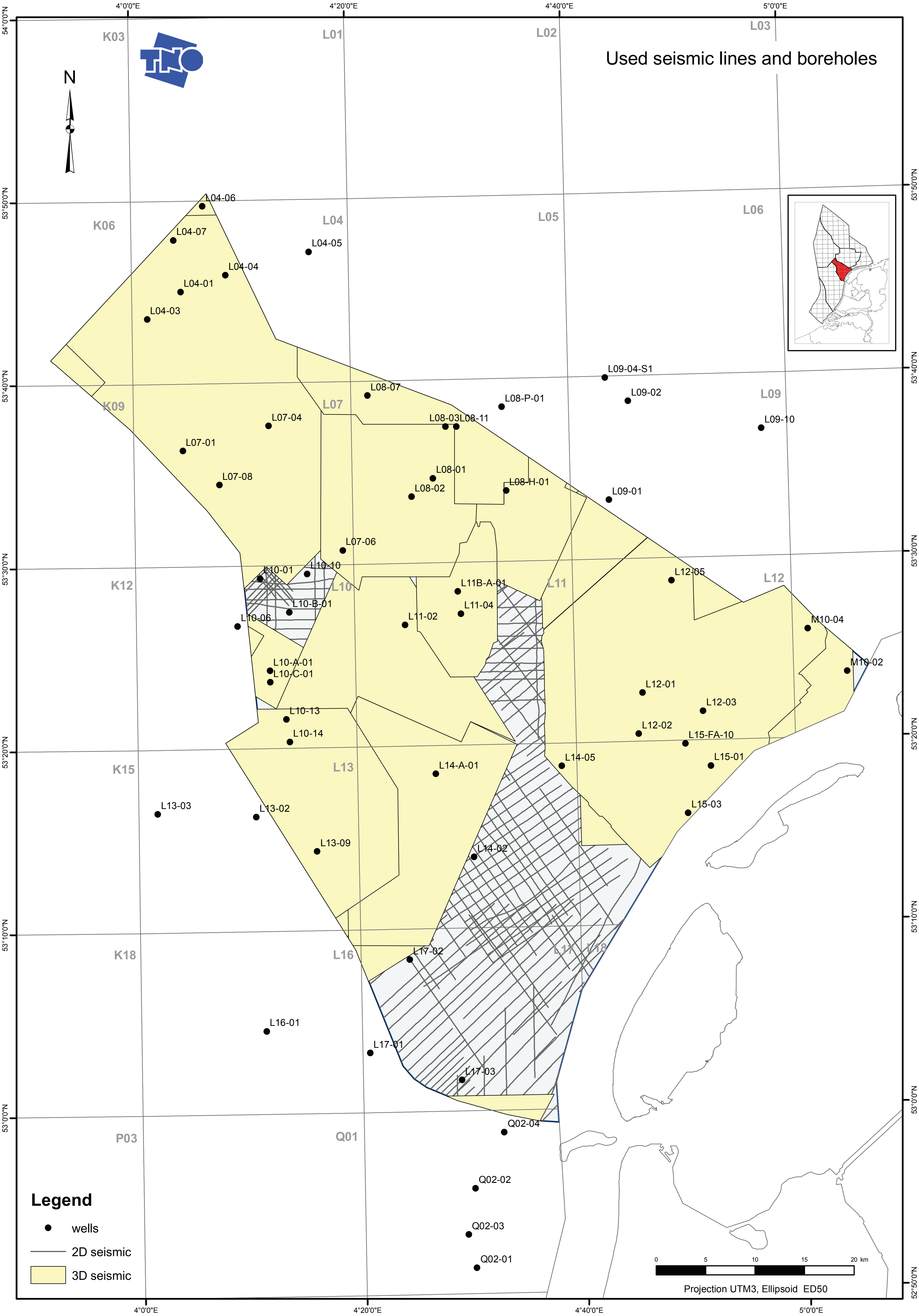
Used seismic lines and boreholes
N
K03
L01
L02
L03
K06
L04
L05
L06
K09
L07
L09
K12
L10
L11
L12
K15
L13
K18
L16
L17
L18
P03
Q01
L04-06
L04-07
L04-05
L04-04
L04-01
L04-03
L09-04-S1
L08-07
L08-P-01
L09-02
L07-04
L08-03
L08-11
L09-10
L07-01
L08-01
L08-02
L08-H-01
L07-08
L09-01
L07-06
L10-01
L10-10
L12-05
L11B-A-01
L10-B-01
L11-04
L10-06
L11-02
M10-04
L10-A-01
L10-C-01
M10-02
L12-01
L12-03
L10-13
L10-14
L12-02
L15-FA-10
L14-A-01
L14-05
L15-01
L13-03
L13-02
L15-03
L13-09
L14-02
L17-02
L16-01
L17-01
L17-03
Q02-04
Q02-02
Q02-03
Q02-01
4°0'0"E
4°20'0"E
4°40'0"E
5°0'0"E
54°0'0"N
53°50'0"N
53°40'0"N
53°30'0"N
53°20'0"N
53°10'0"N
53°0'0"N
52°50'0"N
0
5
10
15
20 km
Projection UTM3, Ellipsoid ED50
Legend
wells
2D seismic
3D seismic

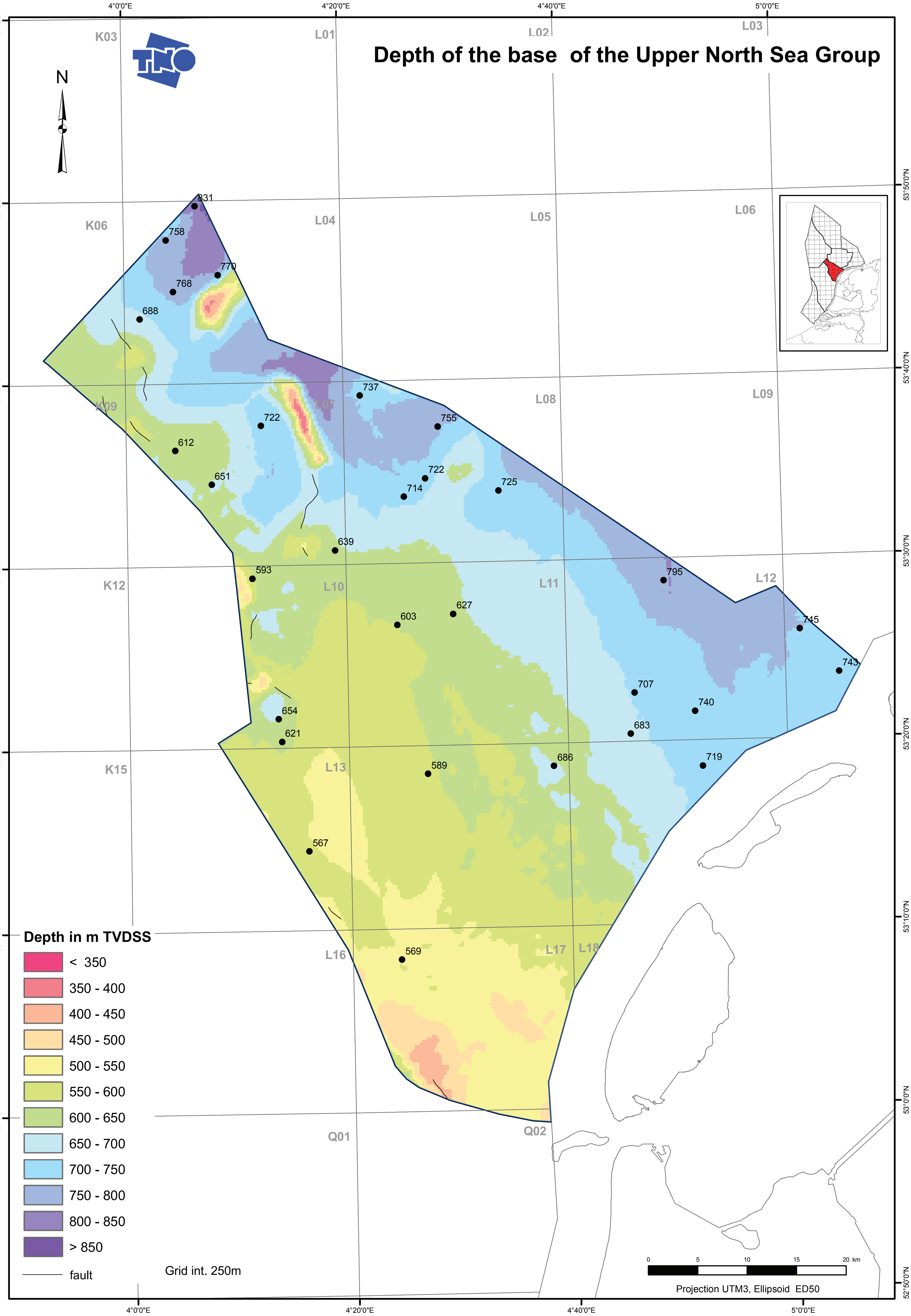

Depth of the base of the Upper North Sea Group
N
Depth in m TVDSS
< 350
350 - 400
400 - 450
450 - 500
500 - 550
550 - 600
600 - 650
650 - 700
700 - 750
750 - 800
800 - 850
> 850
fault
Grid int. 250m
Projection UTM3, Ellipsoid ED50
0 5 10 15 20 km
K03
L01
L02
L03
K06
L04
L05
L06
K09
L07
L08
L09
K12
L10
L11
L12
K15
L13
L16
L17
L18
Q01
Q02
4°0'0"E
4°20'0"E
4°40'0"E
5°0'0"E
54°0'0"N
53°50'0"N
53°40'0"N
53°30'0"N
53°20'0"N
53°10'0"N
53°0'0"N
52°50'0"N
831
758
770
768
688
737
722
755
612
651
722
714
725
639
593
795
745
627
603
743
707
740
654
621
683
686
719
589
567
569

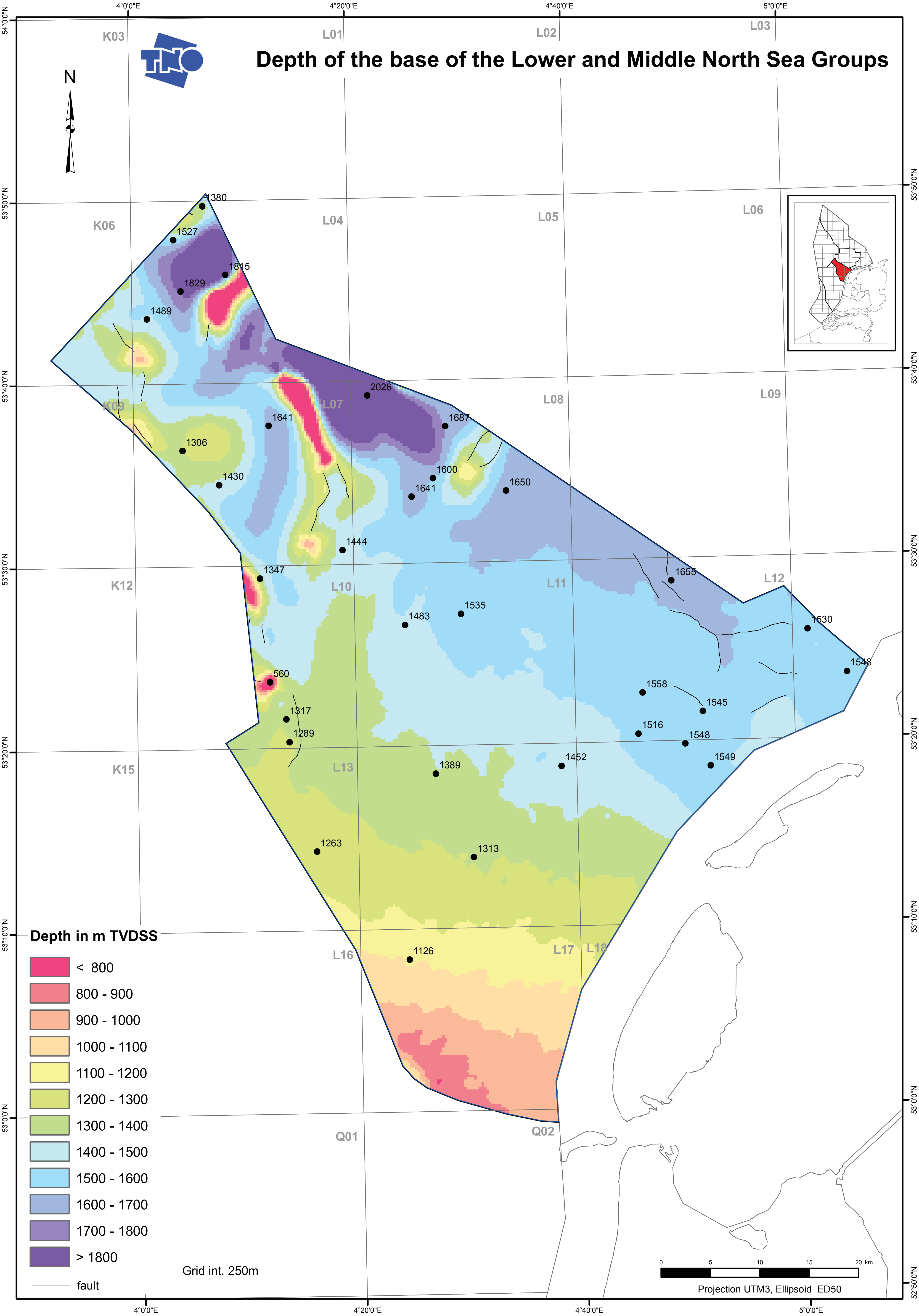
Depth of the base of the Lower and Middle North Sea Groups
N
K03
L01
L02
L03
K06
L04
L05
L06
K09
L07
L08
L09
K12
L10
L11
L12
K15
L13
L16
L17
L18
Q01
Q02
1380
1527
1815
1829
1489
2026
1641
1687
1306
1600
1641
1650
1430
1444
1347
1655
1535
1483
1530
1548
560
1558
1545
1317
1516
1289
1548
1452
1549
1389
1263
1313
1126
Depth in m TVDSS
< 800
800 - 900
900 - 1000
1000 - 1100
1100 - 1200
1200 - 1300
1300 - 1400
1400 - 1500
1500 - 1600
1600 - 1700
1700 - 1800
> 1800
fault
Grid int. 250m
0 5 10 15 20 km
Projection UTM3, Ellipsoid ED50
4°0'0"E
4°20'0"E
4°40'0"E
5°0'0"E
54°0'0"N
53°50'0"N
53°40'0"N
53°30'0"N
53°20'0"N
53°10'0"N
53°0'0"N
52°50'0"N

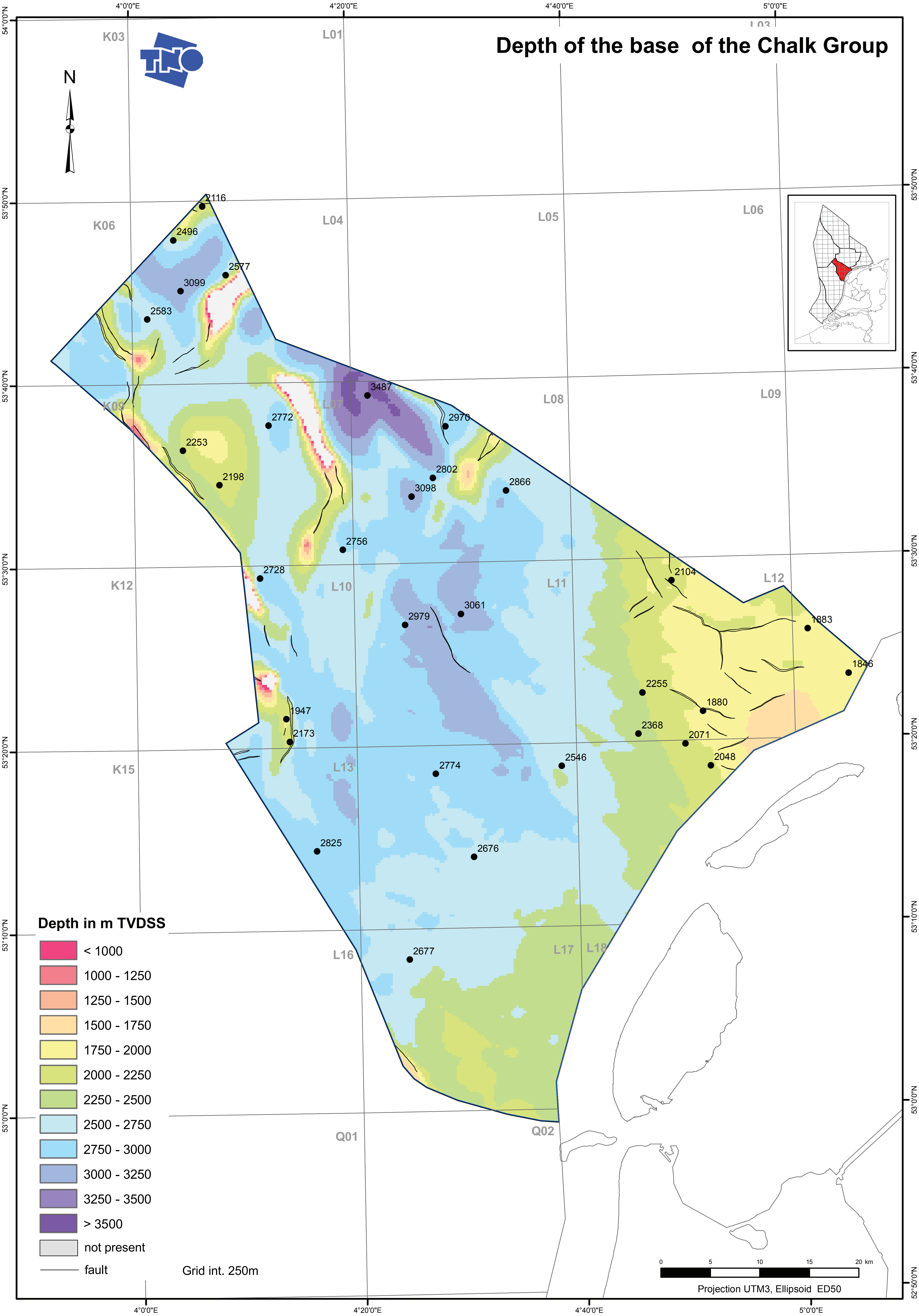
Depth of the base of the Chalk Group
N
K03
L01
L03
K06
L04
L05
L06
K09
L07
L08
L09
K12
L10
L11
L12
K15
L13
L16
L17
L18
Q01
Q02
2116
2496
2577
3099
2583
3487
2772
2970
2253
2198
2802
3098
2866
2756
2728
2104
3061
2979
1883
1846
2255
1880
1947
2173
2368
2071
2546
2048
2774
2825
2676
2677
Depth in m TVDSS
< 1000
1000 - 1250
1250 - 1500
1500 - 1750
1750 - 2000
2000 - 2250
2250 - 2500
2500 - 2750
2750 - 3000
3000 - 3250
3250 - 3500
> 3500
not present
fault
Grid int. 250m
Projection UTM3, Ellipsoid ED50
0
5
10
15
20 km
4°0'0"E
4°20'0"E
4°40'0"E
5°0'0"E
54°0'0"N
53°50'0"N
53°40'0"N
53°30'0"N
53°20'0"N
53°10'0"N
53°0'0"N
52°50'0"N

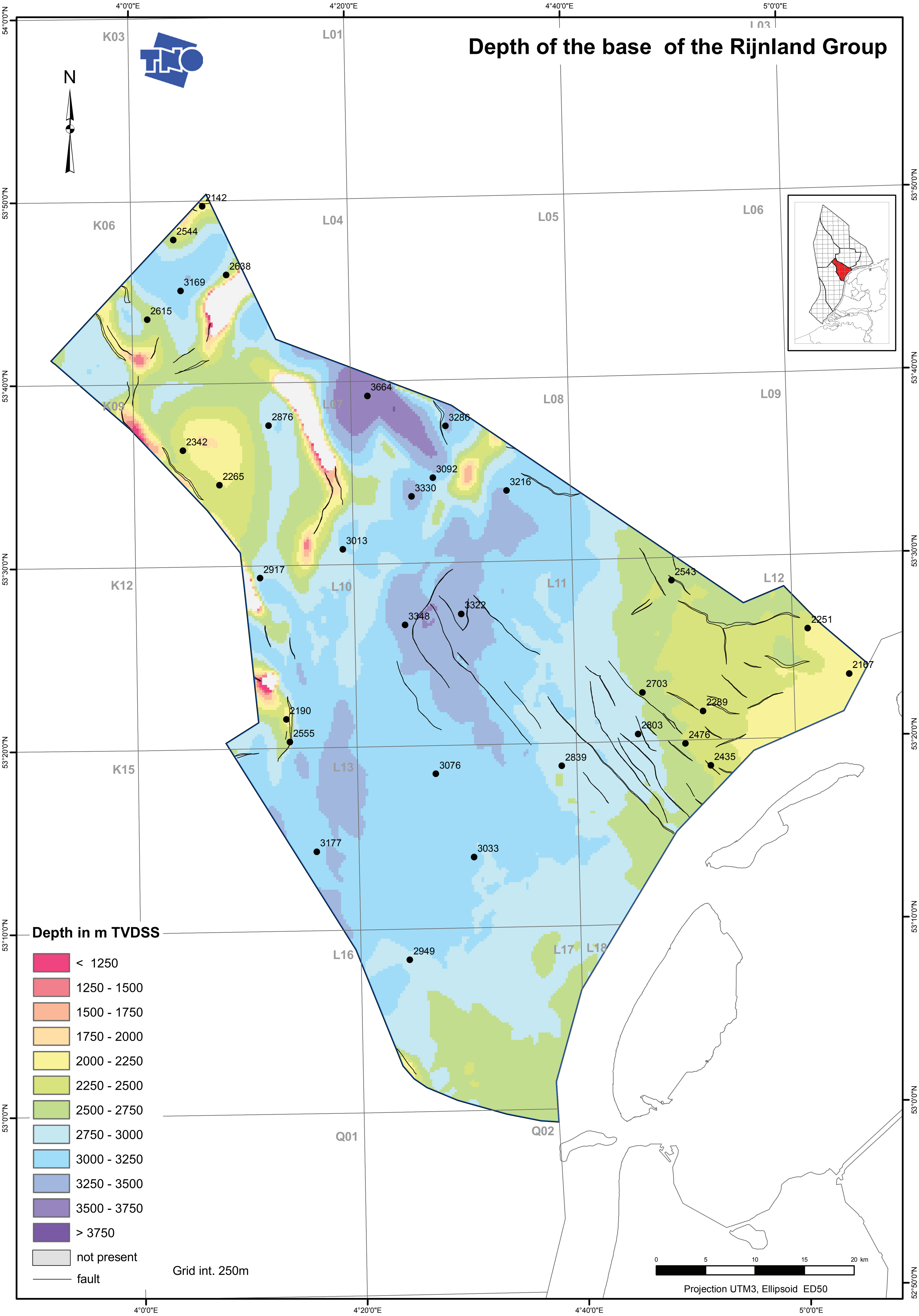
Depth of the base of the Rijnland Group
N
K03
L01
L03
K06
L04
L05
L06
K09
L07
L08
L09
K12
L10
L11
L12
K15
L13
L16
L17
L18
Q01
Q02
2142
2544
2638
3169
2615
3664
2876
3286
2342
2265
3092
3330
3216
3013
2917
2543
3322
3348
2251
2167
2703
2289
2190
2803
2555
2476
2435
2839
3076
3177
3033
2949
Depth in m TVDSS
< 1250
1250 - 1500
1500 - 1750
1750 - 2000
2000 - 2250
2250 - 2500
2500 - 2750
2750 - 3000
3000 - 3250
3250 - 3500
3500 - 3750
> 3750
not present
fault
Grid int. 250m
0
5
10
15
20 km
Projection UTM3, Ellipsoid ED50
4°0'0"E
4°20'0"E
4°40'0"E
5°0'0"E
54°0'0"N
53°50'0"N
53°40'0"N
53°30'0"N
53°20'0"N
53°10'0"N
53°0'0"N
52°50'0"N

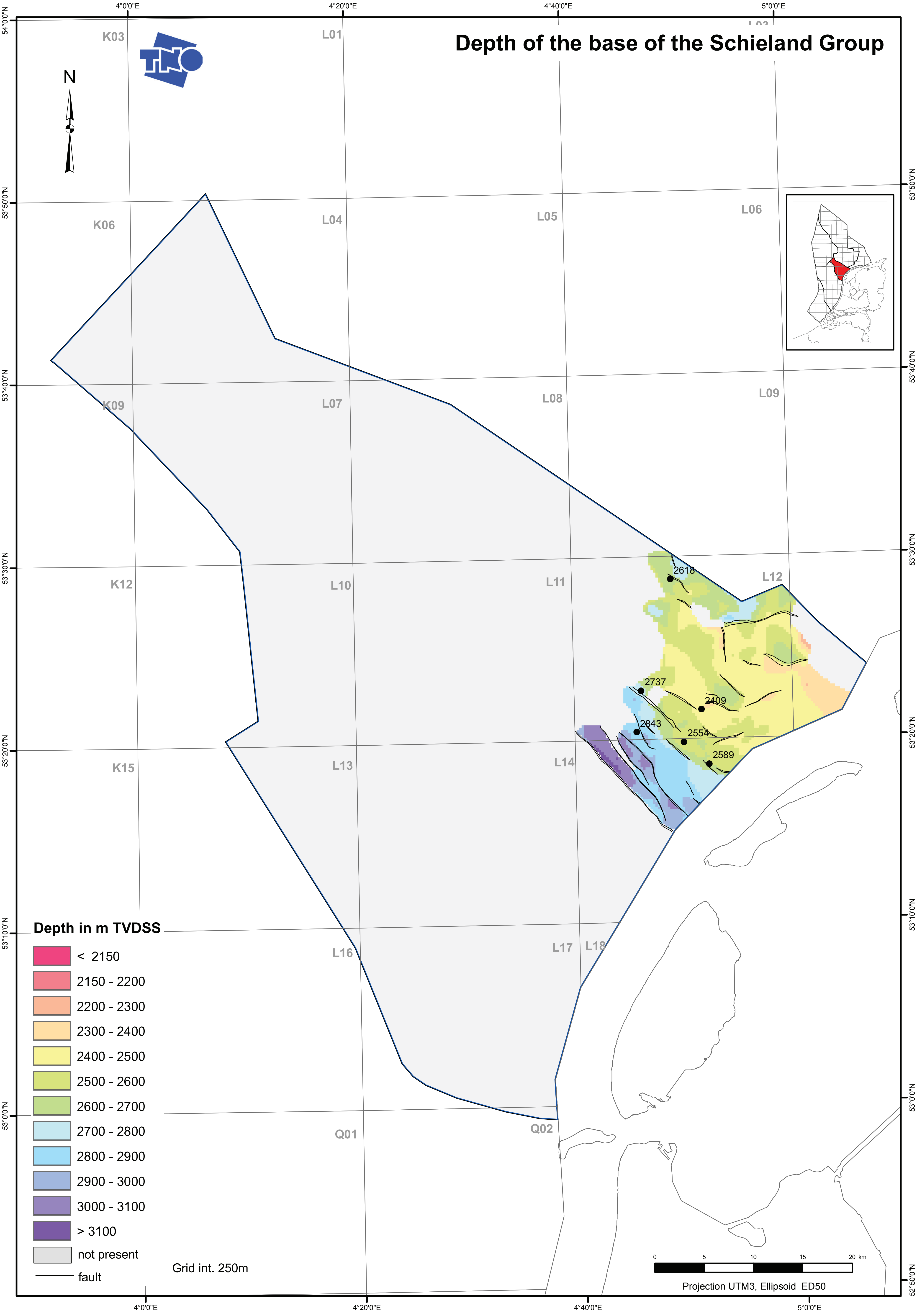

Depth of the base of the Schieland Group
N
K03
L01
K06
L04
L05
L06
K09
L07
L08
L09
K12
L10
L11
L12
K15
L13
L14
L16
L17
L18
Q01
Q02
2618
2737
2409
2843
2554
2589
4°0'0"E
4°20'0"E
4°40'0"E
5°0'0"E
54°0'0"N
53°50'0"N
53°40'0"N
53°30'0"N
53°20'0"N
53°10'0"N
53°0'0"N
52°50'0"N
Depth in m TVDSS
< 2150
2150 - 2200
2200 - 2300
2300 - 2400
2400 - 2500
2500 - 2600
2600 - 2700
2700 - 2800
2800 - 2900
2900 - 3000
3000 - 3100
> 3100
not present
fault
Grid int. 250m
0
5
10
15
20 km
Projection UTM3, Ellipsoid ED50

Depth of the base of the Upper Germanic Trias Group

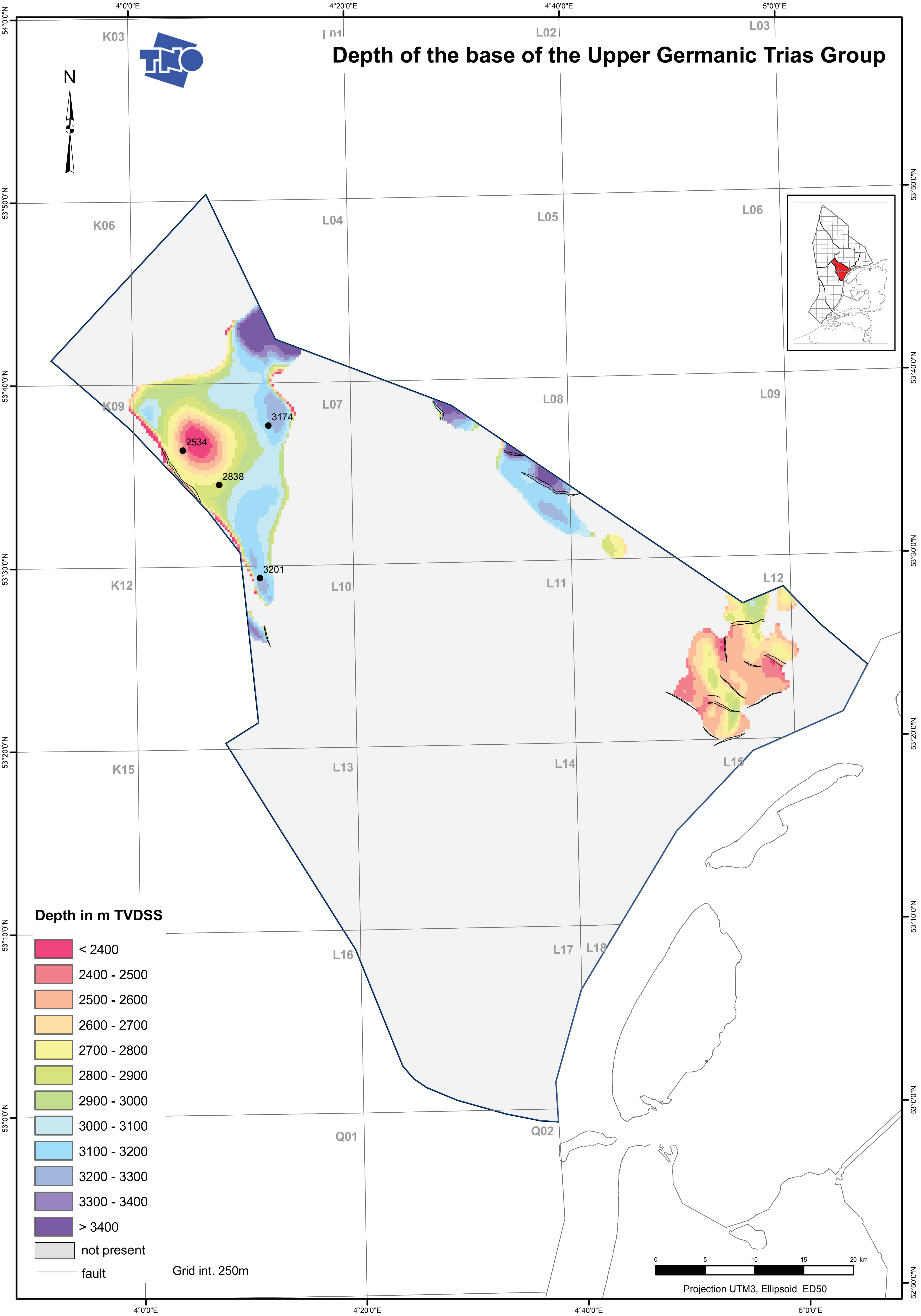

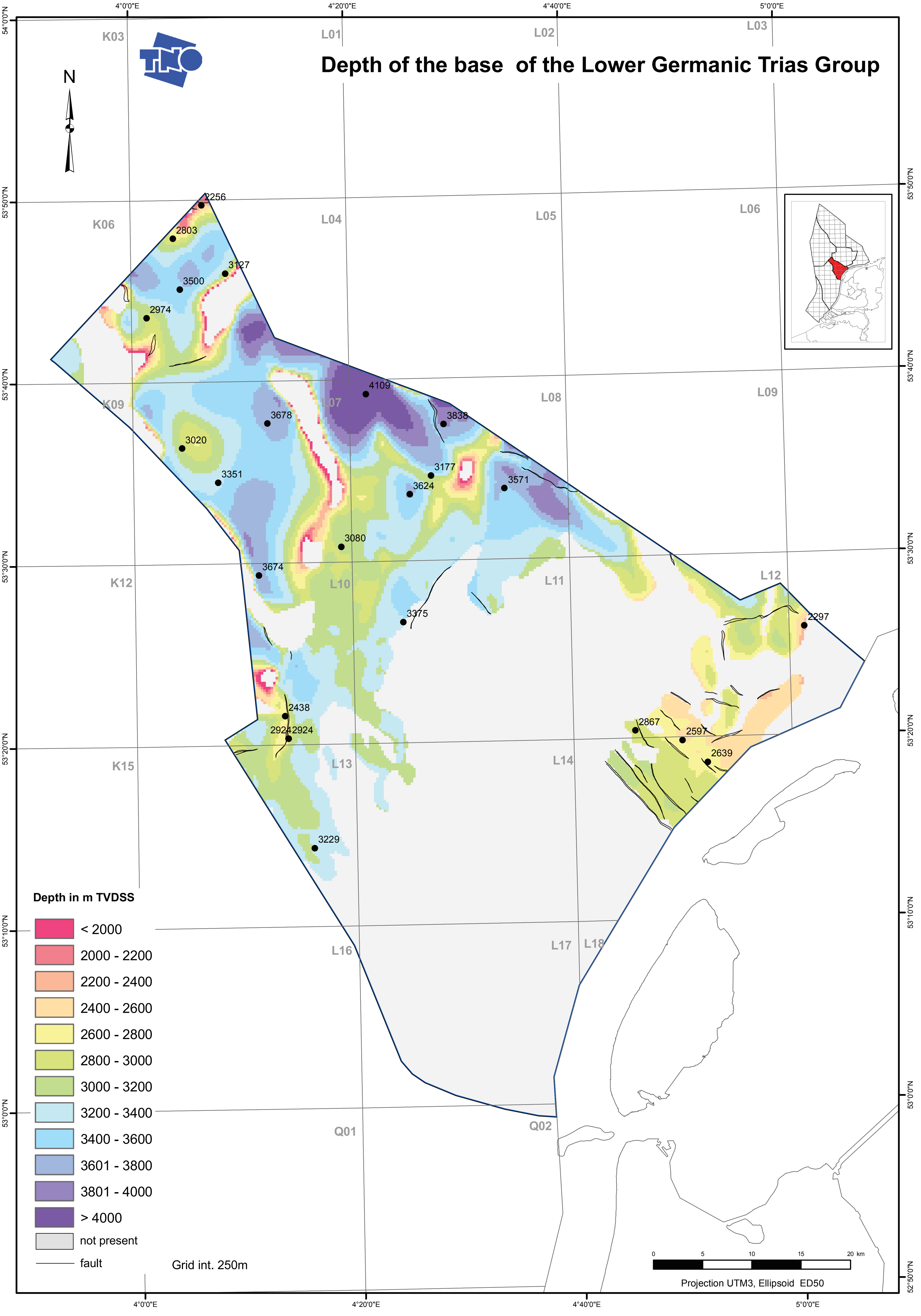
Depth of the base of the Lower Germanic Trias Group
N
K03
L01
L02
L03
K06
L04
L05
L06
K09
L07
L08
L09
K12
L10
L11
L12
K15
L13
L14
L16
L17
L18
Q01
Q02
2256
2803
3127
3500
2974
4109
3678
3838
3020
3177
3624
3571
3351
3080
3674
3375
2297
2438
2924
2924
2867
2597
2639
3229
Depth in m TVDSS
< 2000
2000 - 2200
2200 - 2400
2400 - 2600
2600 - 2800
2800 - 3000
3000 - 3200
3200 - 3400
3400 - 3600
3601 - 3800
3801 - 4000
> 4000
not present
fault
Grid int. 250m
0
5
10
15
20 km
Projection UTM3, Ellipsoid ED50
4°0'0"E
4°20'0"E
4°40'0"E
5°0'0"E
54°0'0"N
53°50'0"N
53°40'0"N
53°30'0"N
53°20'0"N
53°10'0"N
53°0'0"N
52°50'0"N

Depth of the base of the Zechstein Group

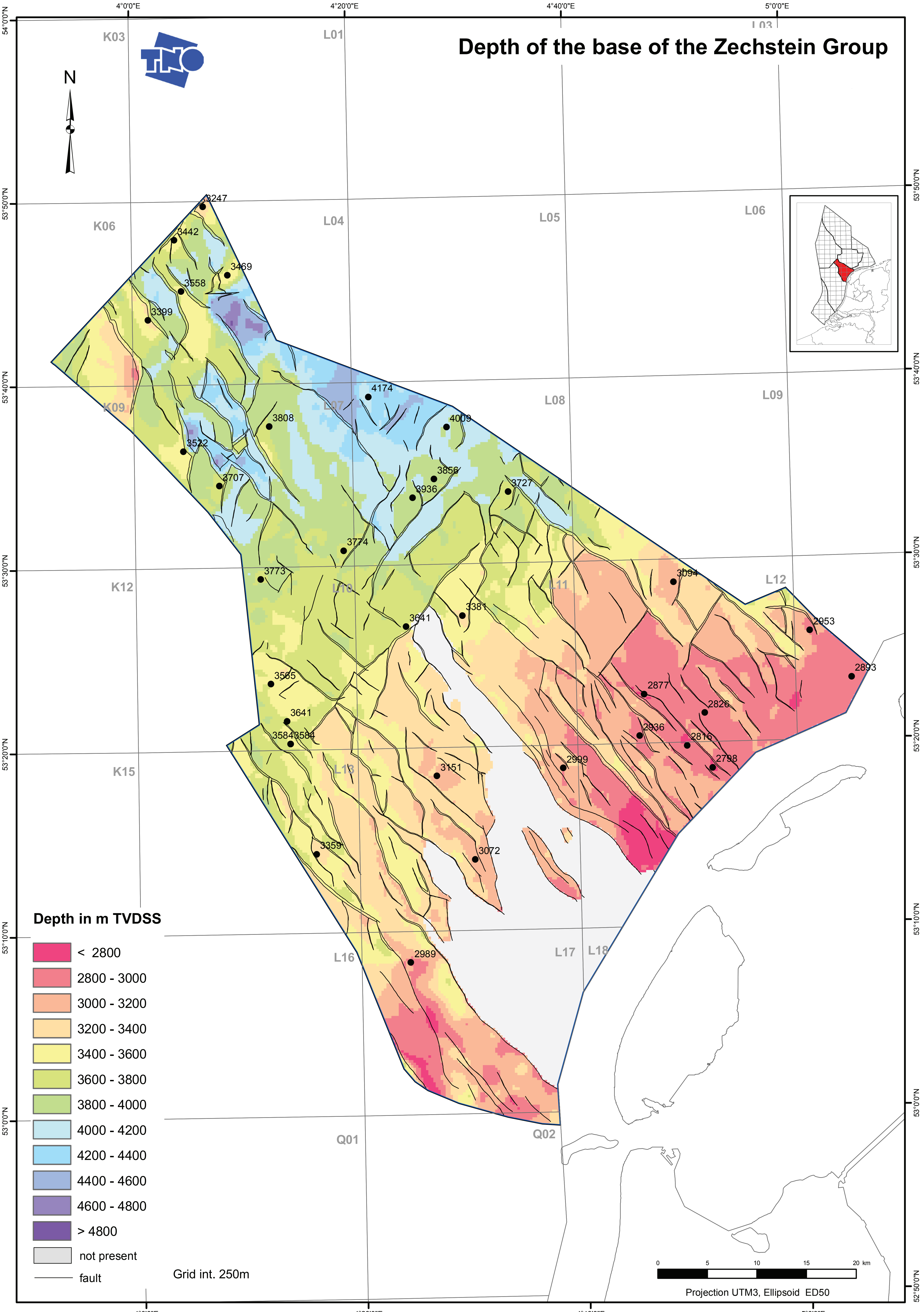

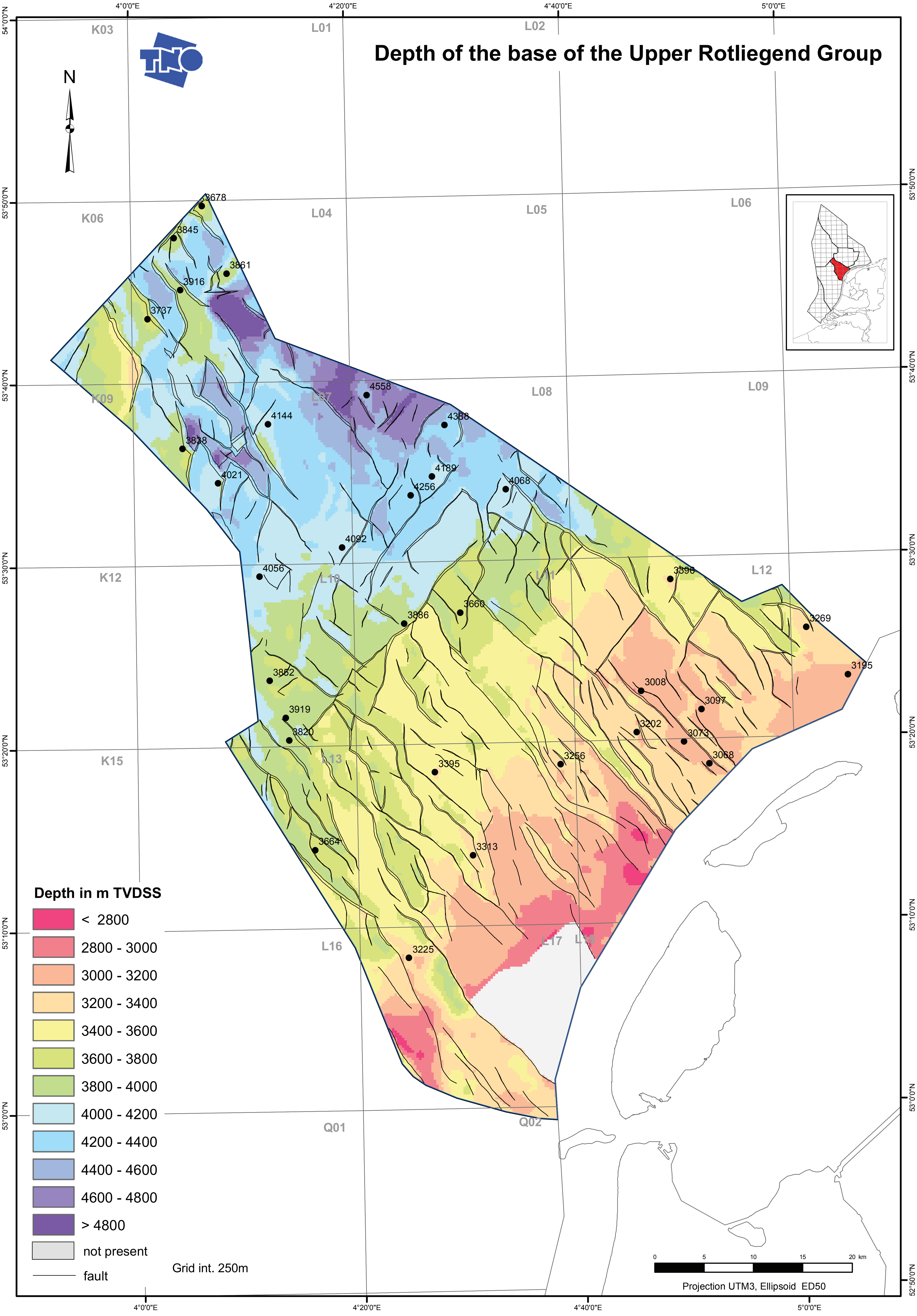
Depth of the base of the Upper Rotliegend Group
N
K03
L01
L02
K06
L04
L05
L06
K09
L07
L08
L09
K12
L10
L11
L12
K15
L13
L16
L17
L18
Q01
Q02
3678
3845
3861
3916
3737
4558
4144
4388
3838
4189
4021
4256
4068
4092
4056
3398
3660
3886
3269
3195
3852
3008
3097
3919
3202
3820
3073
3256
3068
3395
3664
3313
3225
4°0'0"E
4°20'0"E
4°40'0"E
5°0'0"E
54°0'0"N
53°50'0"N
53°40'0"N
53°30'0"N
53°20'0"N
53°10'0"N
53°0'0"N
52°50'0"N
Depth in m TVDSS
< 2800
2800 - 3000
3000 - 3200
3200 - 3400
3400 - 3600
3600 - 3800
3800 - 4000
4000 - 4200
4200 - 4400
4400 - 4600
4600 - 4800
> 4800
not present
fault
Grid int. 250m
0
5
10
15
20 km
Projection UTM3, Ellipsoid ED50

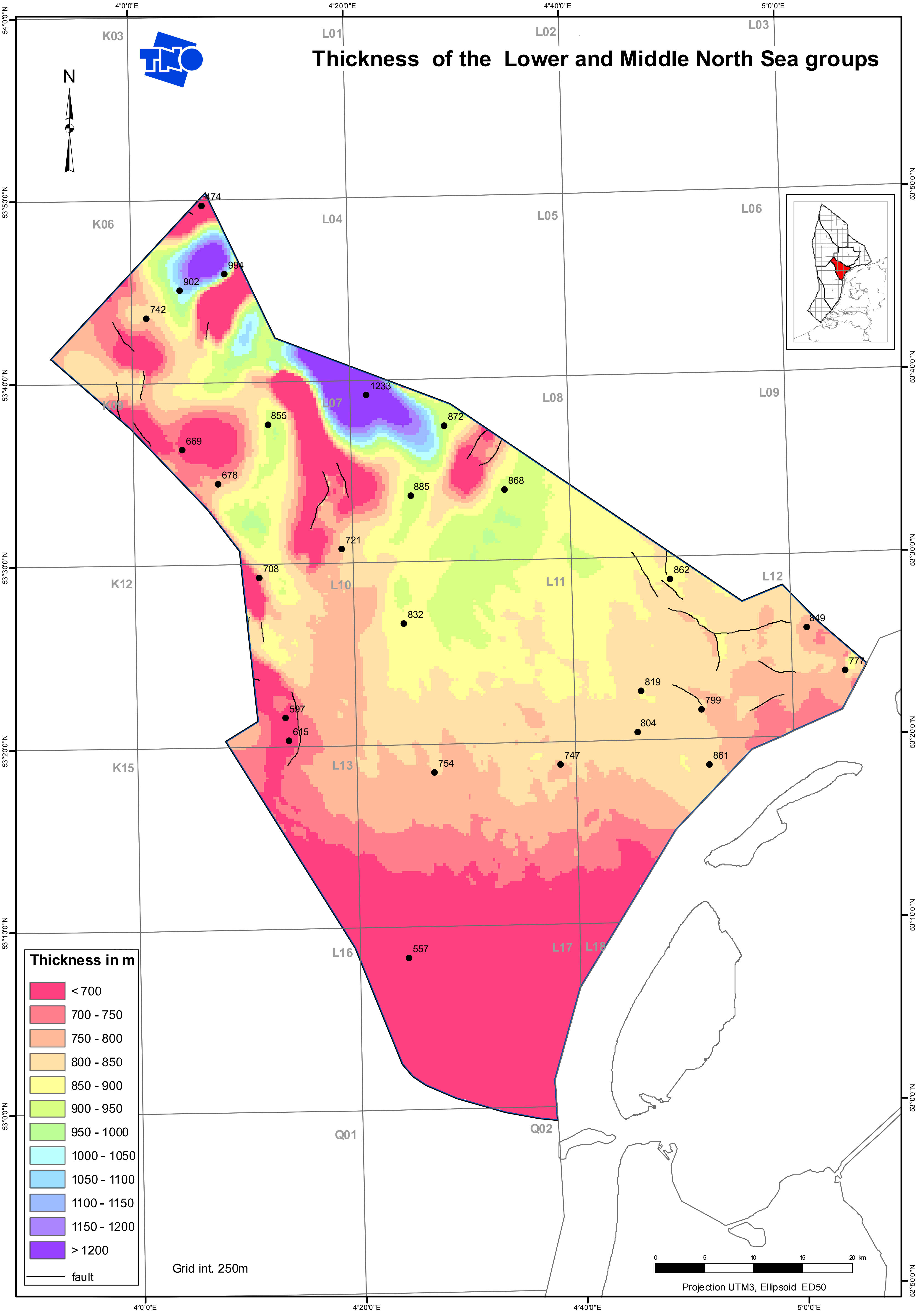
Thickness of the Lower and Middle North Sea groups
N
K03
L01
L02
L03
K06
L04
L05
L06
K09
L07
L08
L09
K12
L10
L11
L12
K15
L13
L16
L17
L18
Q01
Q02
474
994
902
742
1233
855
872
669
678
885
868
721
708
862
832
849
777
819
799
597
615
804
747
754
861
557
4°0'0"E
4°20'0"E
4°40'0"E
5°0'0"E
54°0'0"N
53°50'0"N
53°40'0"N
53°30'0"N
53°20'0"N
53°10'0"N
53°0'0"N
52°50'0"N
Thickness in m
< 700
700 - 750
750 - 800
800 - 850
850 - 900
900 - 950
950 - 1000
1000 - 1050
1050 - 1100
1100 - 1150
1150 - 1200
> 1200
fault
Grid int. 250m
0
5
10
15
20 km
Projection UTM3, Ellipsoid ED50

Annex C2

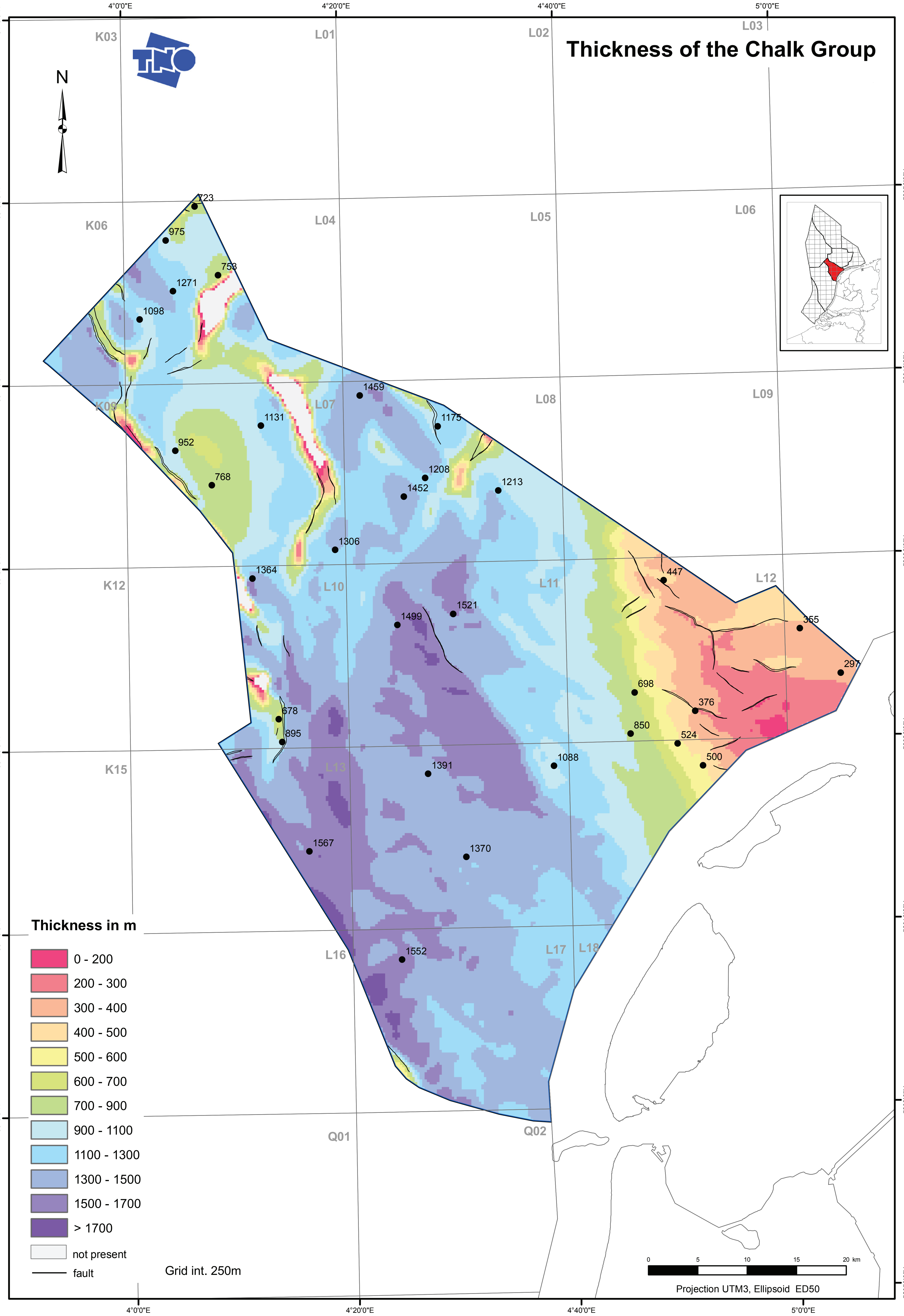

Thickness of the Chalk Group
N
4°0'0"E
4°20'0"E
4°40'0"E
5°0'0"E
54°0'0"N
53°50'0"N
53°40'0"N
53°30'0"N
53°20'0"N
53°10'0"N
53°0'0"N
52°50'0"N
K03
L01
L02
L03
K06
L04
L05
L06
K09
L07
L08
L09
K12
L10
L11
L12
K15
L13
L16
L17
L18
Q01
Q02
723
975
758
1271
1098
1459
1131
1175
952
1208
768
1452
1213
1306
1364
447
1521
1499
355
297
698
376
678
895
850
524
1088
500
1391
1567
1370
1552
Thickness in m
0 - 200
200 - 300
300 - 400
400 - 500
500 - 600
600 - 700
700 - 900
900 - 1100
1100 - 1300
1300 - 1500
1500 - 1700
> 1700
not present
fault
Grid int. 250m
0
5
10
15
20 km
Projection UTM3, Ellipsoid ED50

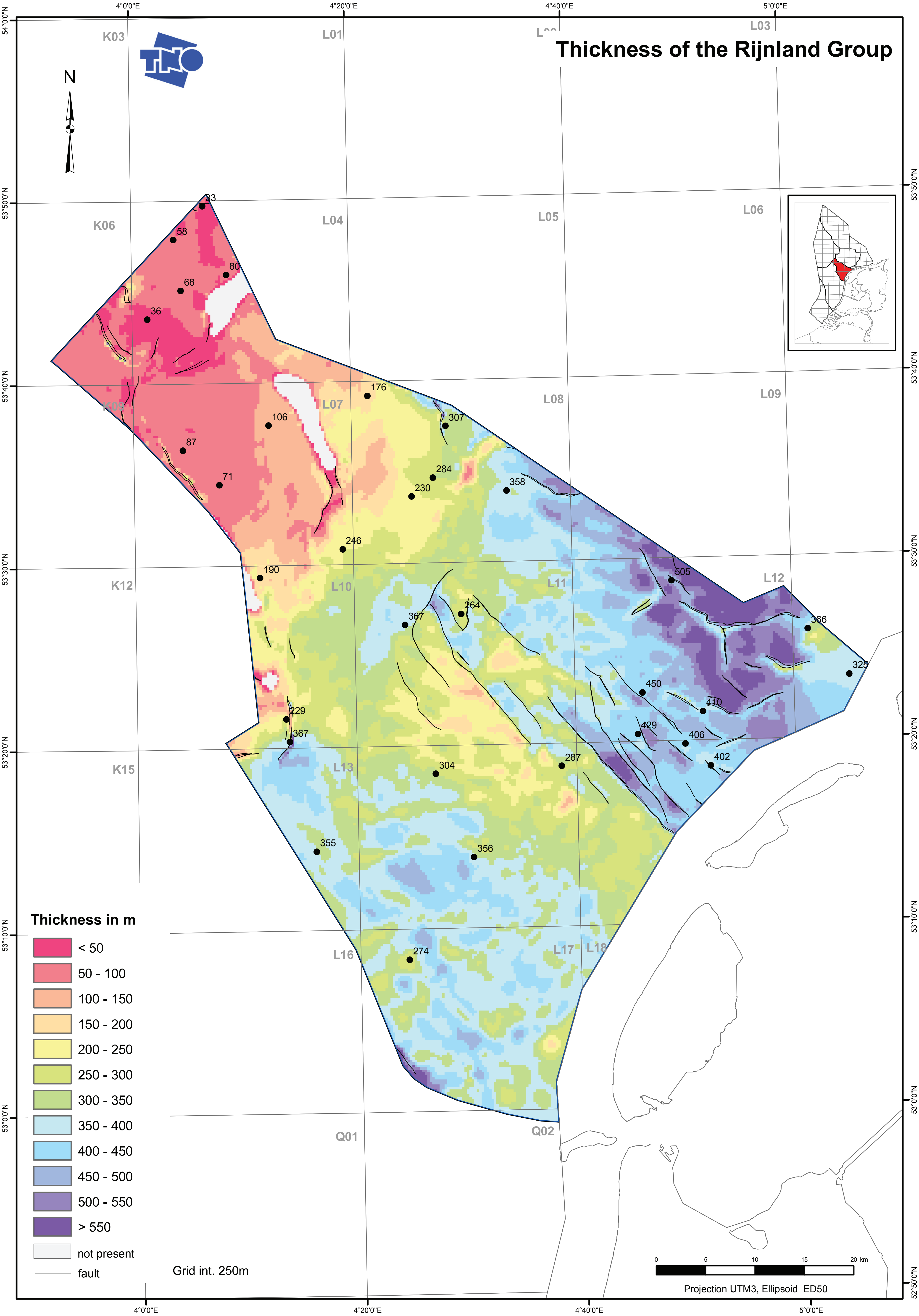
Thickness of the Rijnland Group
4°0'0"E
4°20'0"E
4°40'0"E
5°0'0"E
54°0'0"N
53°50'0"N
53°40'0"N
53°30'0"N
53°20'0"N
53°10'0"N
53°0'0"N
52°50'0"N
N
K03
L01
L03
K06
L04
L05
L06
K09
L07
L08
L09
K12
L10
L11
L12
K15
L13
L16
L17
L18
Q01
Q02
33
58
80
68
36
176
106
307
87
284
71
230
358
246
190
505
264
367
366
325
450
410
229
429
367
406
287
304
402
355
356
274
Thickness in m
< 50
50 - 100
100 - 150
150 - 200
200 - 250
250 - 300
300 - 350
350 - 400
400 - 450
450 - 500
500 - 550
> 550
not present
fault
Grid int. 250m
0
5
10
15
20 km
Projection UTM3, Ellipsoid ED50

Annex C4

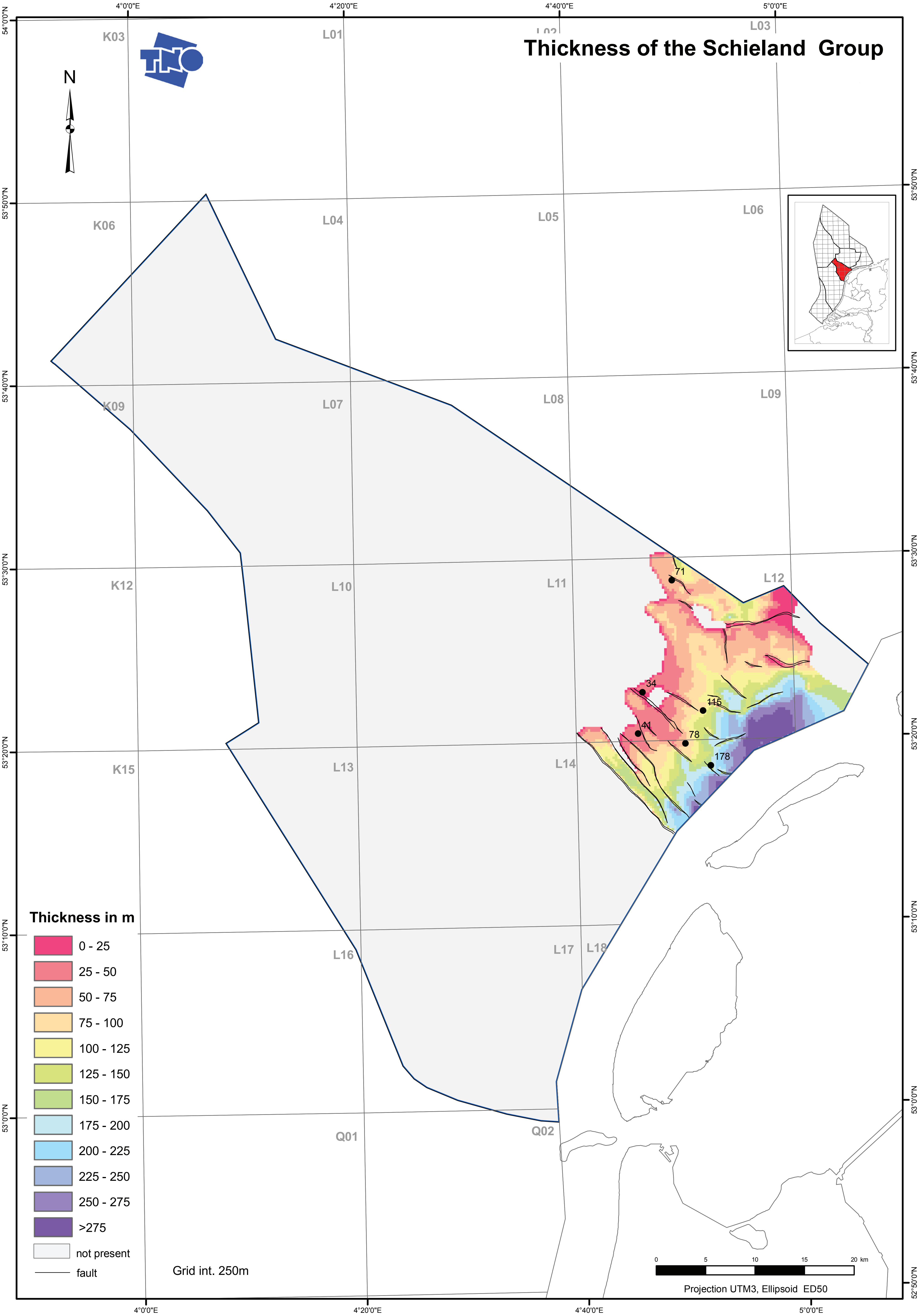

Thickness of the Schieland Group
Thickness in m
0 - 25
25 - 50
50 - 75
75 - 100
100 - 125
125 - 150
150 - 175
175 - 200
200 - 225
225 - 250
250 - 275
>275
not present
fault
Grid int. 250m
Projection UTM3, Ellipsoid ED50
0
5
10
15
20 km
N
K03
L01
L02
L03
K06
L04
L05
L06
K09
L07
L08
L09
K12
L10
L11
L12
K15
L13
L14
L16
L17
L18
Q01
Q02
71
34
115
41
78
178
4°0'0"E
4°20'0"E
4°40'0"E
5°0'0"E
54°0'0"N
53°50'0"N
53°40'0"N
53°30'0"N
53°20'0"N
53°10'0"N
53°0'0"N
52°50'0"N

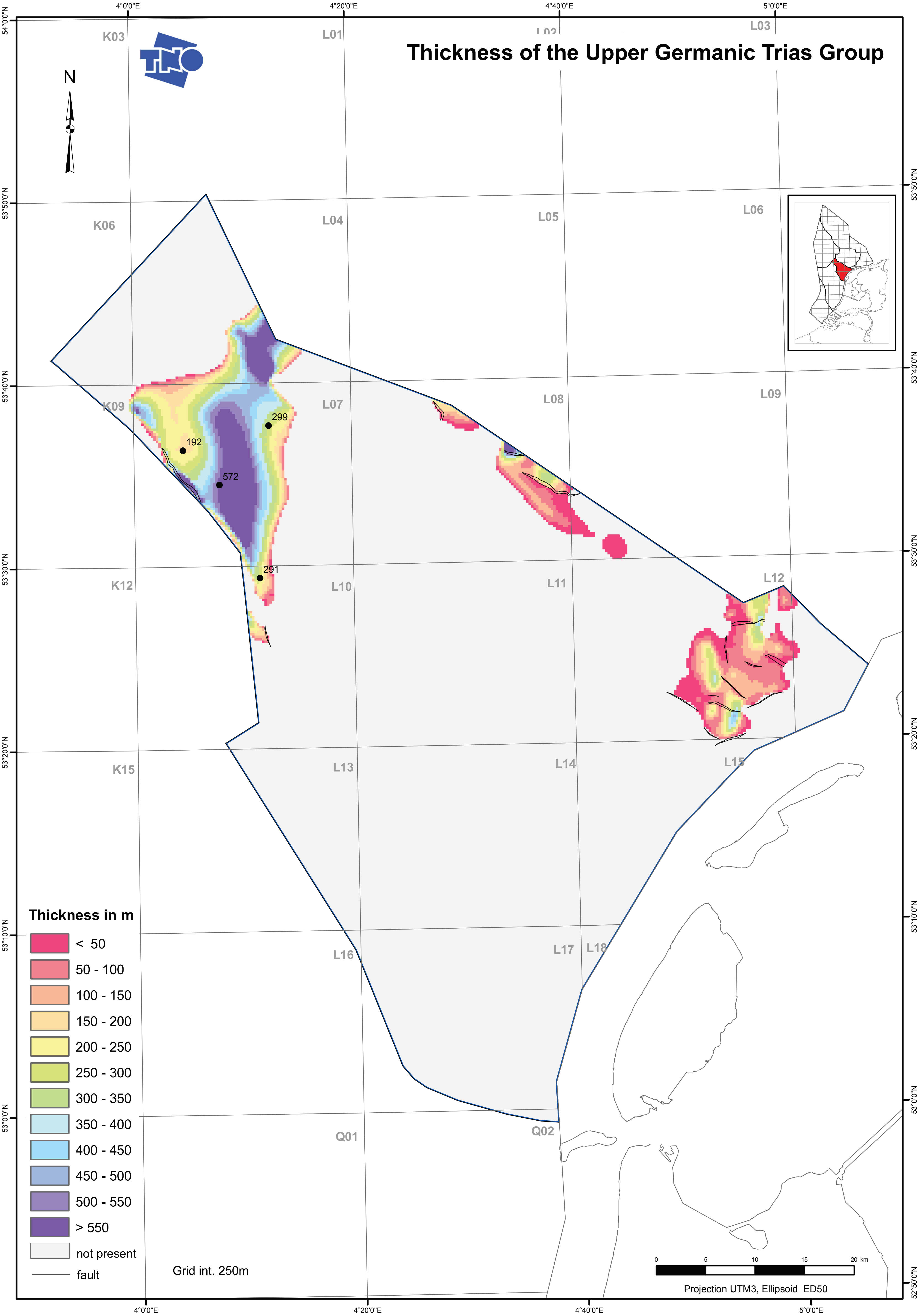
Thickness of the Upper Germanic Trias Group
N
4°0'0"E
4°20'0"E
4°40'0"E
5°0'0"E
54°0'0"N
53°50'0"N
53°40'0"N
53°30'0"N
53°20'0"N
53°10'0"N
53°0'0"N
52°50'0"N
K03
L01
L02
L03
K06
L04
L05
L06
K09
L07
L08
L09
K12
L10
L11
L12
K15
L13
L14
L15
L16
L17
L18
Q01
Q02
192
299
572
291
Thickness in m
< 50
50 - 100
100 - 150
150 - 200
200 - 250
250 - 300
300 - 350
350 - 400
400 - 450
450 - 500
500 - 550
> 550
not present
fault
Grid int. 250m
0
5
10
15
20 km
Projection UTM3, Ellipsoid ED50

Thickness of the Lower Germanic Trias Group

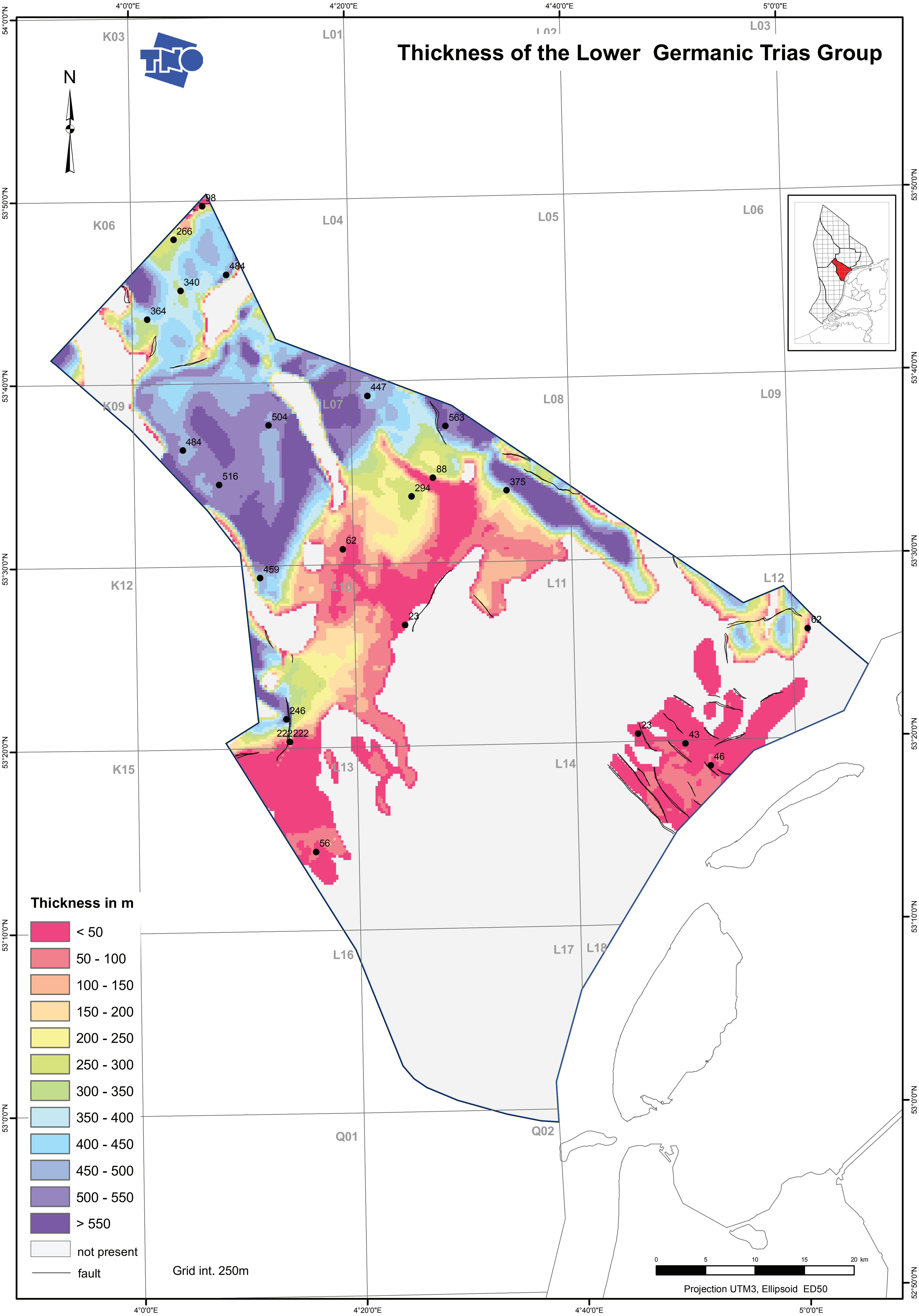

Annex C7

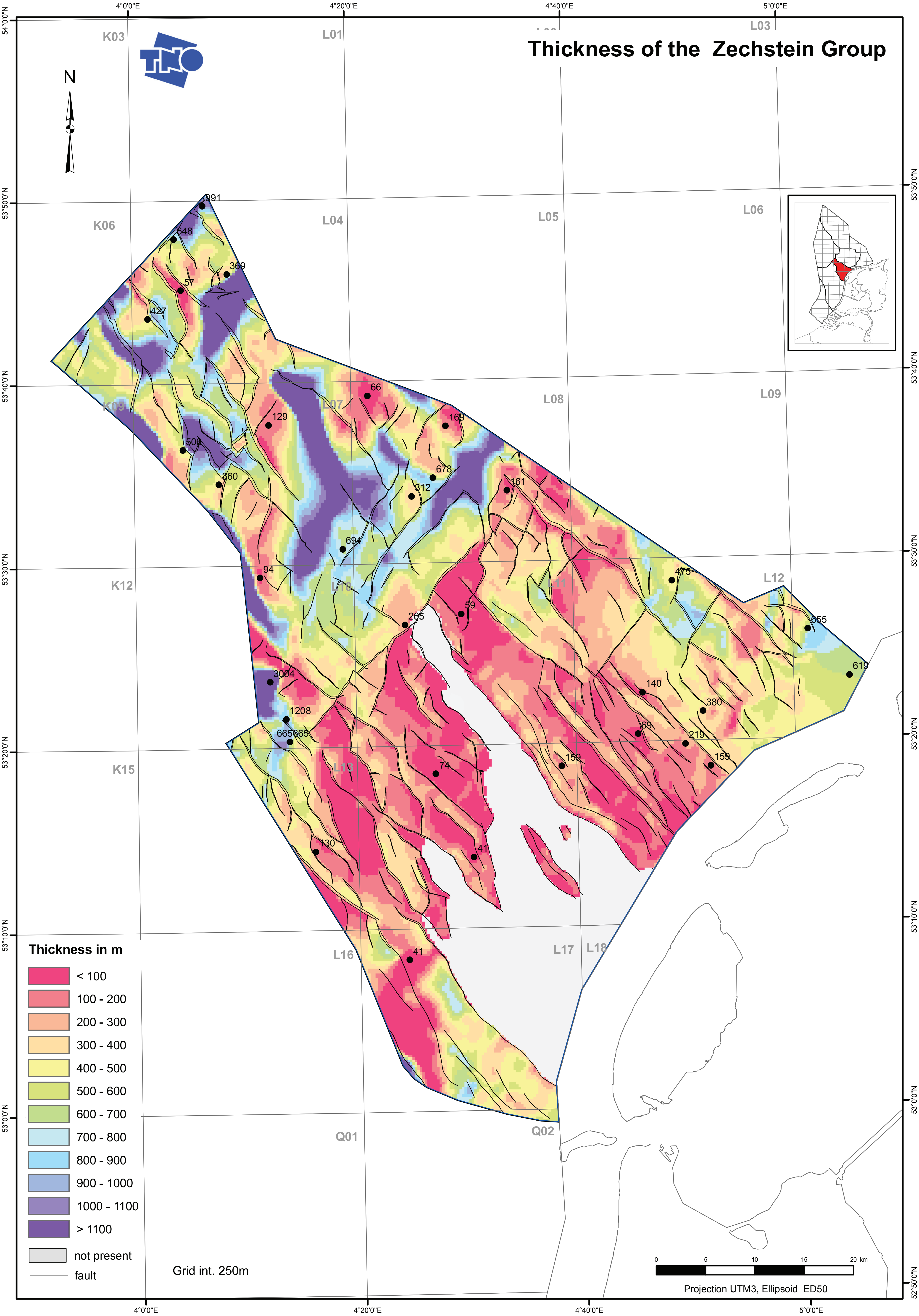
Thickness of the Zechstein Group
N
K03
L01
L03
K06
L04
L05
L06
K09
L07
L08
L09
K12
L10
L11
L12
K15
L13
L16
L17
L18
Q01
Q02
991
648
369
57
427
66
129
169
508
678
360
312
161
694
94
475
59
265
655
619
3004
140
380
1208
665665
69
219
159
159
74
130
41
41
4°0'0"E
4°20'0"E
4°40'0"E
5°0'0"E
54°0'0"N
53°50'0"N
53°40'0"N
53°30'0"N
53°20'0"N
53°10'0"N
53°0'0"N
52°50'0"N
Thickness in m
< 100
100 - 200
200 - 300
300 - 400
400 - 500
500 - 600
600 - 700
700 - 800
800 - 900
900 - 1000
1000 - 1100
> 1100
not present
fault
Grid int. 250m
0
5
10
15
20 km
Projection UTM3, Ellipsoid ED50

Annex C8

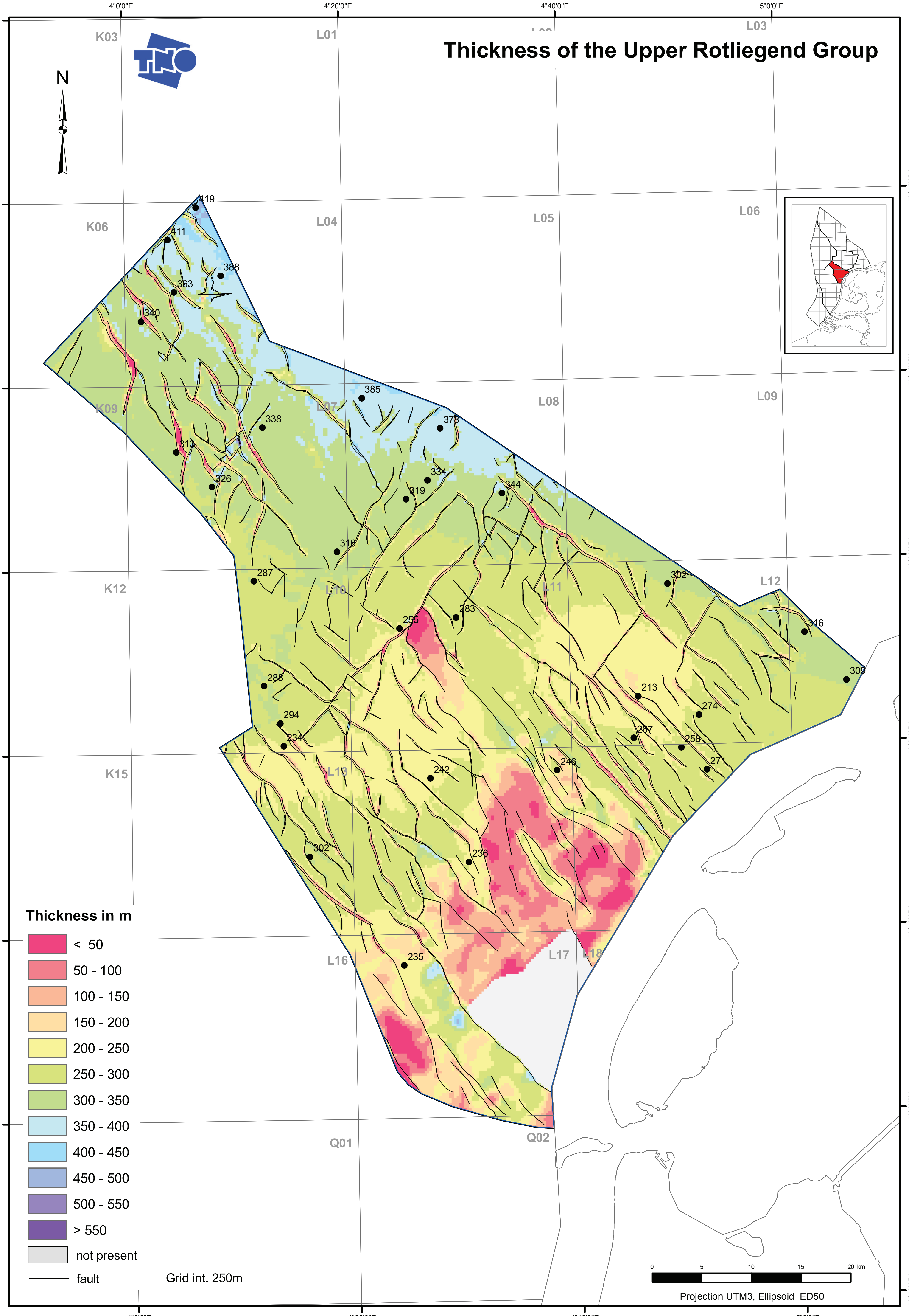

Thickness of the Upper Rotliegend Group
N
Thickness in m
< 50
50 - 100
100 - 150
150 - 200
200 - 250
250 - 300
300 - 350
350 - 400
400 - 450
450 - 500
500 - 550
> 550
not present
fault
Grid int. 250m
Projection UTM3, Ellipsoid ED50
K03
L01
L03
K06
L04
L05
L06
K09
L07
L08
L09
K12
L10
L11
L12
K15
L13
L16
L17
L18
Q01
Q02
4°0'0"E
4°20'0"E
4°40'0"E
5°0'0"E
54°0'0"N
53°50'0"N
53°40'0"N
53°30'0"N
53°20'0"N
53°10'0"N
53°0'0"N
52°50'0"N

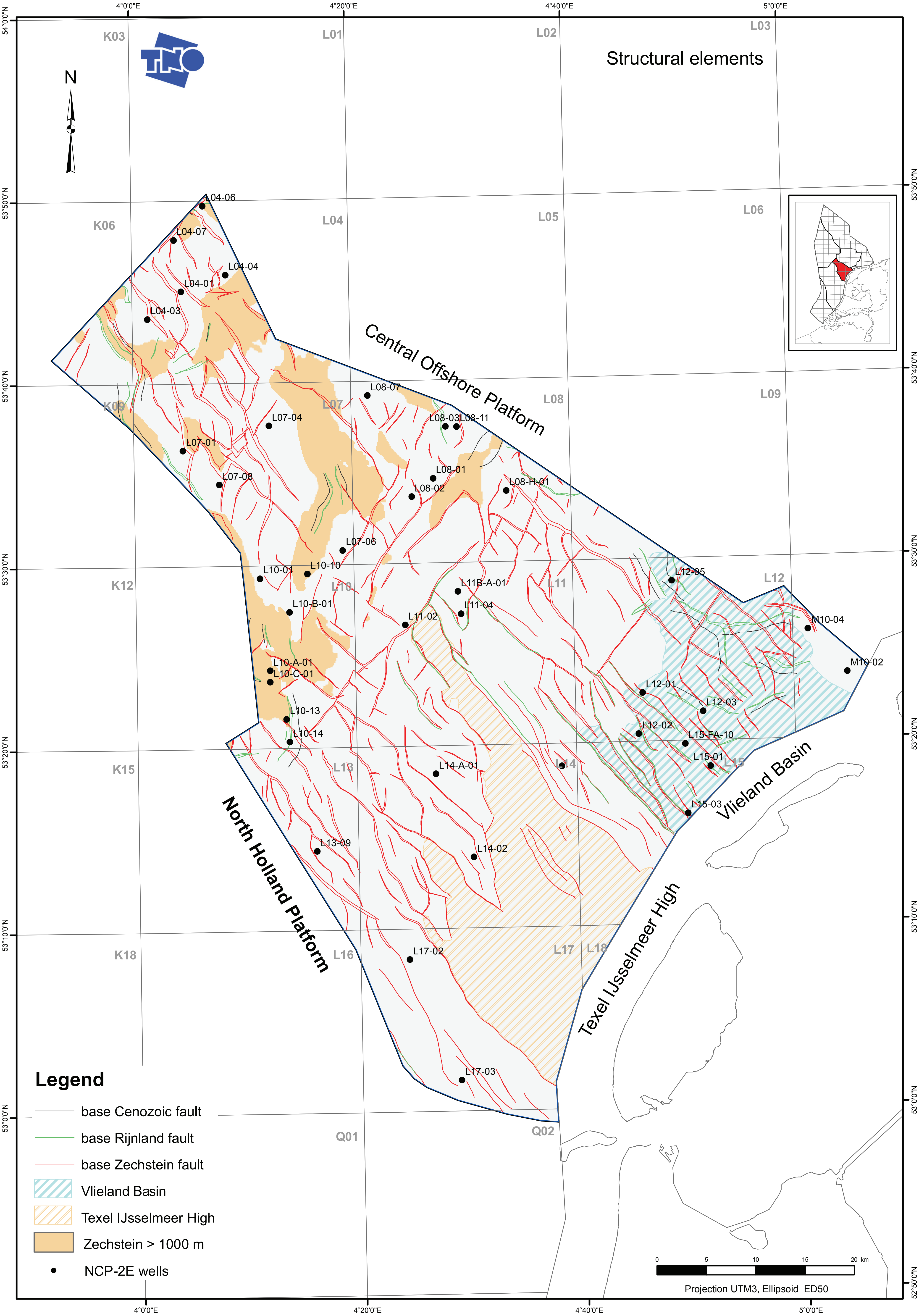

Structural elements
N
Central Offshore Platform
North Holland Platform
Texel IJsselmeer High
Vlieland Basin
K03
L01
L02
L03
K06
L04
L05
L06
K09
L07
L08
L09
K12
L10
L11
L12
K15
L13
L14
L15
K18
L16
L17
L18
Q01
Q02
L04-06
L04-07
L04-04
L04-01
L04-03
L08-07
L07-04
L08-03
L08-11
L07-01
L08-01
L07-08
L08-02
L08-H-01
L07-06
L10-01
L10-10
L12-05
L11B-A-01
L10-B-01
L11-04
L11-02
M10-04
L10-A-01
L10-C-01
M10-02
L12-01
L12-03
L10-13
L12-02
L10-14
L15-FA-10
L15-01
L14-A-01
L15-03
L13-09
L14-02
L17-02
L17-03
4°0'0"E
4°20'0"E
4°40'0"E
5°0'0"E
54°0'0"N
53°50'0"N
53°40'0"N
53°30'0"N
53°20'0"N
53°10'0"N
53°0'0"N
52°50'0"N
Legend
base Cenozoic fault
base Rijnland fault
base Zechstein fault
Vlieland Basin
Texel IJsselmeer High
Zechstein > 1000 m
NCP-2E wells
0
5
10
15
20 km
Projection UTM3, Ellipsoid ED50

Annex E

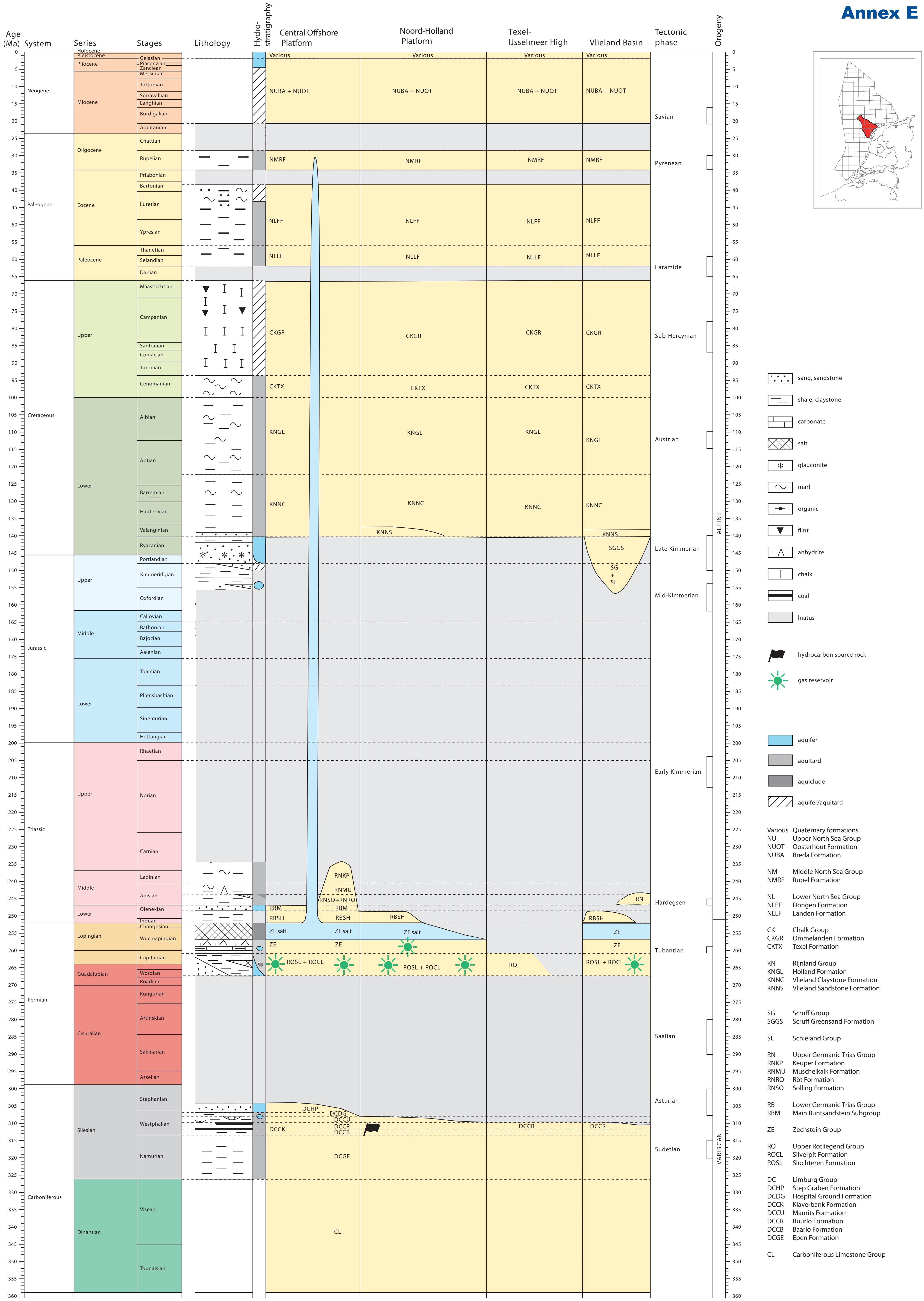

Tectono-stratigraphic chart of the Central Offshore Platform, Noord-Holland Platform, Texel-IJsselmeer High and Vlieland Basin. Time scale according to Gradstein et al. (2004).

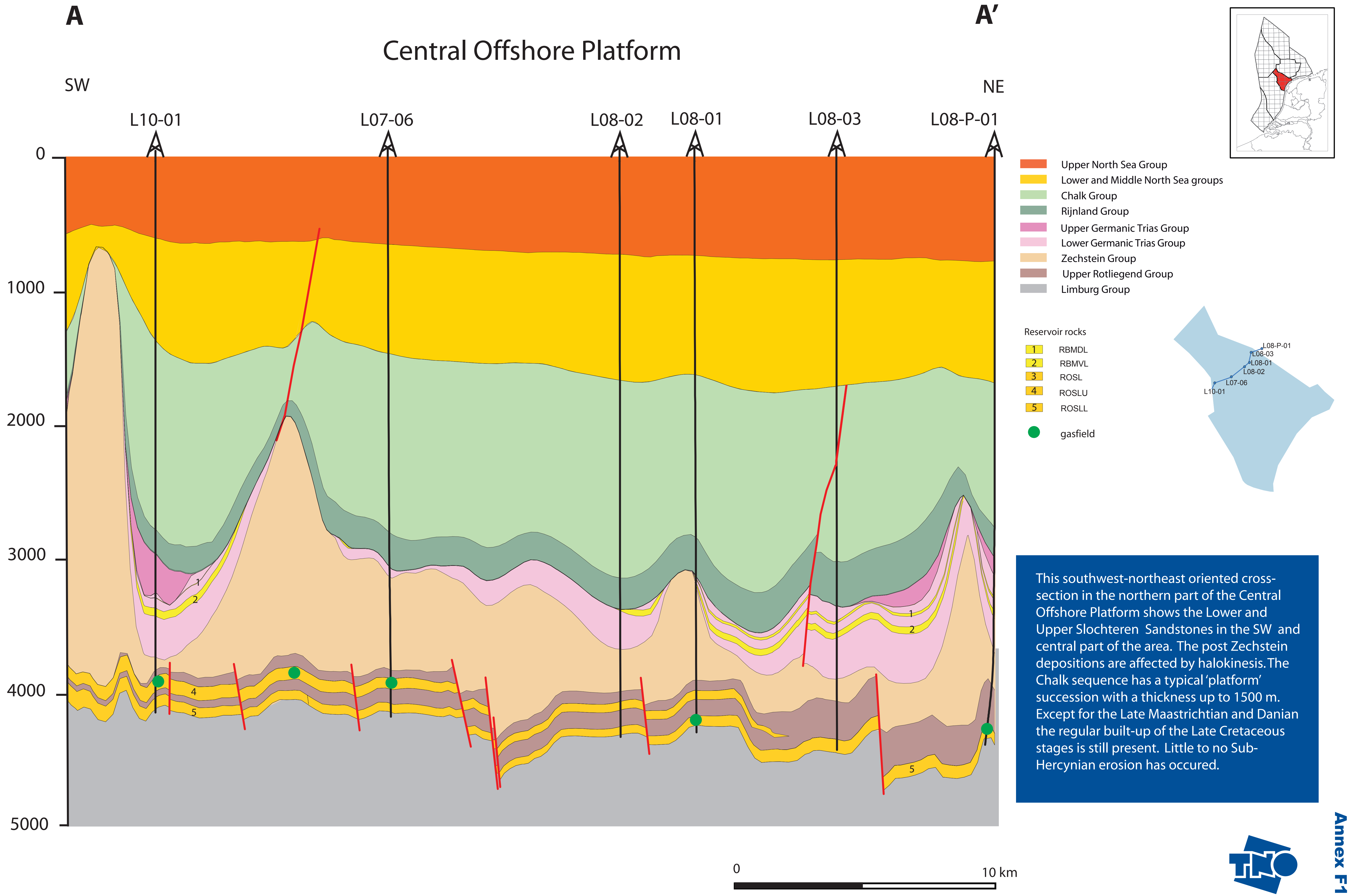

This southwest-northeast oriented cross-section in the northern part of the Central Offshore Platform shows the Lower and Upper Slochteren Sandstones in the SW and central part of the area. The post Zechstein depositions are affected by halokinesis. The Chalk sequence has a typical 'platform' succession with a thickness up to 1500 m. Except for the Late Maastrichtian and Danian the regular built-up of the Late Cretaceous stages is still present. Little to no Sub-Hercynian erosion has occured.

Annex F1

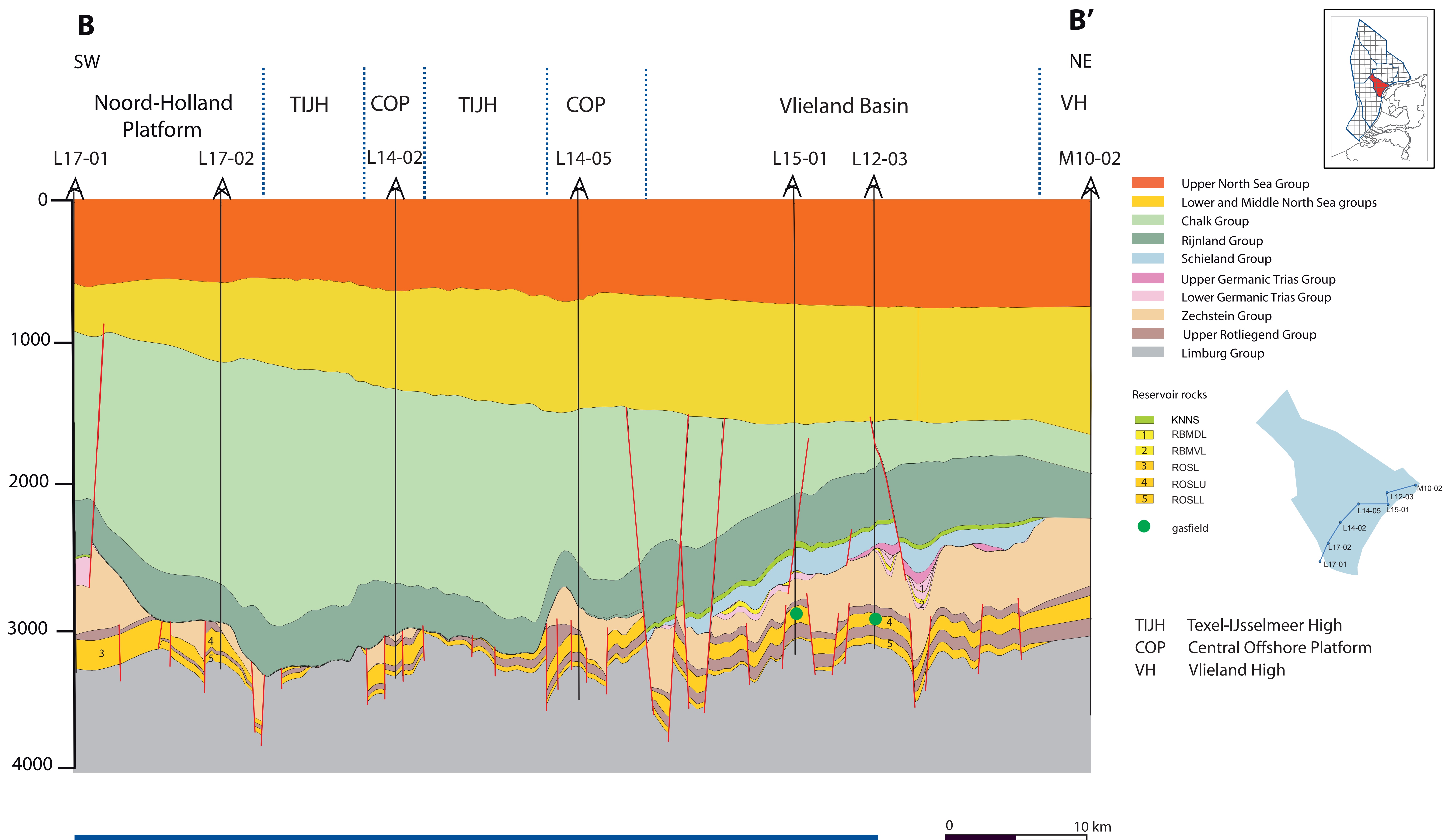

This southwest-northeast cross-section in the southern part of the area shows a differentiated stratigraphic succession. The Texel-IJsselmeer High typically has no Zechstein and locally no Rotliegend present. The platform areas are characterized by thin or absent Triassic deposits. A very thick Chalk sequence has been deposited with most stages present. In the Vlieland Basin however, the Upper Jurassic sediments have been preserved and are overlain by the Lower Cretaceous Friesland Member. The Chalk deposits have been affected by Sub-Hercynian erosion. There's a slight increase in thickness from the southwest to the northeast of the Tertiary are Quaternary deposits.

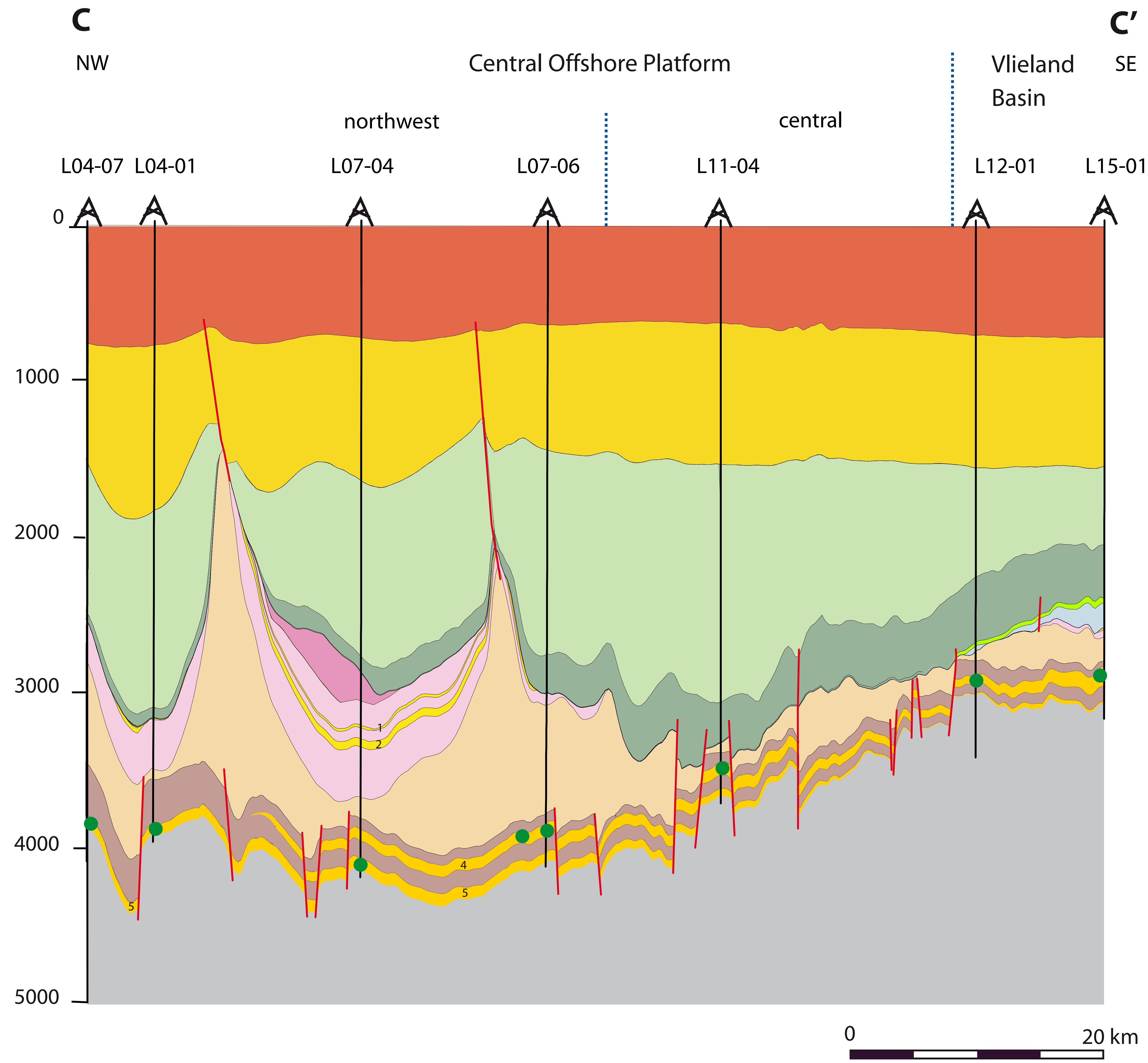

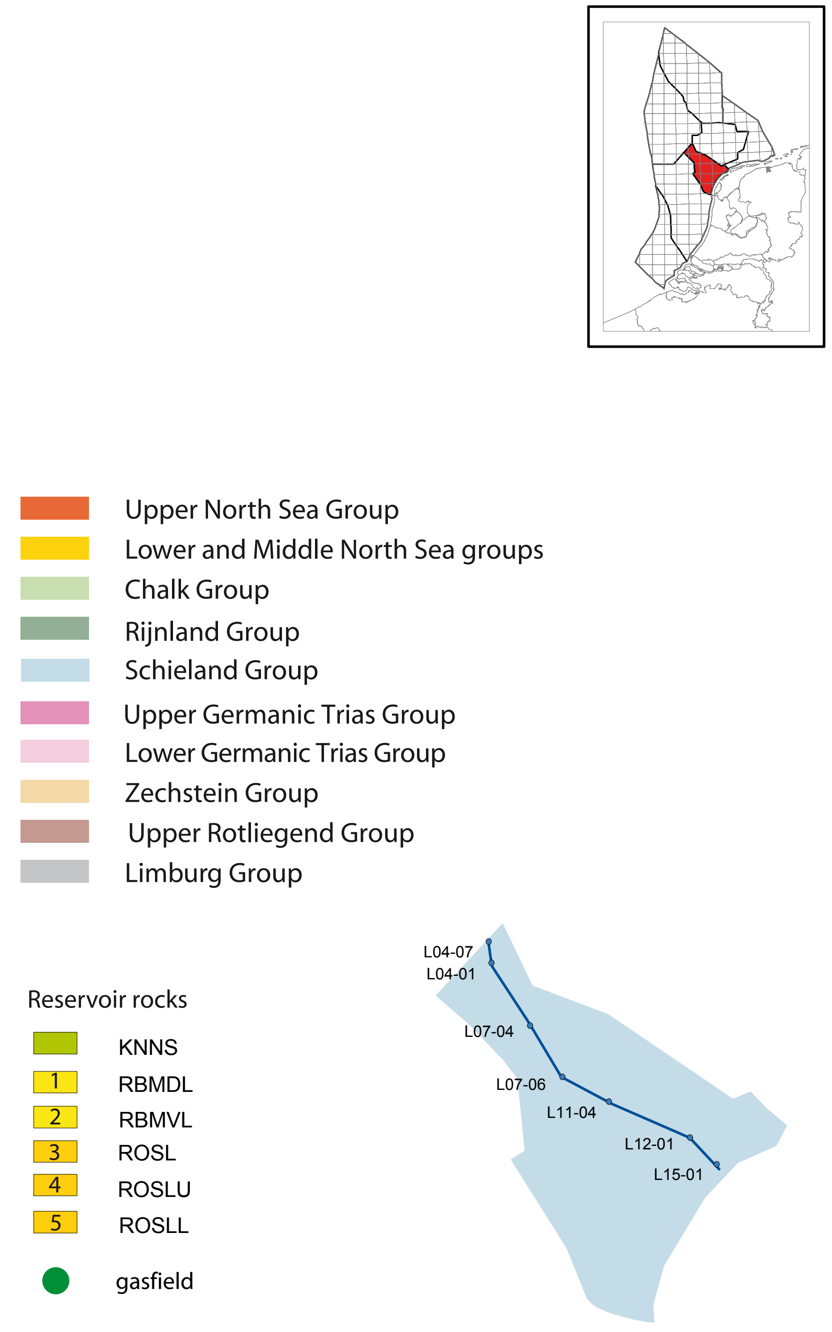

This cross-section shows the pinch-out of the Upper Slochteren Sandstone in northernly direction. Halokinese has affected the post-Permian strata in the northwestern part of the Central Offshore Platform. In the depletion areas Triassic sediments with the Lower Volpriehausen and Lower Detfurth sandstones have been preserved though they are not gas bearing in this area due to salt sealing. In the Vlieland Basin Upper Jurassic and Lower Cretaceous rocks rest on a remnant of the Lower Germanic Trias Group. The Friesland Member is a non-producing reservoir rock in this area.

Playbacks

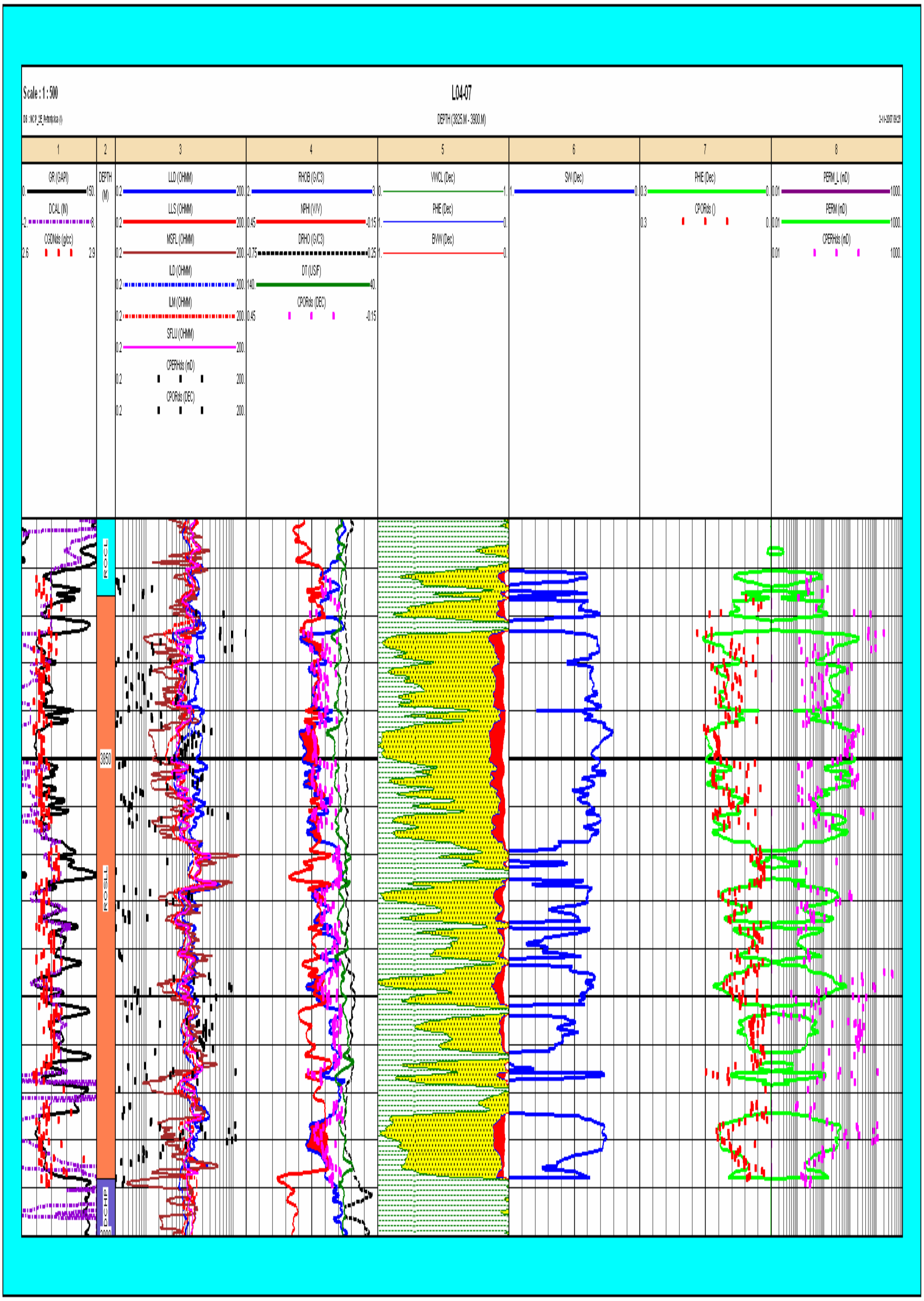

Playback 1 Petrophysical analysis Lower Slochteren Sandstone L04-07

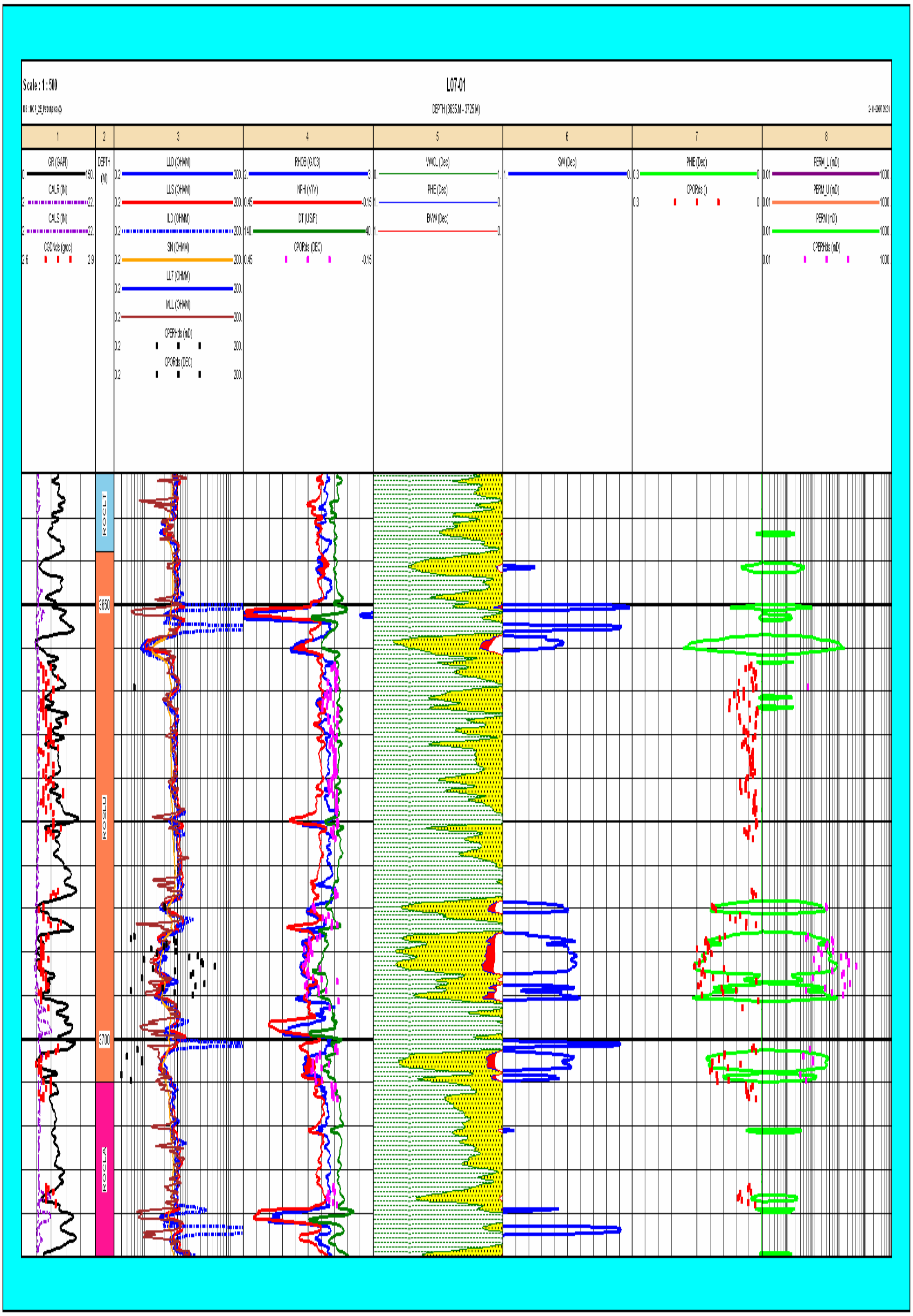

Playback 2a Petrophysical analysis Upper Slochteren Sandstone L07-01

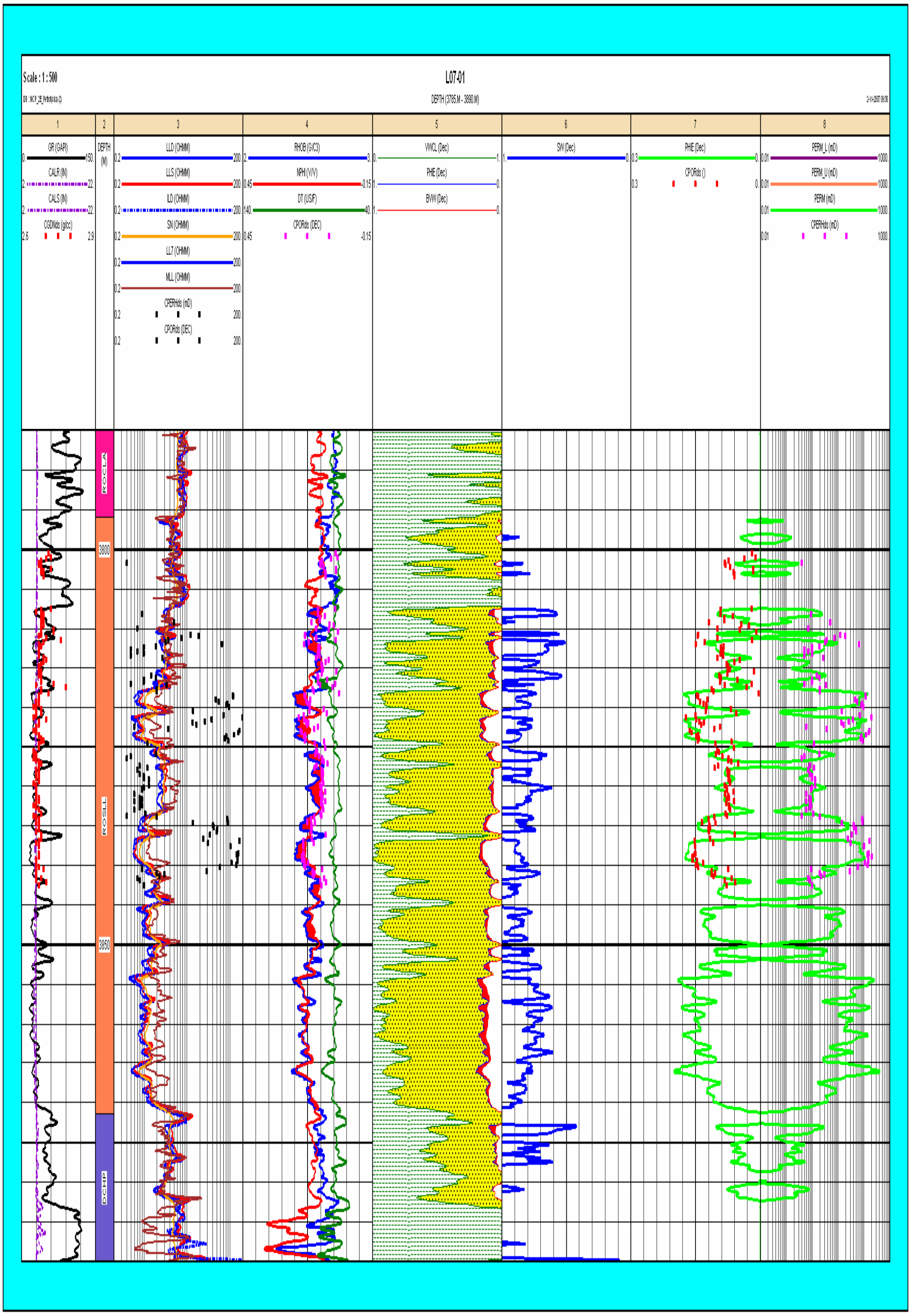

Playback 2b Petrophysical analysis Lower Slochteren Sandstone L07-01

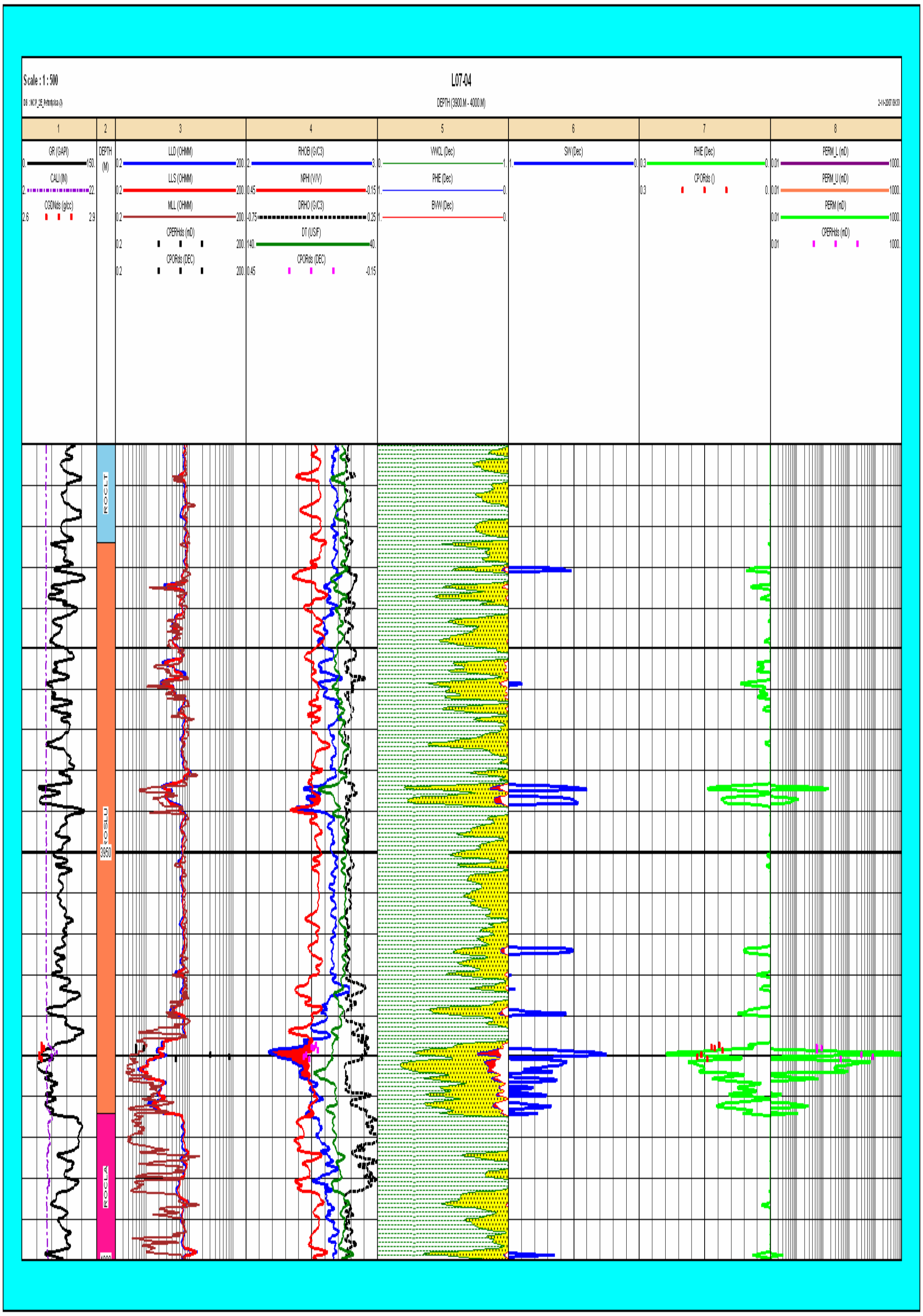

Playback 3a Petrophysical analysis Upper Slochteren Sandstone L07-04

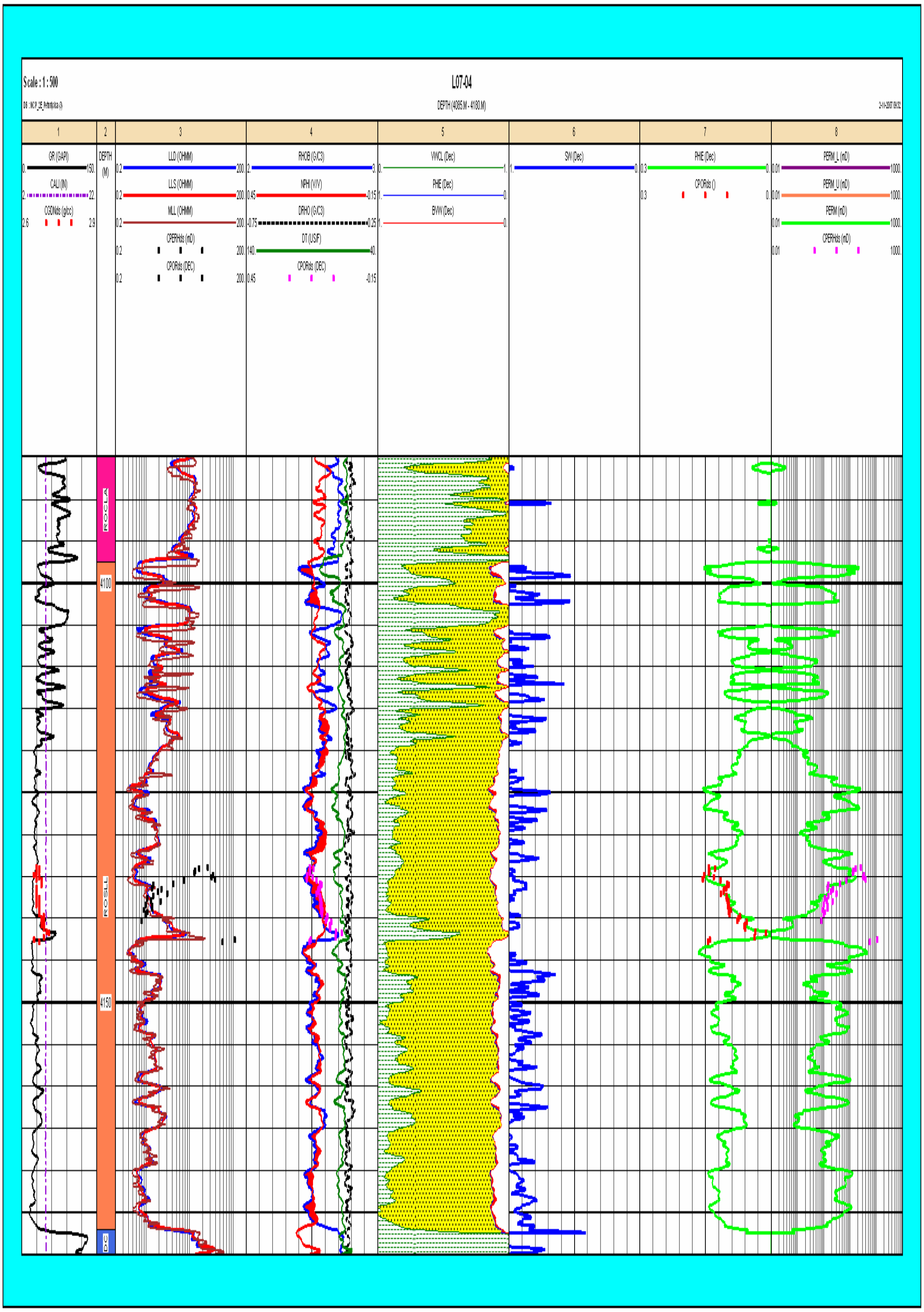

Playback 3b Petrophysical analysis Lower Slochteren Sandstone L07-04

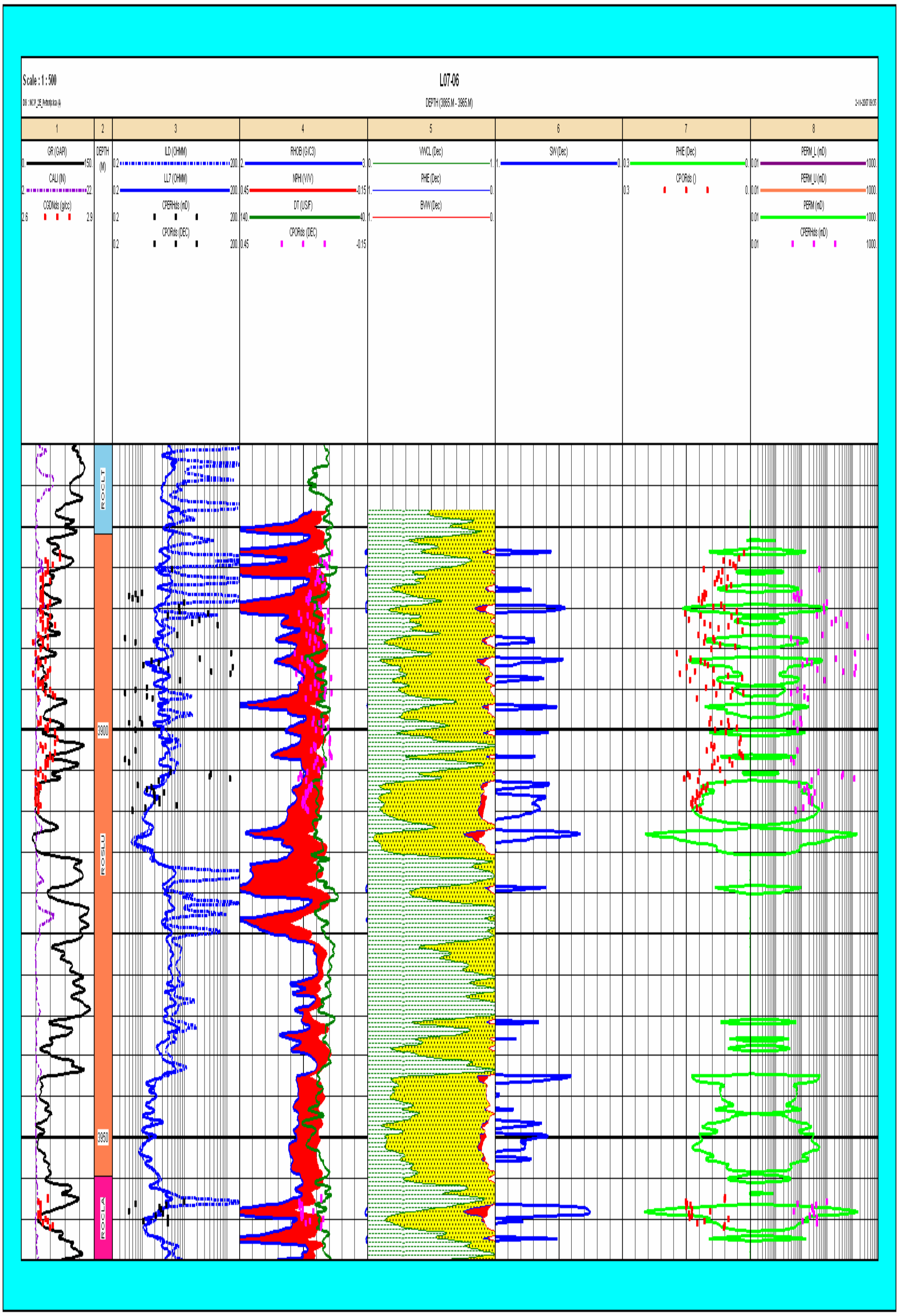

Playback 4a Petrophysical analysis Upper Slochteren Sandstone L07-06

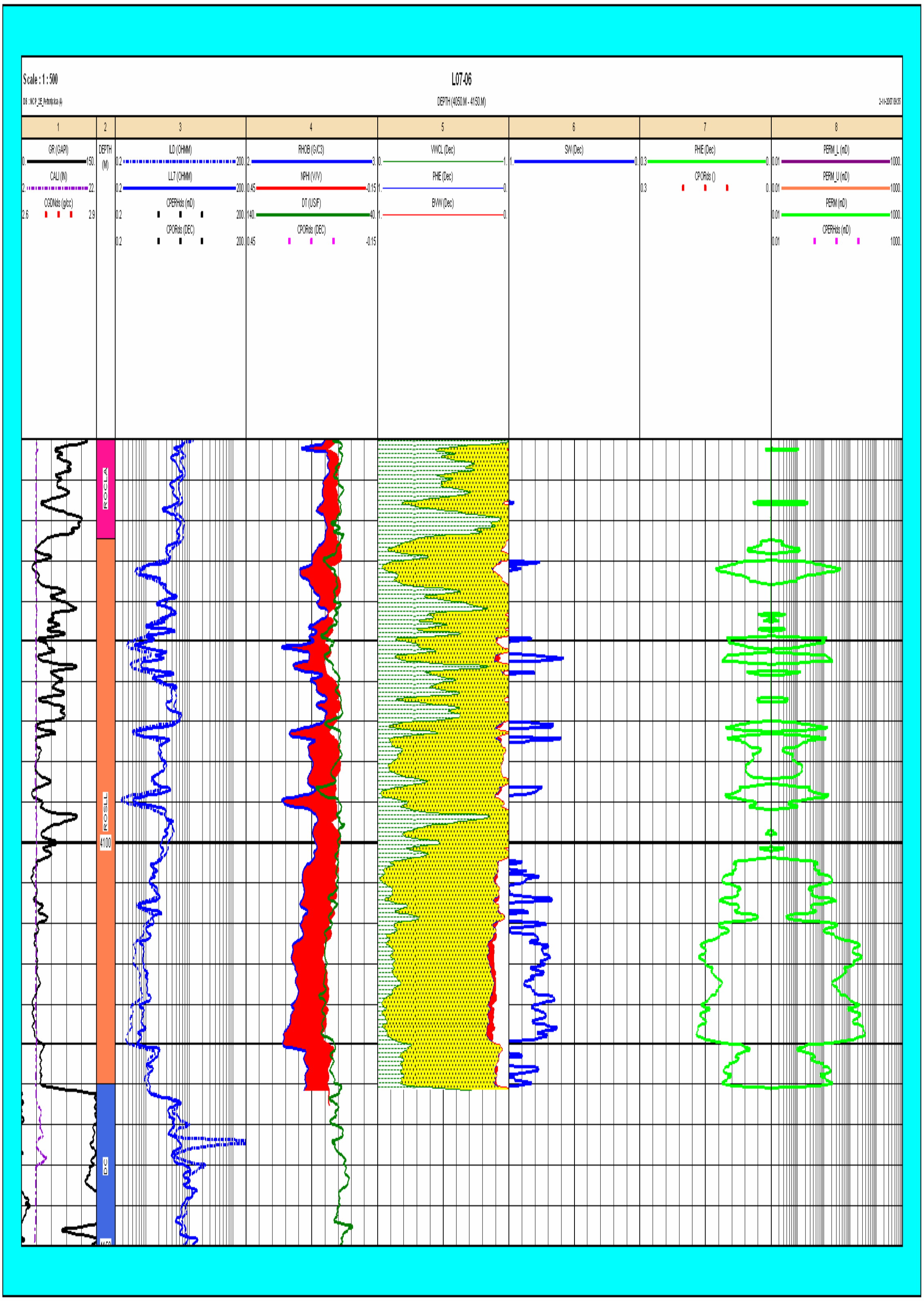

Playback 4b Petrophysical analysis Lower Slochteren Sandstone L07-06

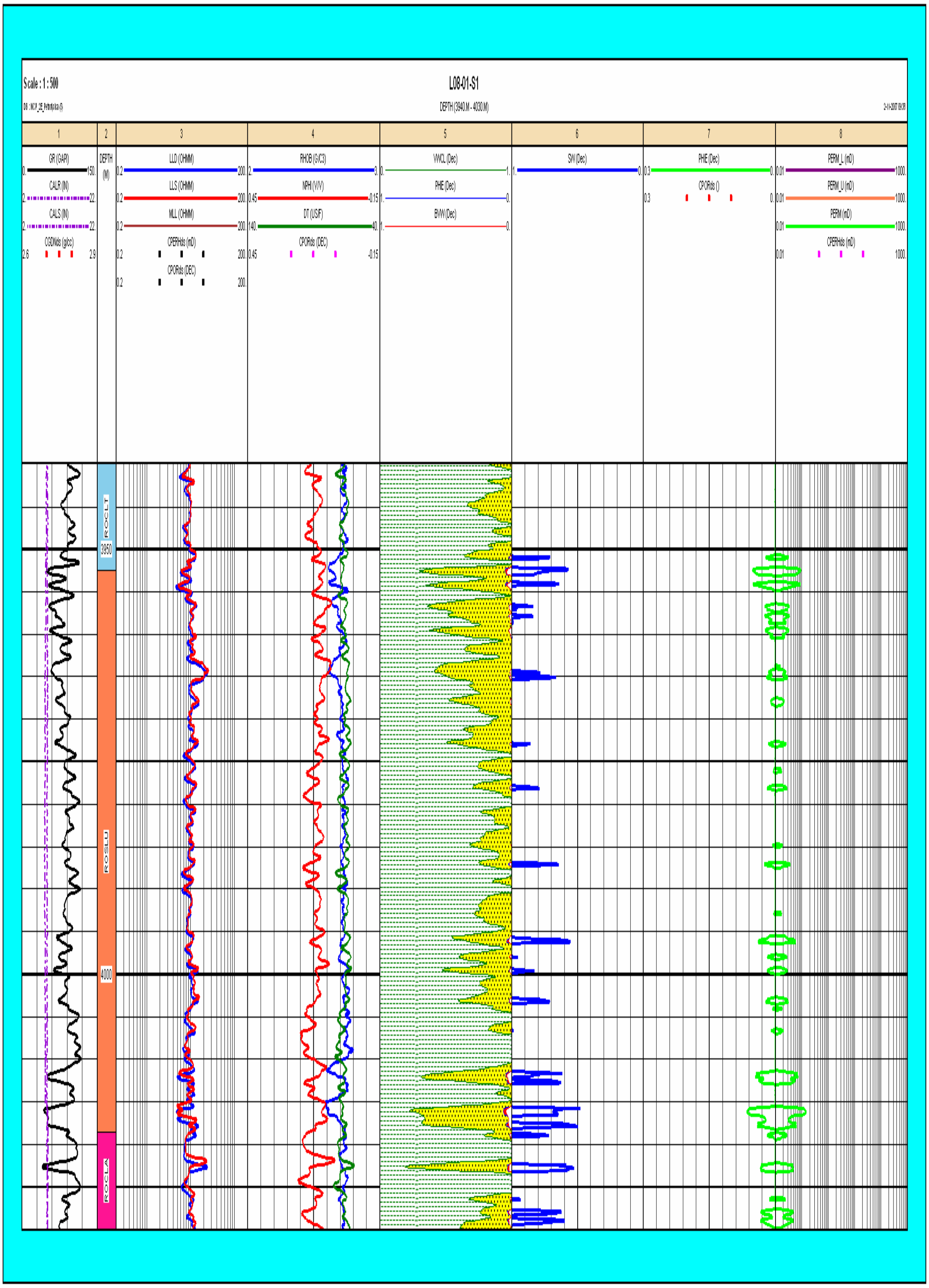

Playback 5a Petrophysical analysis Upper Slochteren Sandstone L08-01-S1

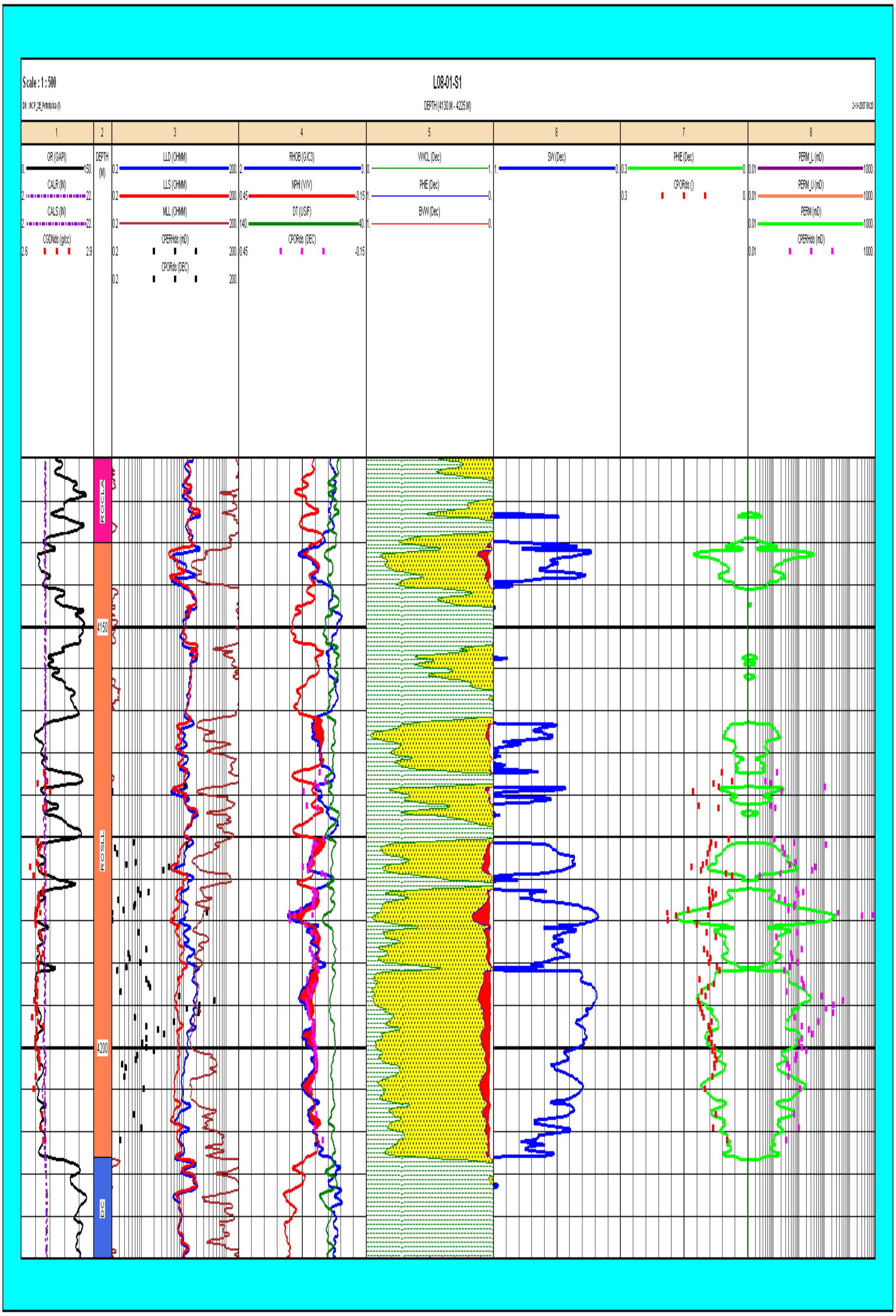

Playback 5b Petrophysical analysis Lower Slochteren Sandstone L08-01-S1

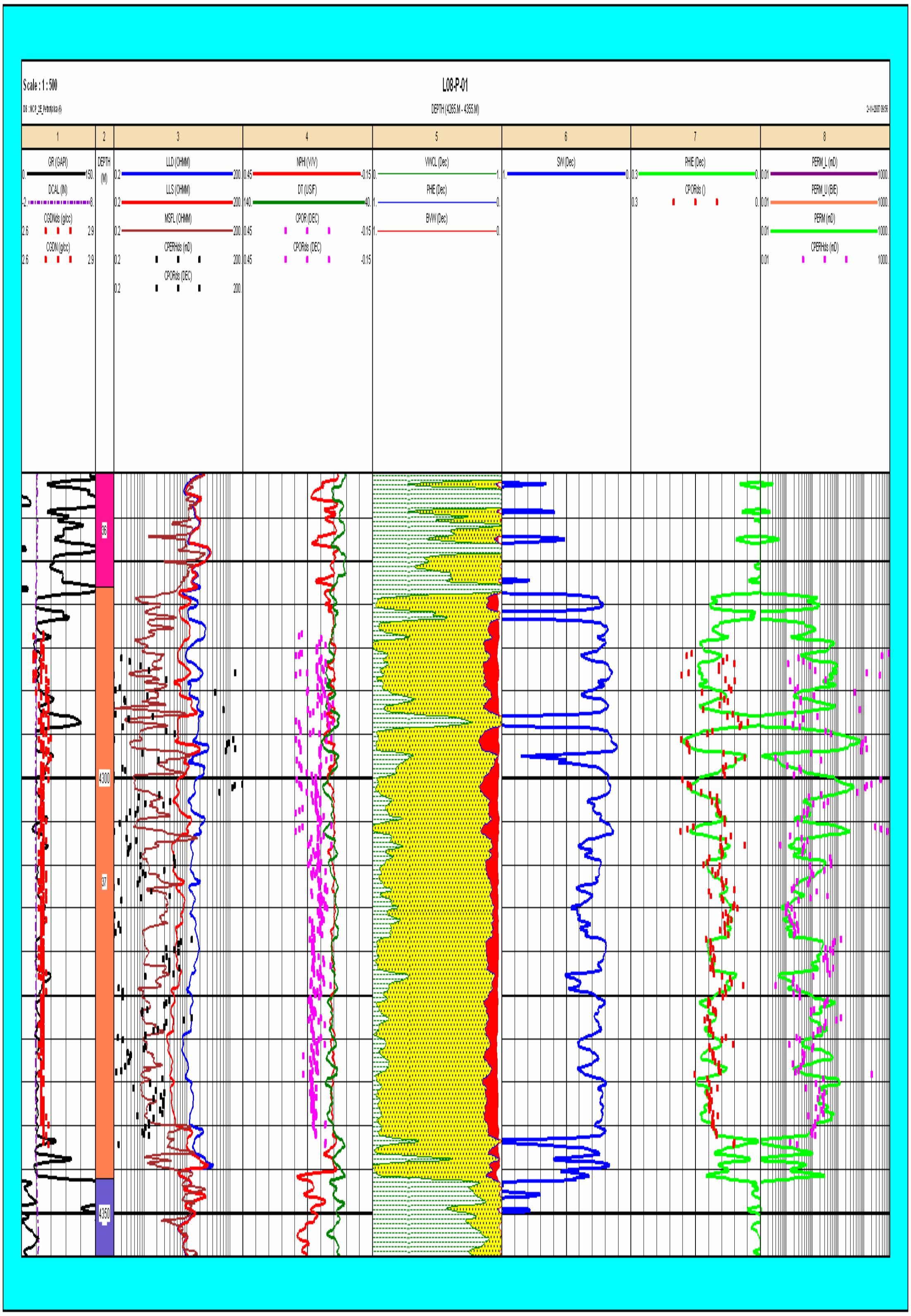

Playback 6 Petrophysical analysis Lower Slochteren Sandstone L08-P-01

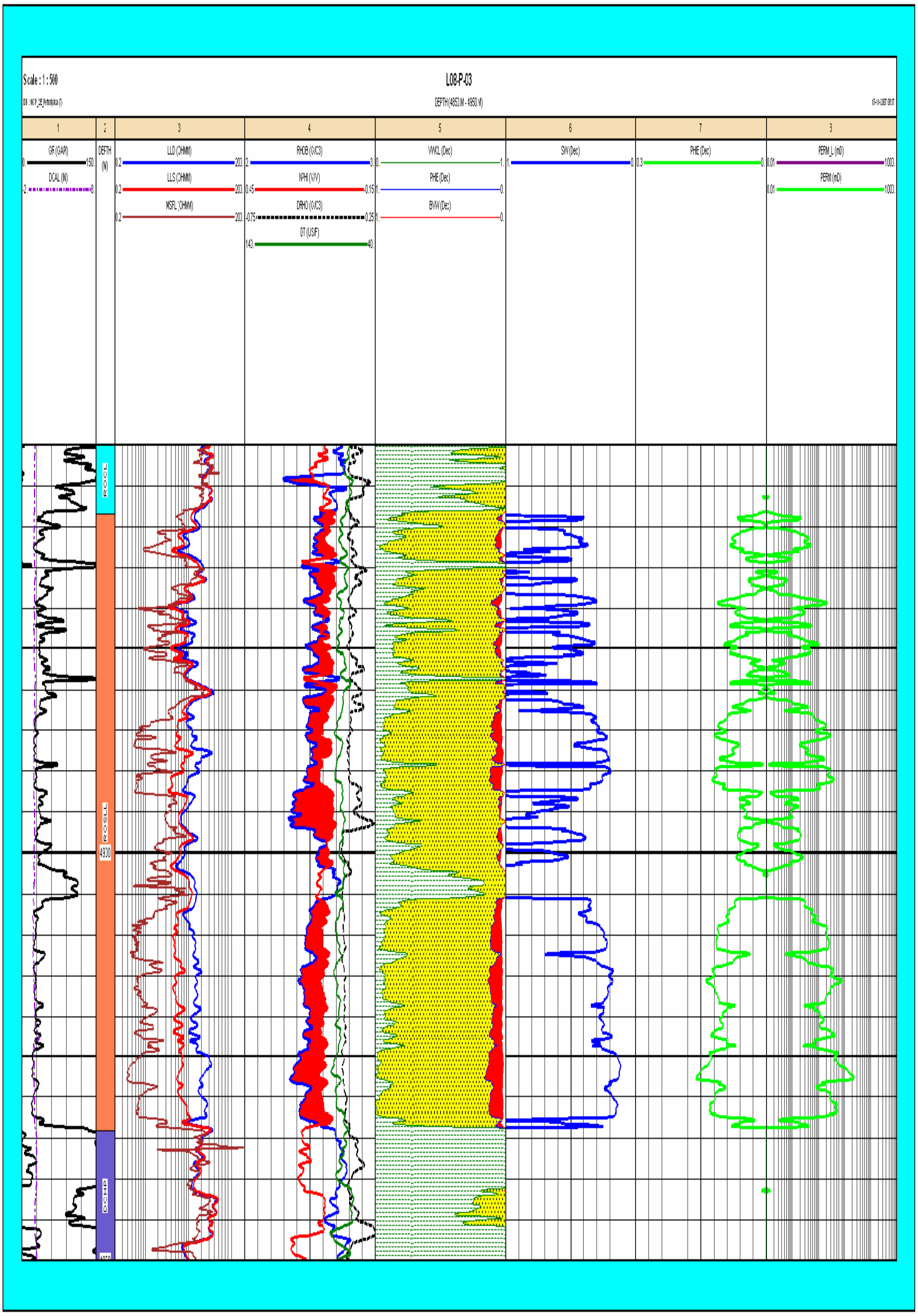

Playback 7 Petrophysical analysis Lower Slochteren Sandstone L08-P-03

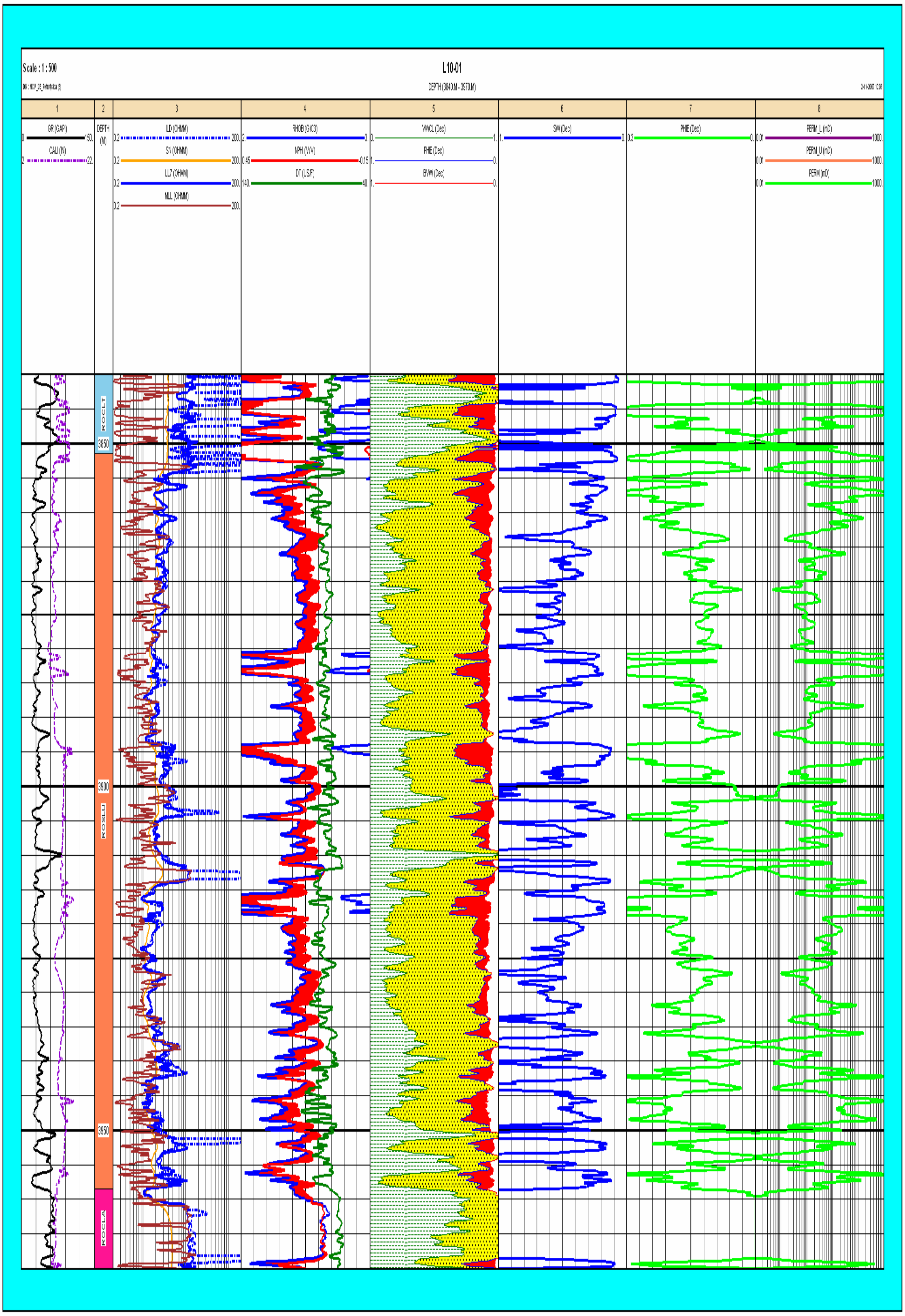

Playback 8a Petrophysical analysis Upper Slochteren Sandstone L10-01

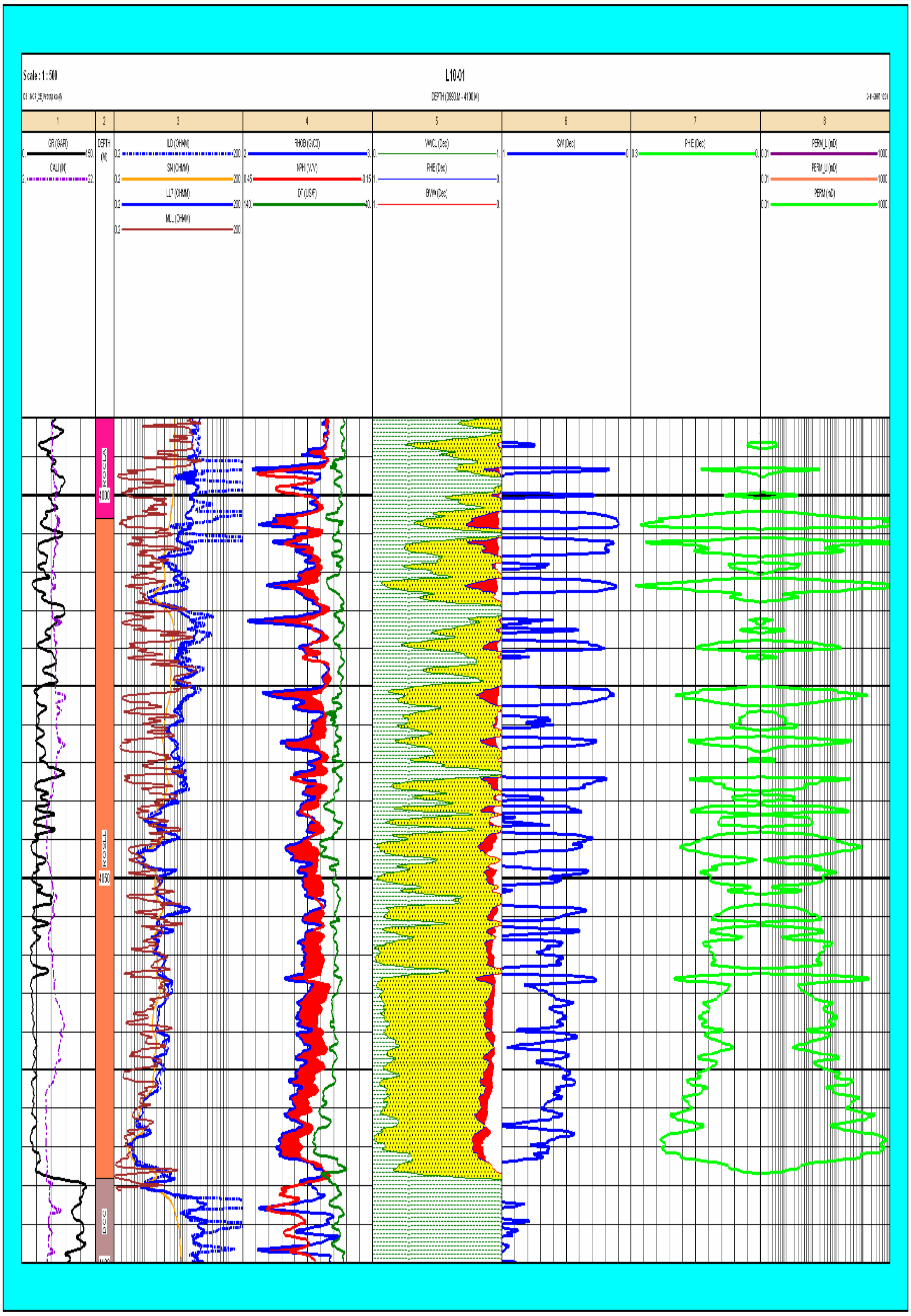

Playback 8b Petrophysical analysis Lower Slochteren Sandstone L10-01

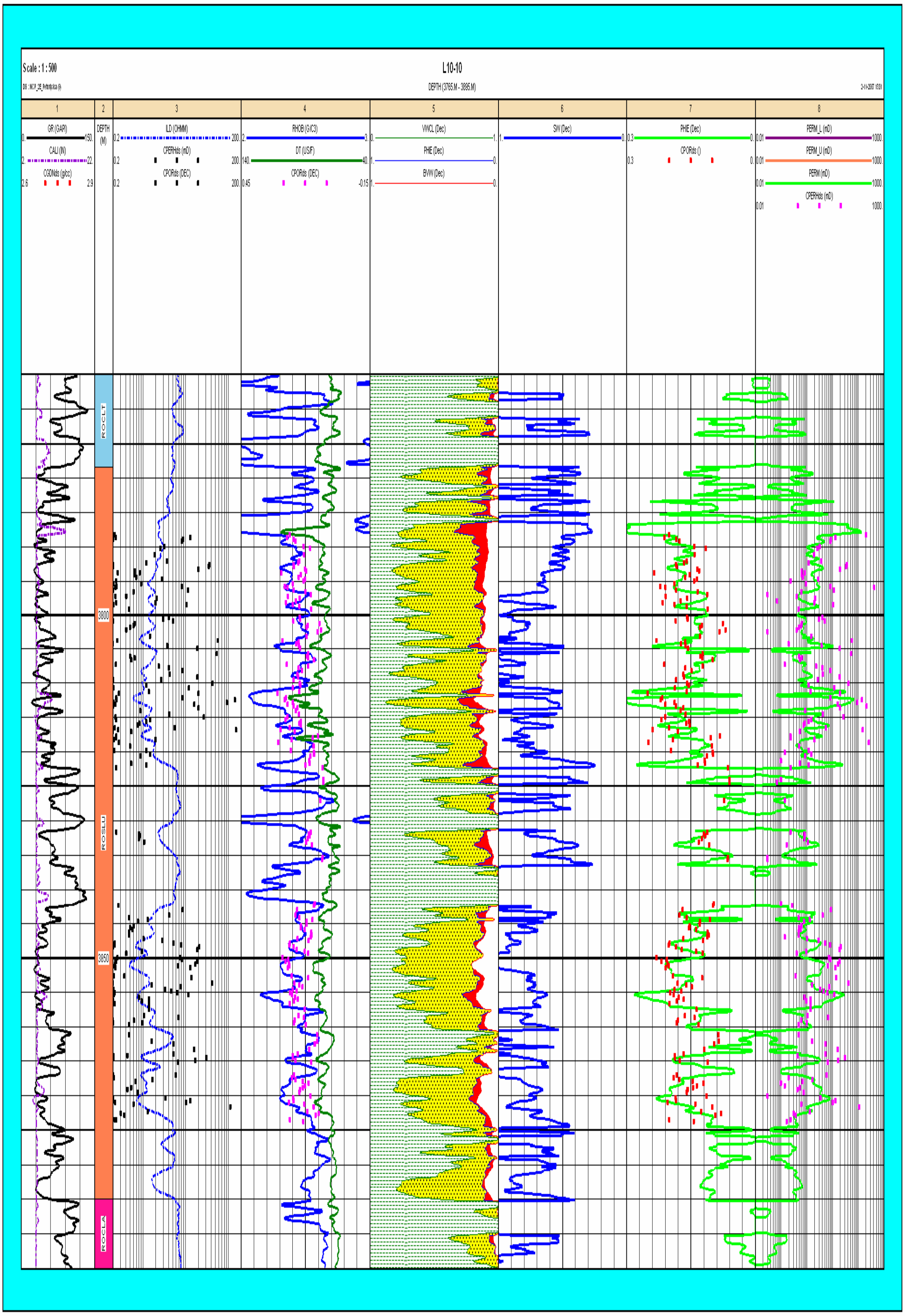

Playback 9a Petrophysical analysis Upper Slochteren Sandstone L10-10

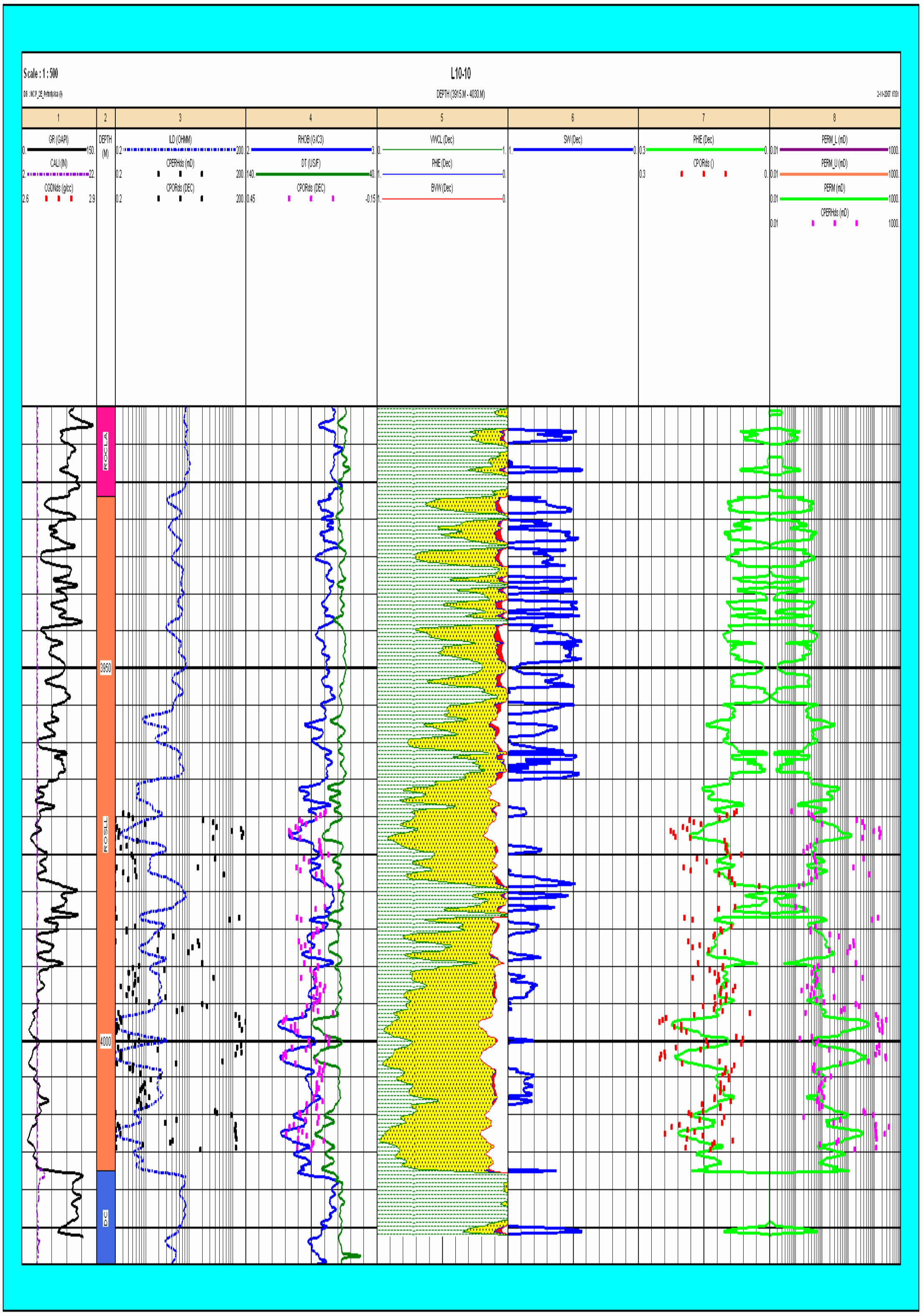

Playback 9b Petrophysical analysis Lower Slochteren Sandstone L10-10

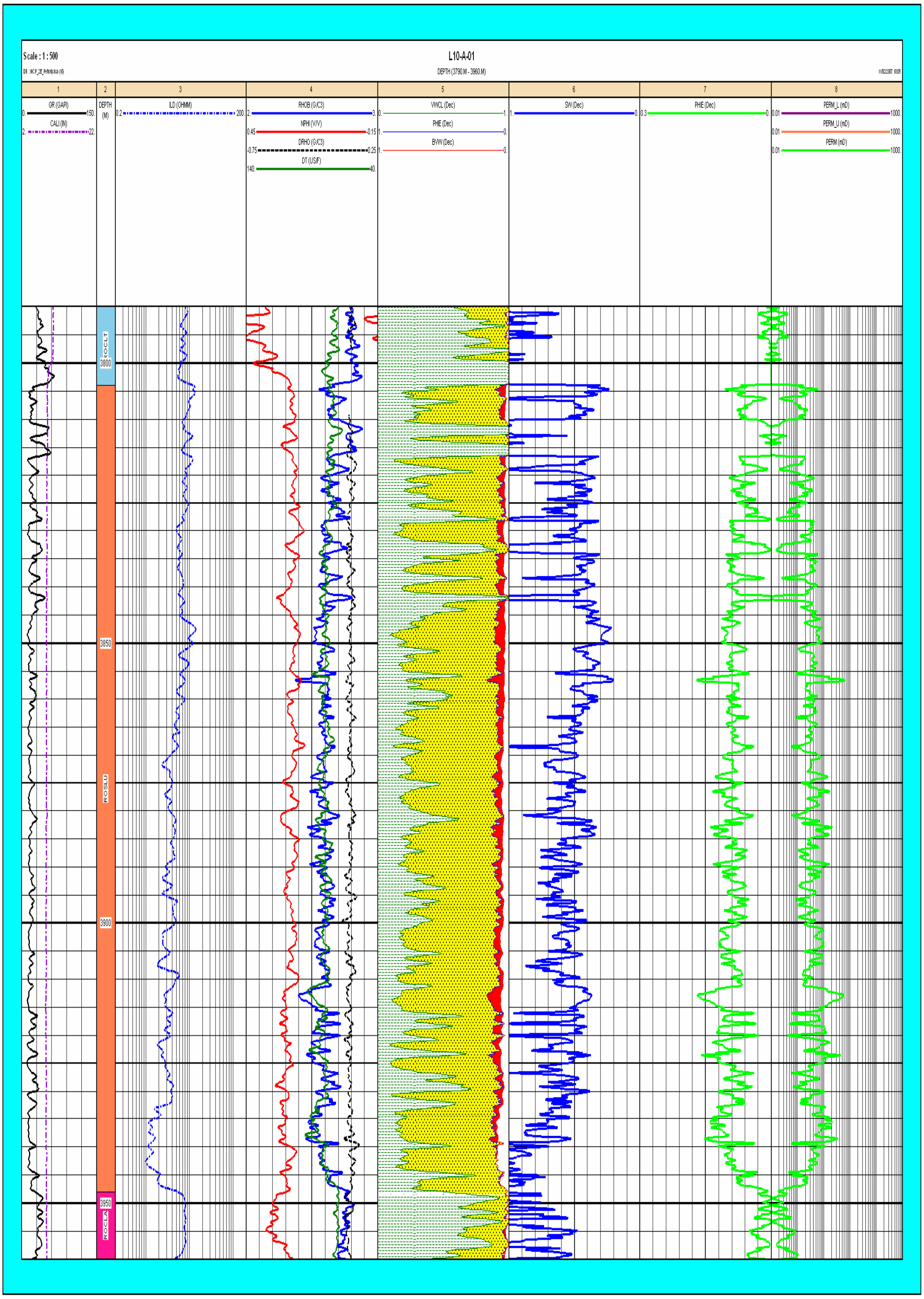

Playback 10a Petrophysical analysis Upper Slochteren Sandstone L10-A-01

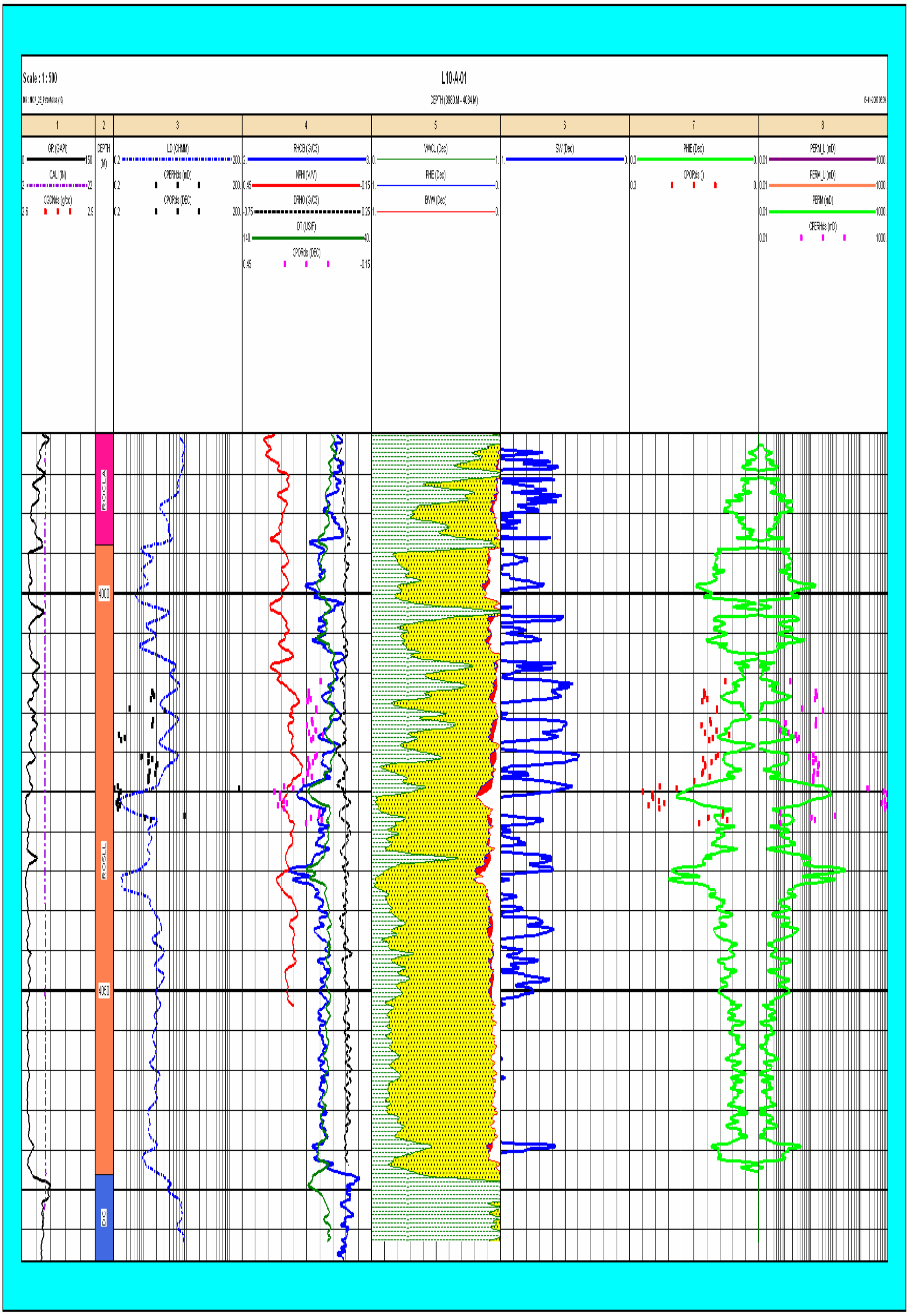

Playback 10b Petrophysical analysis Lower Slochteren Sandstone L10-A-01

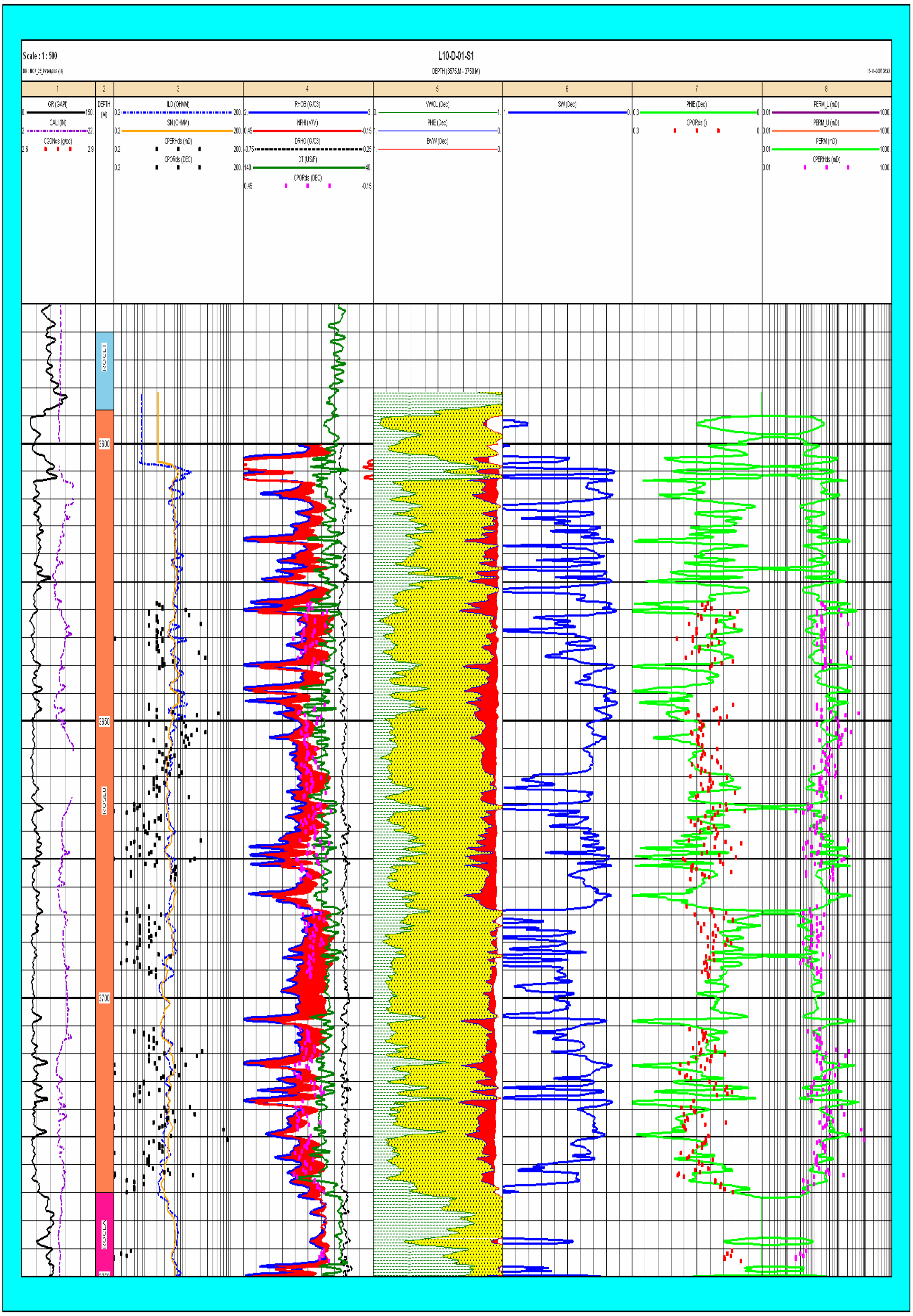

Playback 11a Petrophysical analysis Upper Slochteren Sandstone L10-D-01-S1

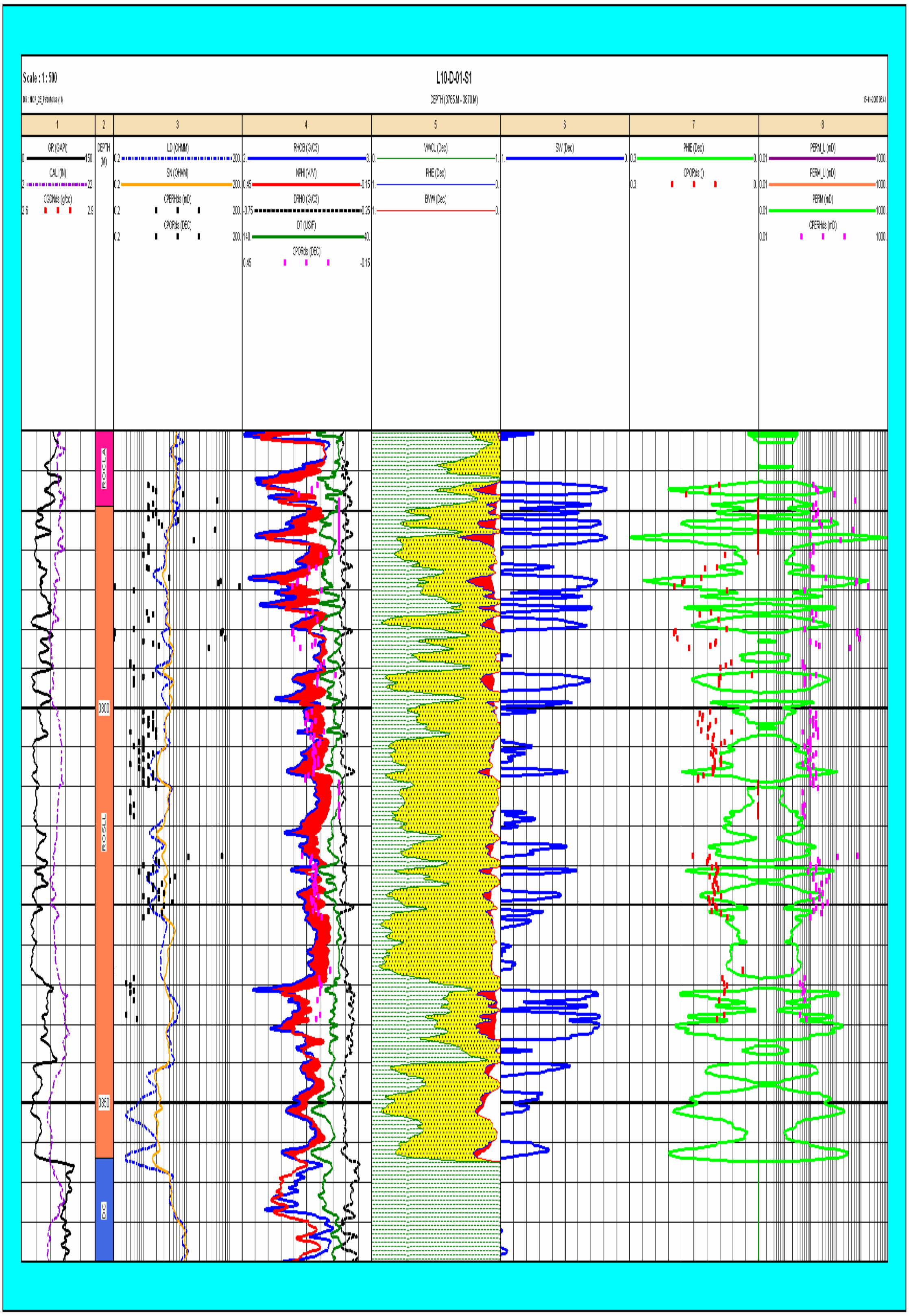

Playback 11b Petrophysical analysis Lower Slochteren Sandstone L10-D-01-S1

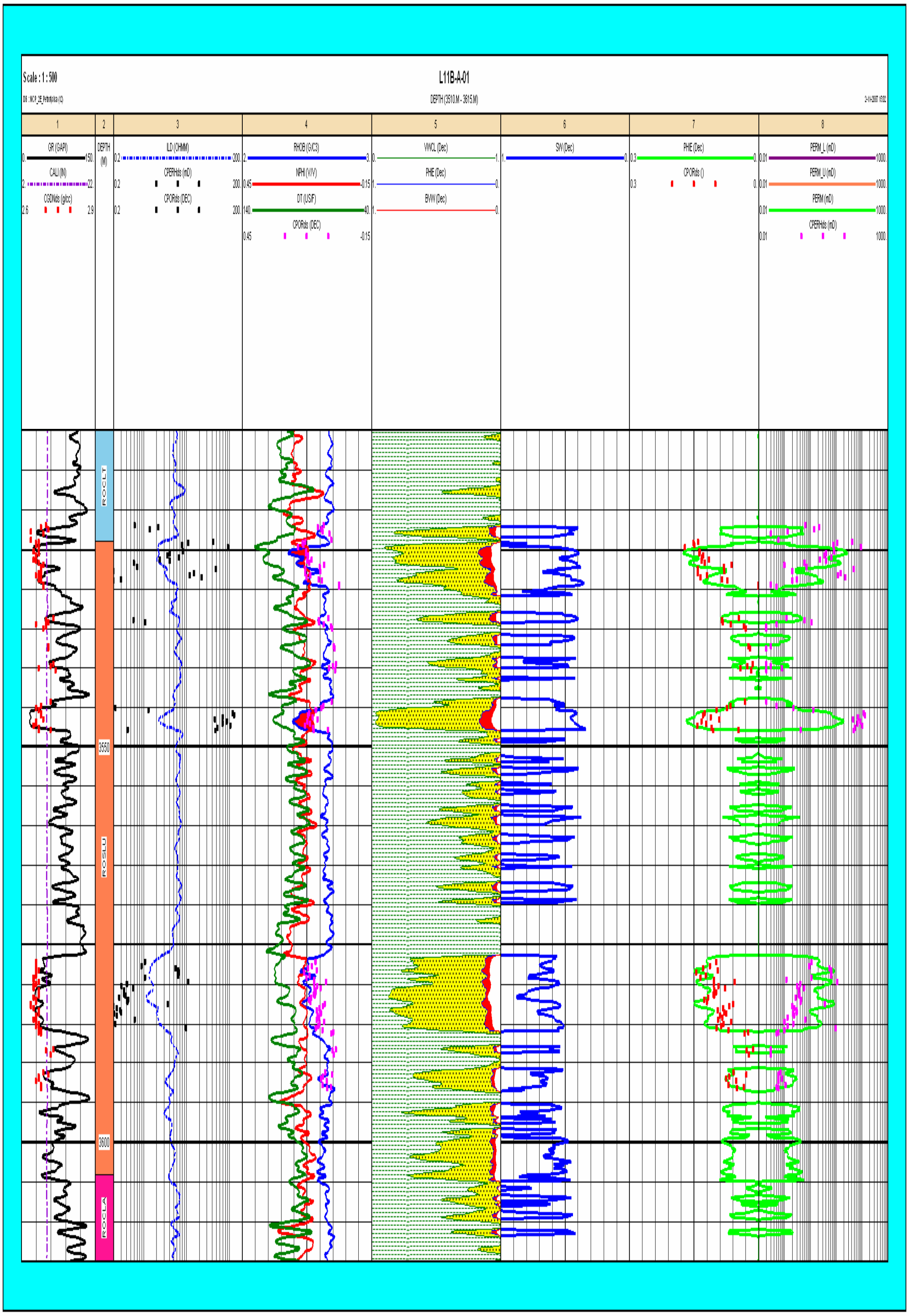

Playback 12a Petrophysical analysis Upper Slochteren Sandstone L11B-A-01

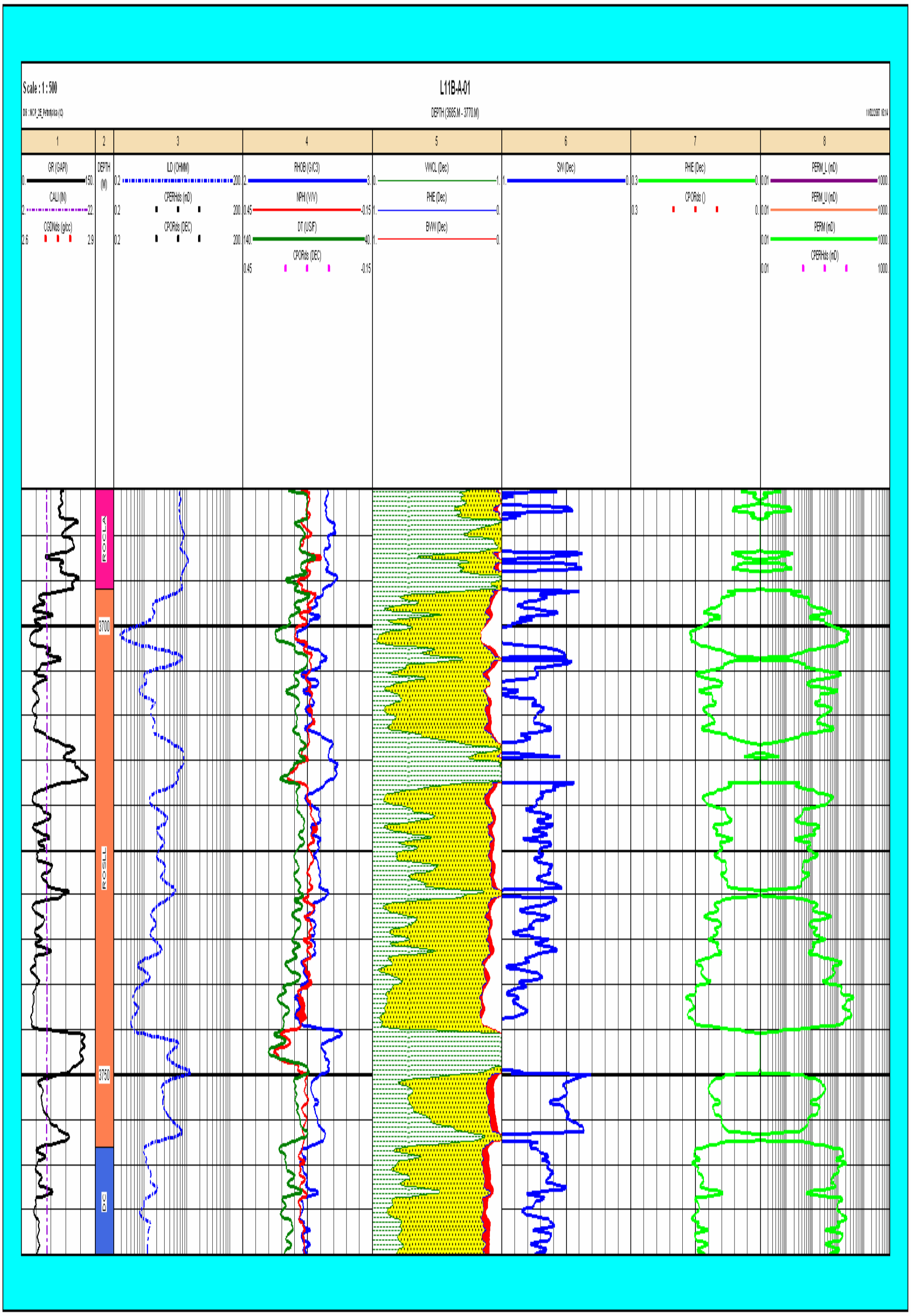

Playback 12b Petrophysical analysis Lower Slochteren Sandstone L11B-A-01

Annex G22

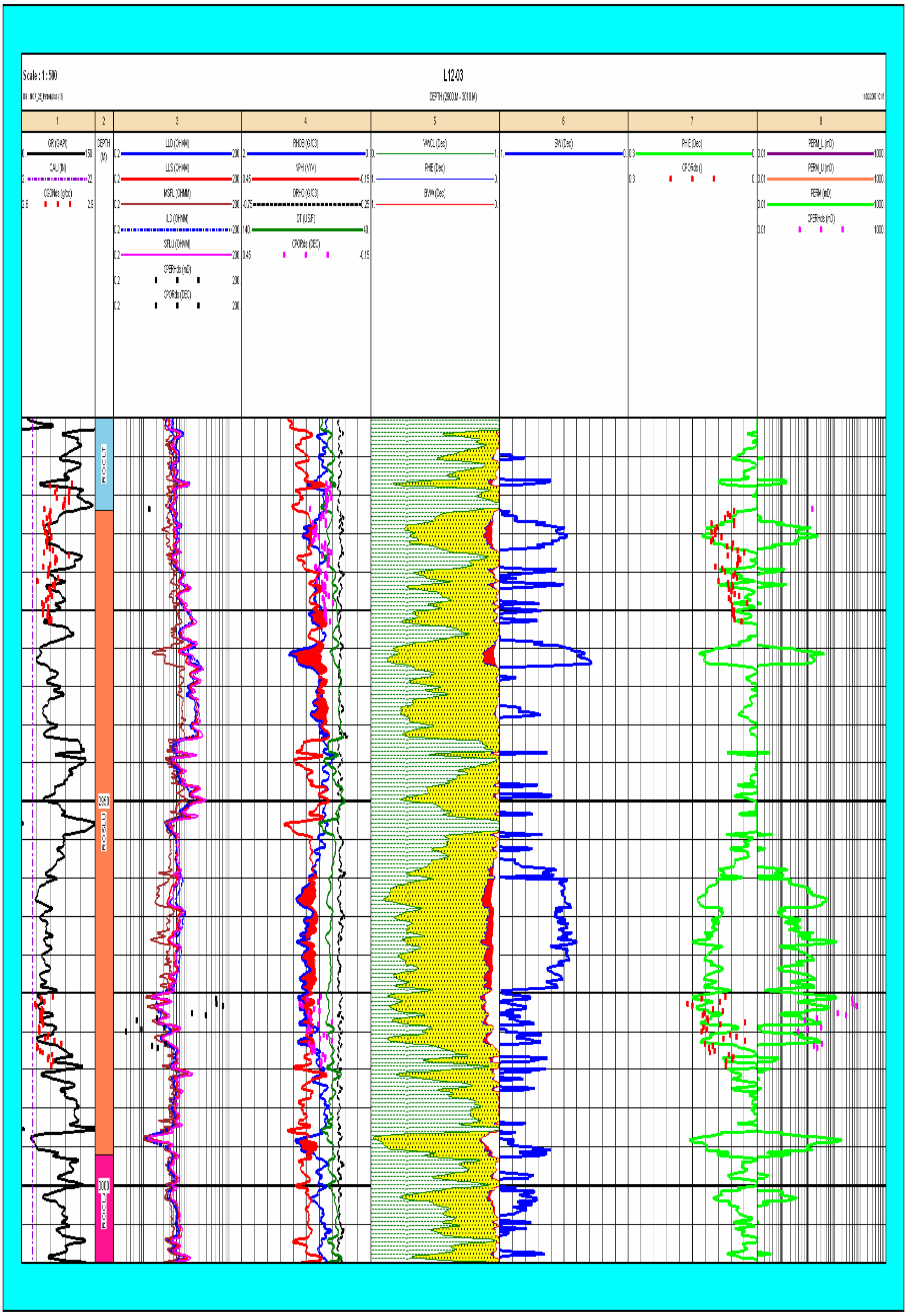

Playback 13a Petrophysical analysis Upper Slochteren Sandstone L12-03

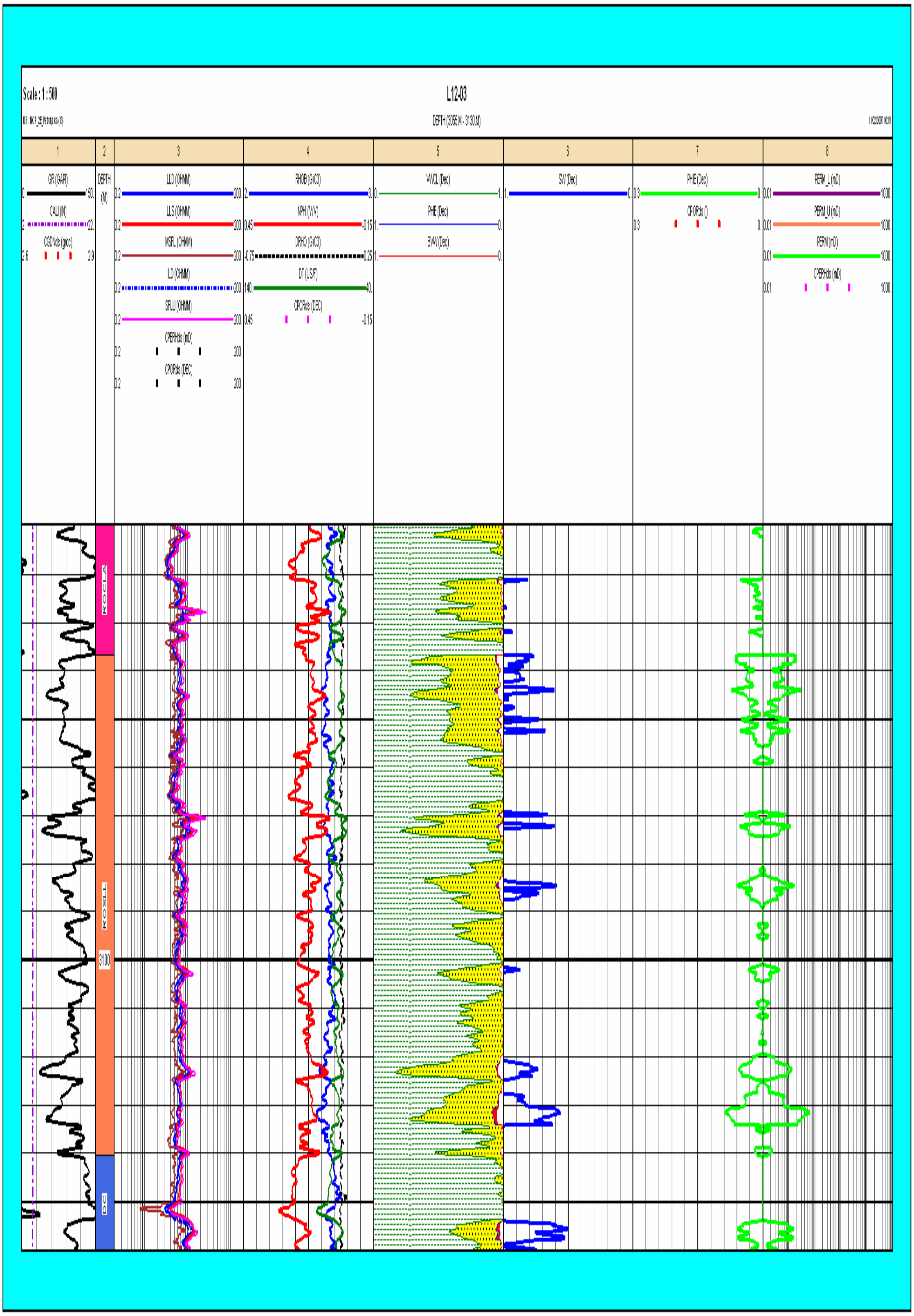

Playback 13b Petrophysical analysis Lower Slochteren Sandstone L12-03

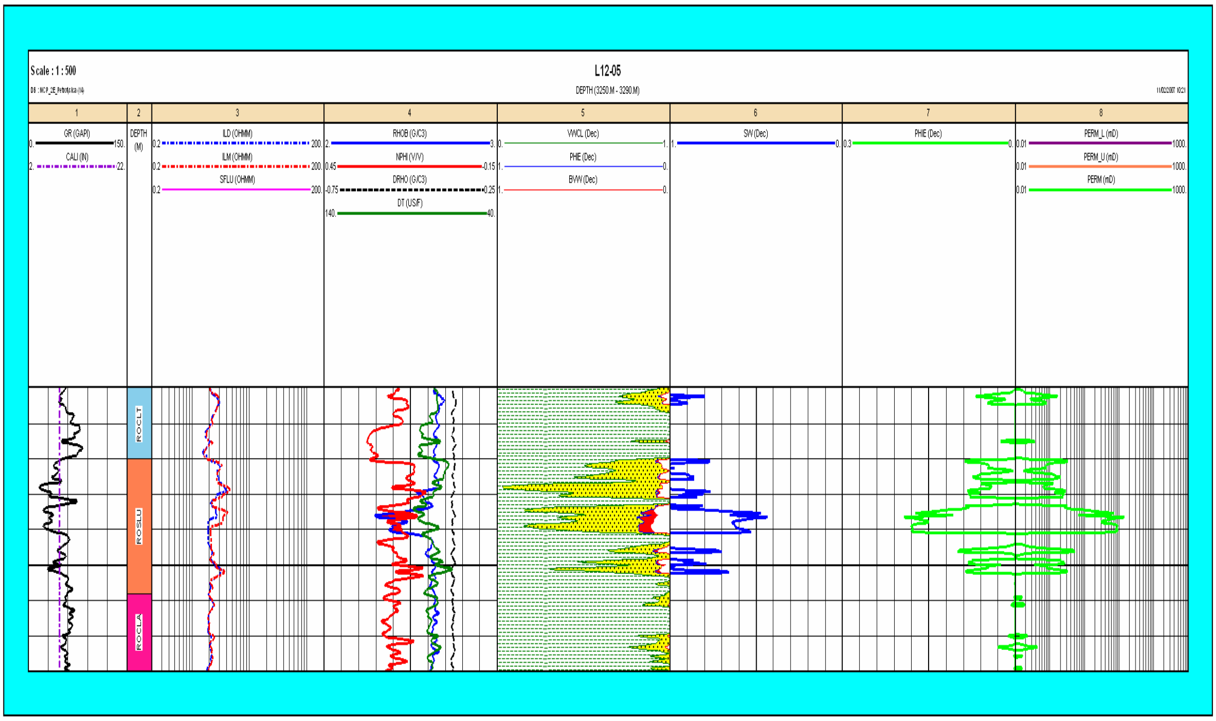

Playback 14a Petrophysical analysis Upper Slochteren Sandstone L12-05

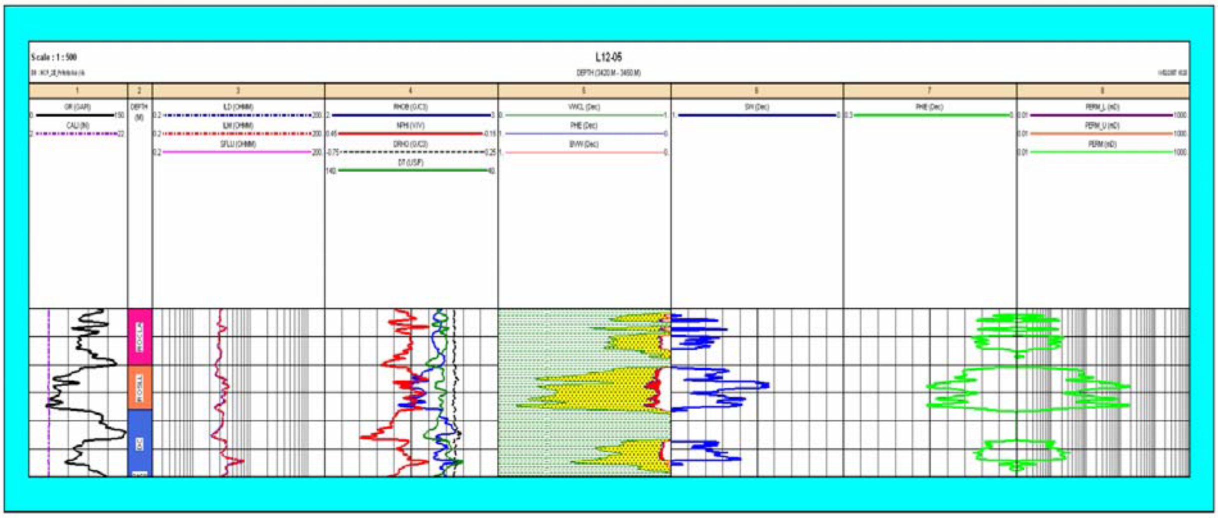

Playback 14b Petrophysical analysis Lower Slochteren Sandstone L12-05

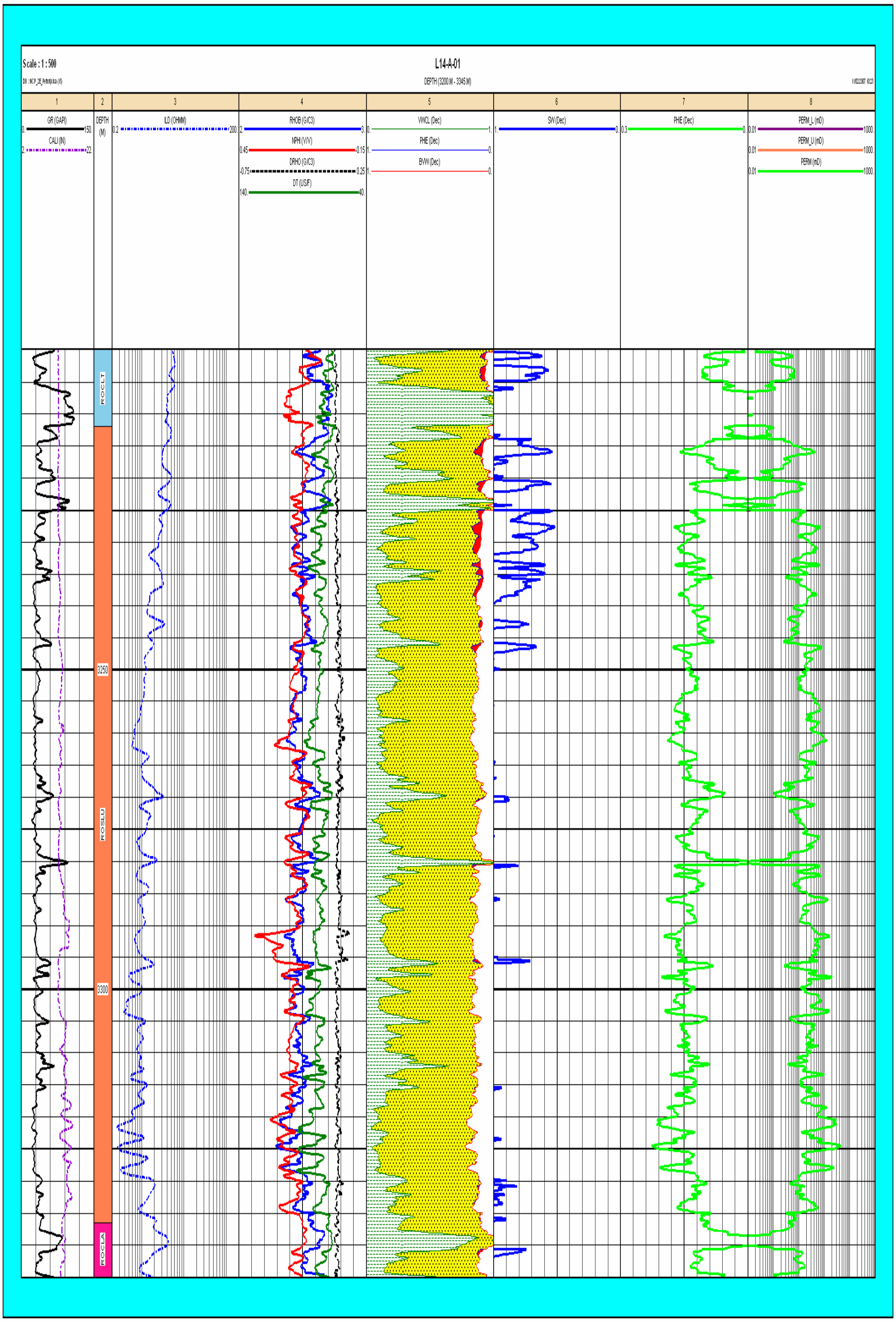

Playback 15a Petrophysical analysis Upper Slochteren Sandstone L14-A-01

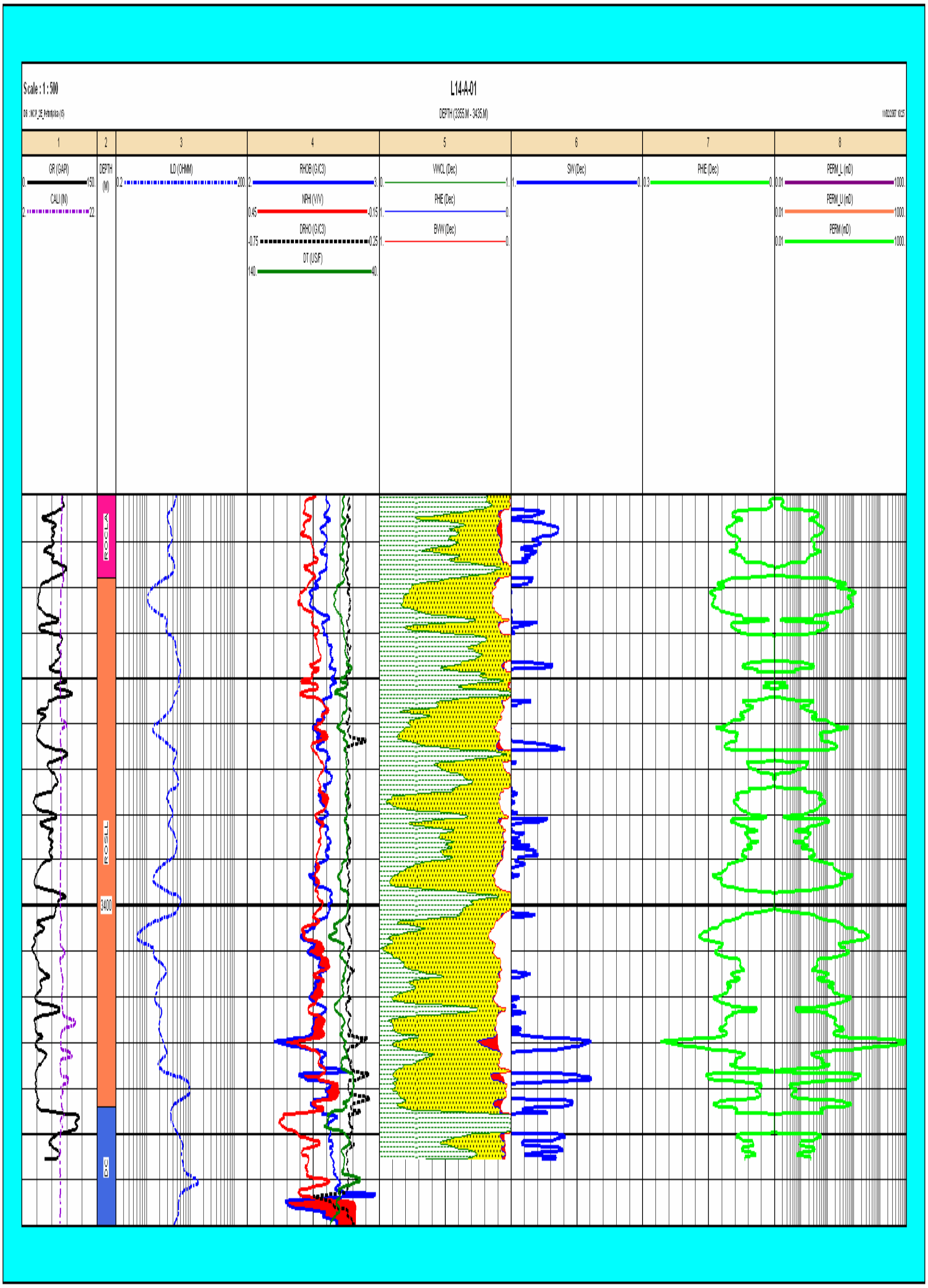

Playback 15b Petrophysical analysis Lower Slochteren Sandstone L14-A-01

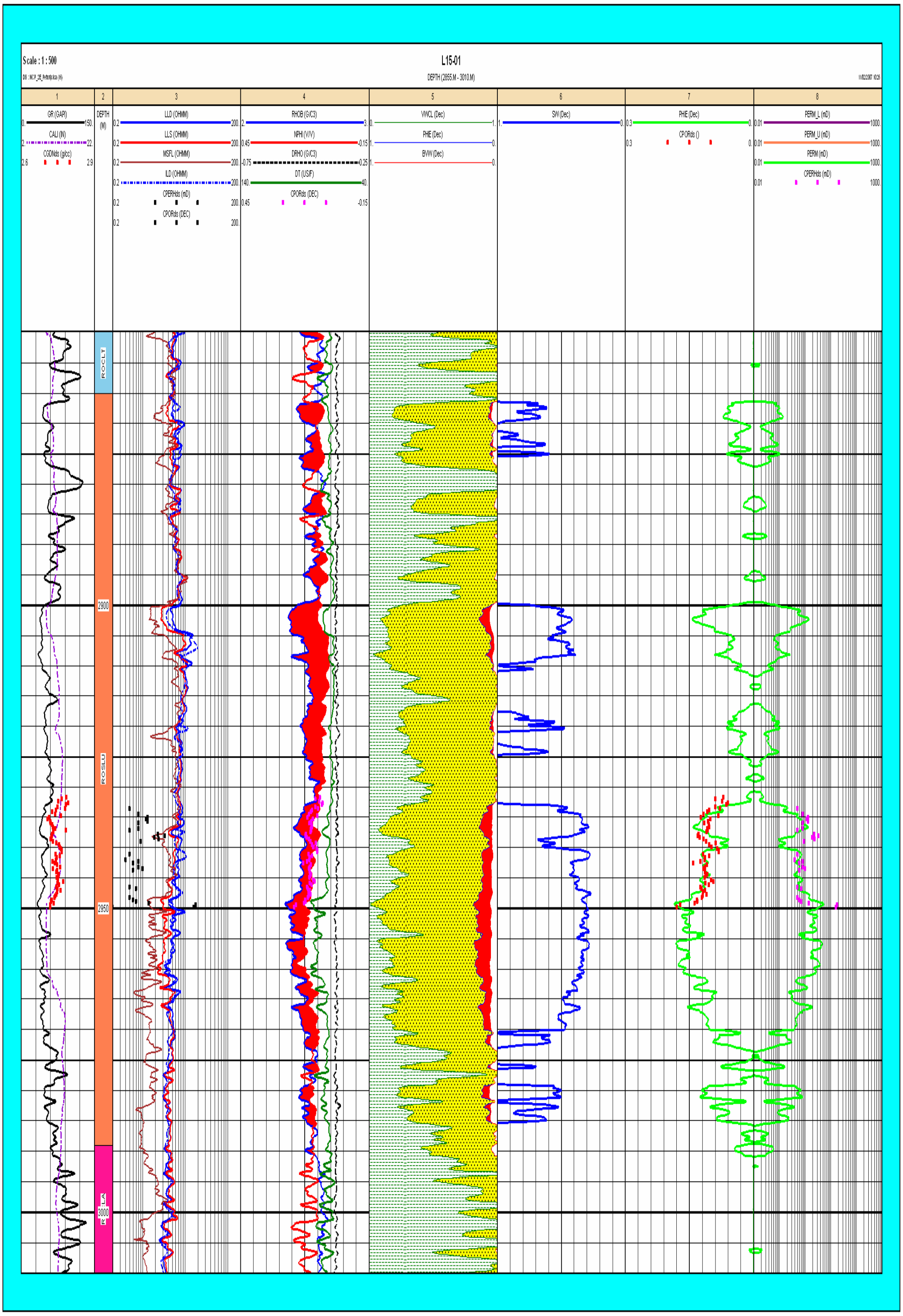

Playback 16a Petrophysical analysis Upper Slochteren Sandstone L15-01

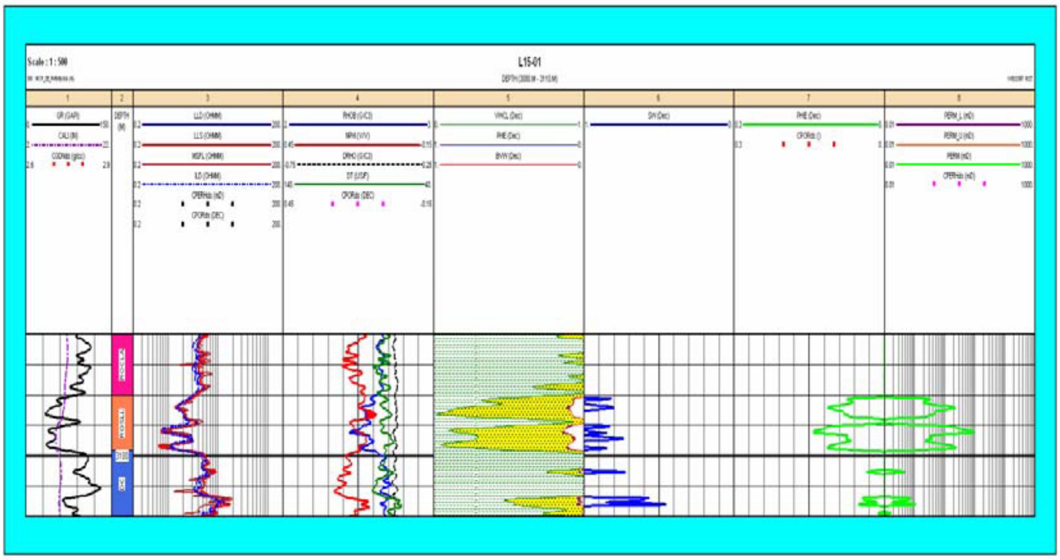

Playback 16b Petrophysical analysis Lower Slochteren Sandstone L15-01

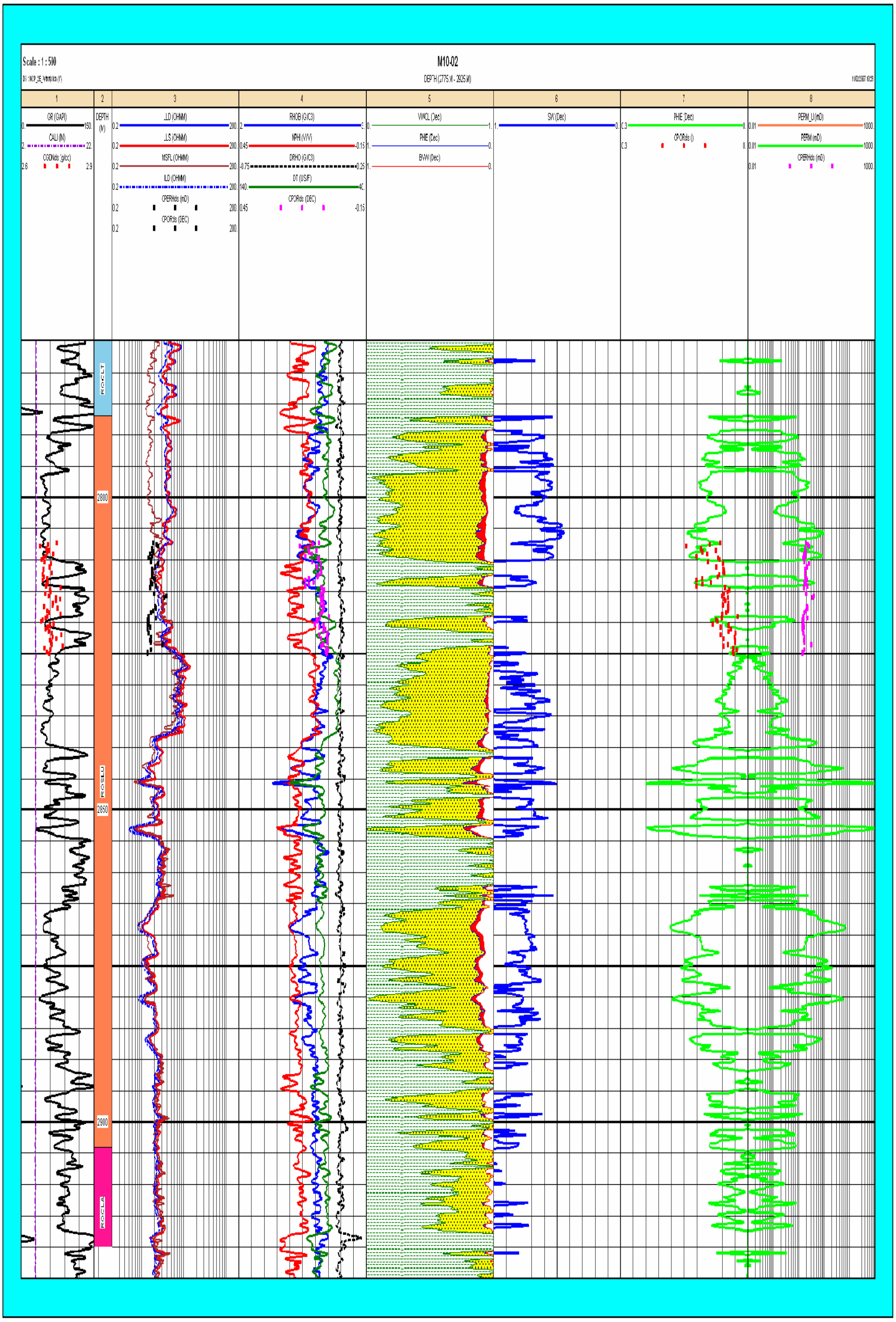

Playback 17a Petrophysical analysis Upper Slochteren Sandstone M10-02

Annex H1

Thickness of the Lower Detfurth Sandstone Member

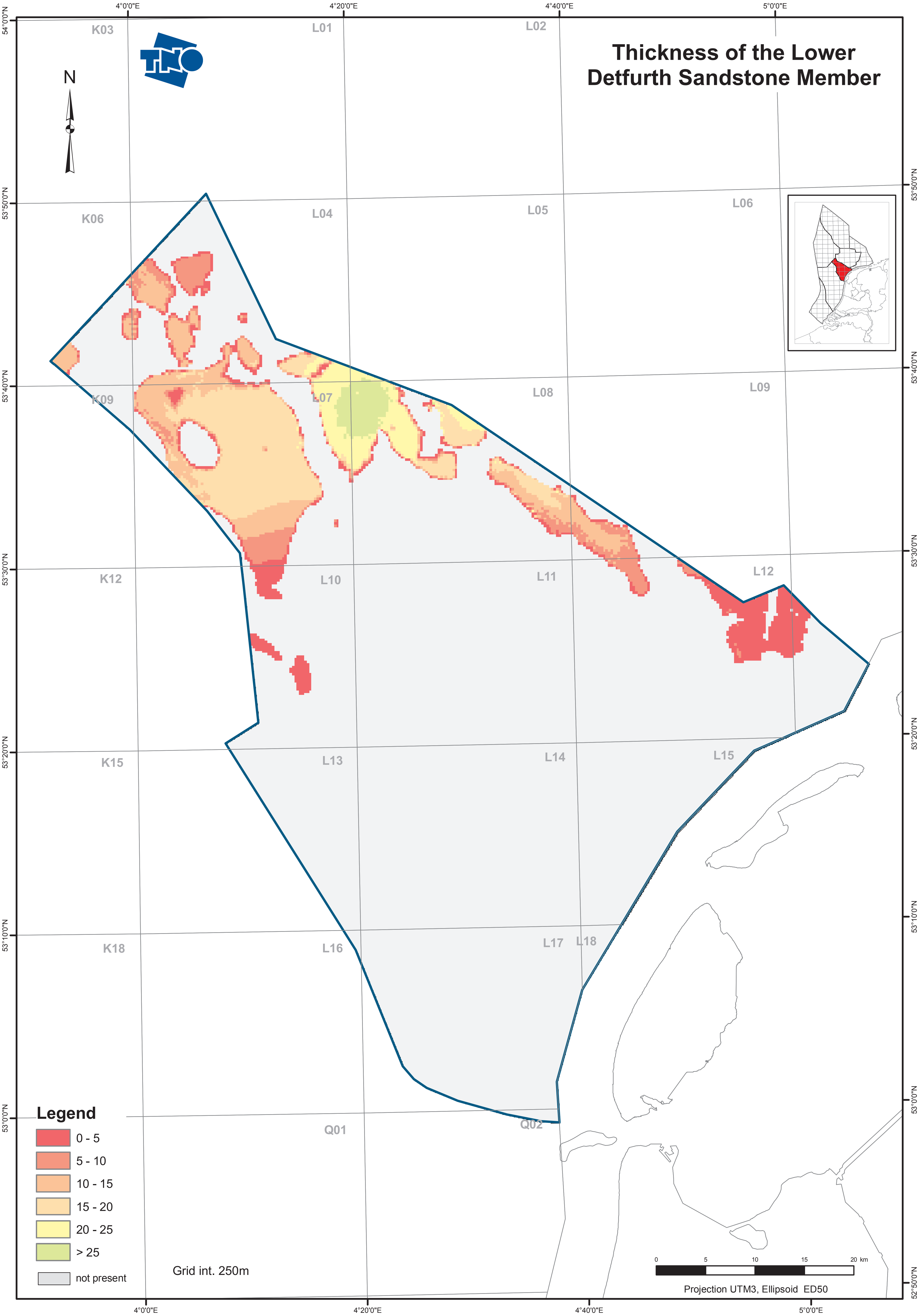

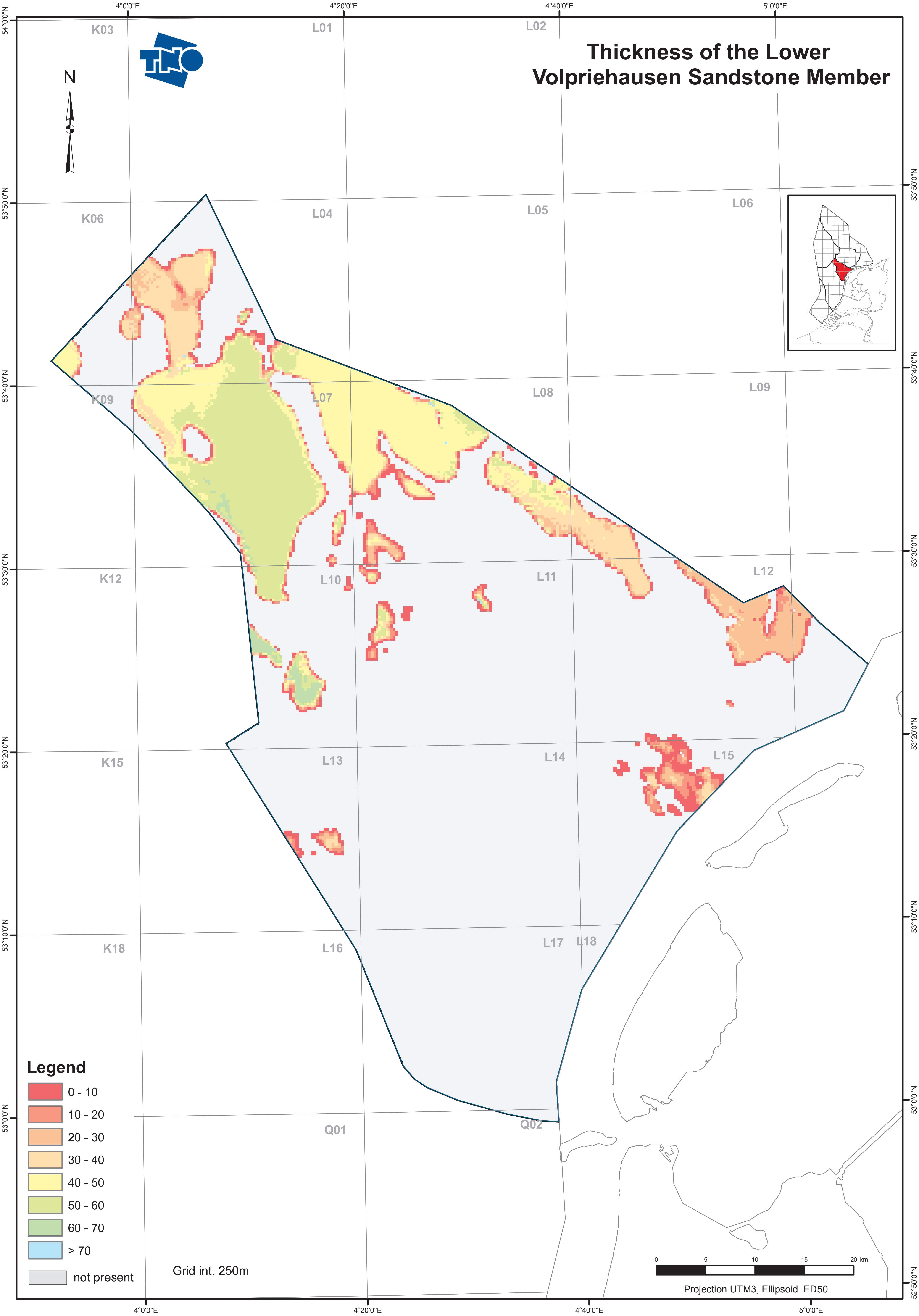
Thickness of the Lower
Volpriehausen Sandstone Member
N
K03
L01
L02
K06
L04
L05
L06
K09
L07
L08
L09
K12
L10
L11
L12
K15
L13
L14
L15
K18
L16
L17
L18
Q01
Q02
4°0'0"E
4°20'0"E
4°40'0"E
5°0'0"E
54°0'0"N
53°50'0"N
53°40'0"N
53°30'0"N
53°20'0"N
53°10'0"N
53°0'0"N
52°50'0"N
Legend
0 - 10
10 - 20
20 - 30
30 - 40
40 - 50
50 - 60
60 - 70
> 70
not present
Grid int. 250m
0
5
10
15
20 km
Projection UTM3, Ellipsoid ED50

Thickness of the Slochteren Formation

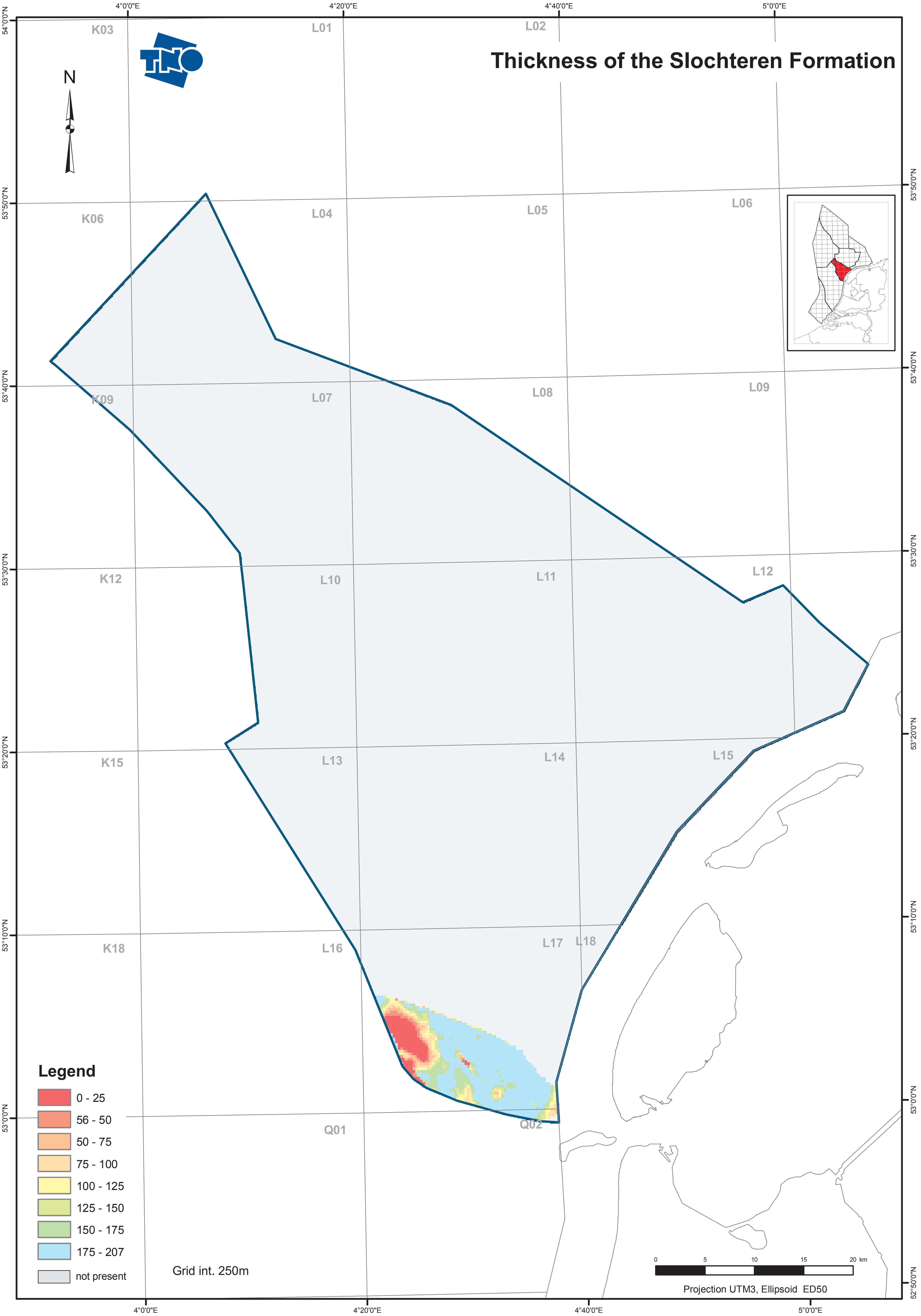

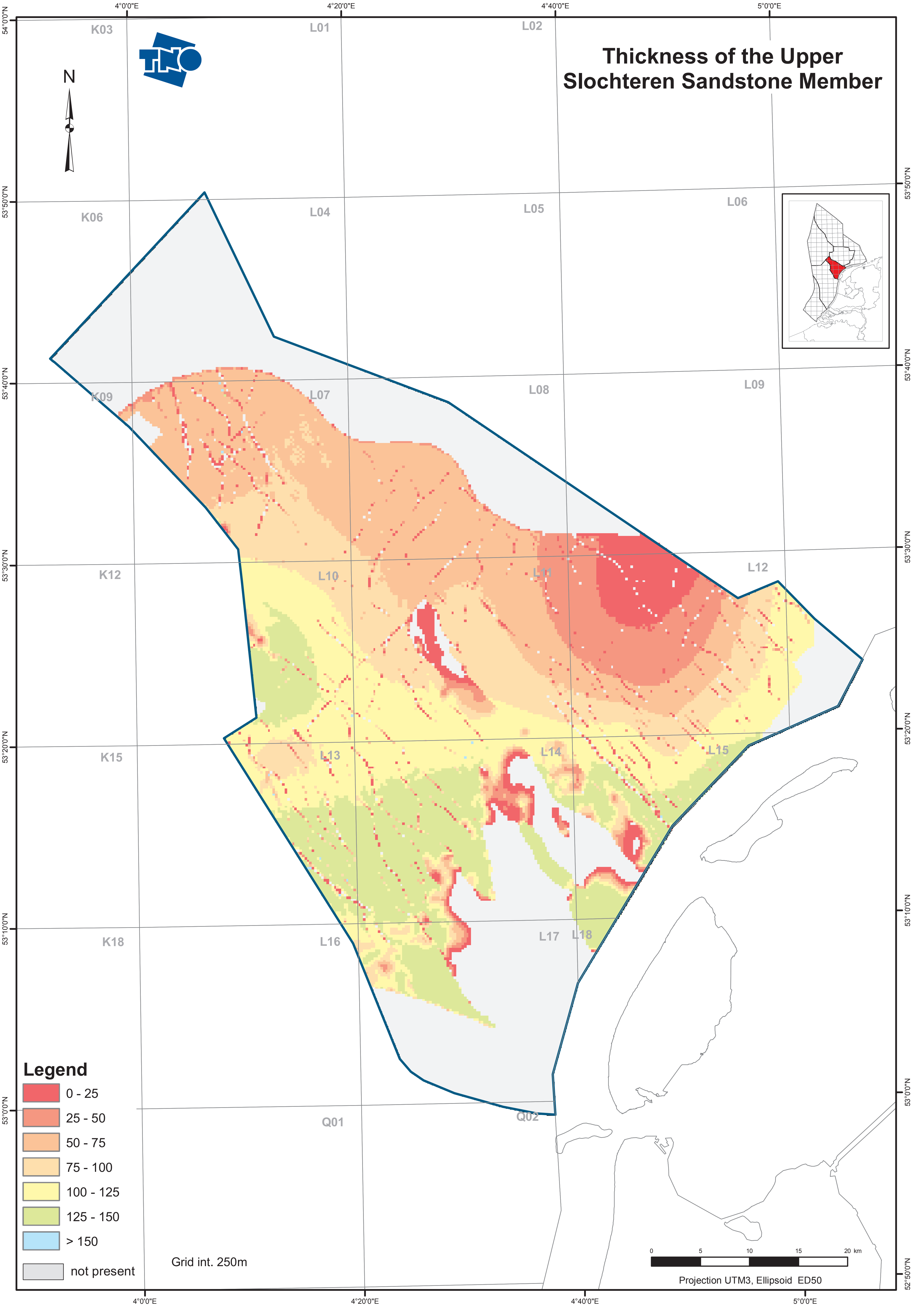
Thickness of the Upper
Slochteren Sandstone Member
N
K03
L01
L02
K06
L04
L05
L06
K09
L07
L08
L09
K12
L10
L11
L12
K15
L13
L14
L15
K18
L16
L17
L18
Q01
Q02
4°0'0"E
4°20'0"E
4°40'0"E
5°0'0"E
54°0'0"N
53°50'0"N
53°40'0"N
53°30'0"N
53°20'0"N
53°10'0"N
53°0'0"N
52°50'0"N
Legend
0 - 25
25 - 50
50 - 75
75 - 100
100 - 125
125 - 150
> 150
not present
Grid int. 250m
0
5
10
15
20 km
Projection UTM3, Ellipsoid ED50

Annex H5

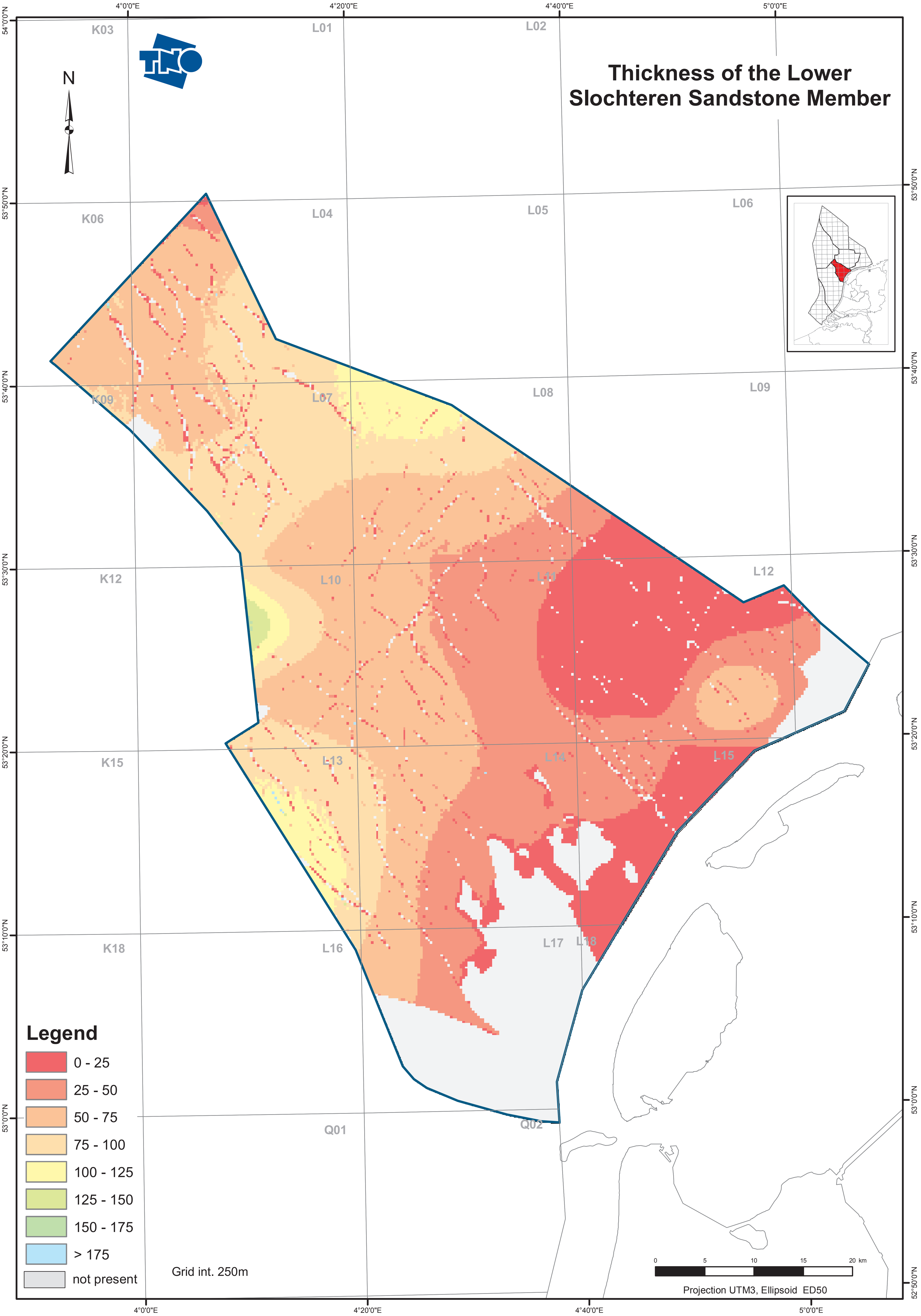

Thickness of the Lower Slochteren Sandstone Member
N
K03
L01
L02
K06
L04
L05
L06
K09
L07
L08
L09
K12
L10
L11
L12
K15
L13
L14
L15
K18
L16
L17
L18
Q01
Q02
4°0'0"E
4°20'0"E
4°40'0"E
5°0'0"E
54°0'0"N
53°50'0"N
53°40'0"N
53°30'0"N
53°20'0"N
53°10'0"N
53°0'0"N
52°50'0"N
Legend
0 - 25
25 - 50
50 - 75
75 - 100
100 - 125
125 - 150
150 - 175
> 175
not present
Grid int. 250m
0
5
10
15
20 km
Projection UTM3, Ellipsoid ED50

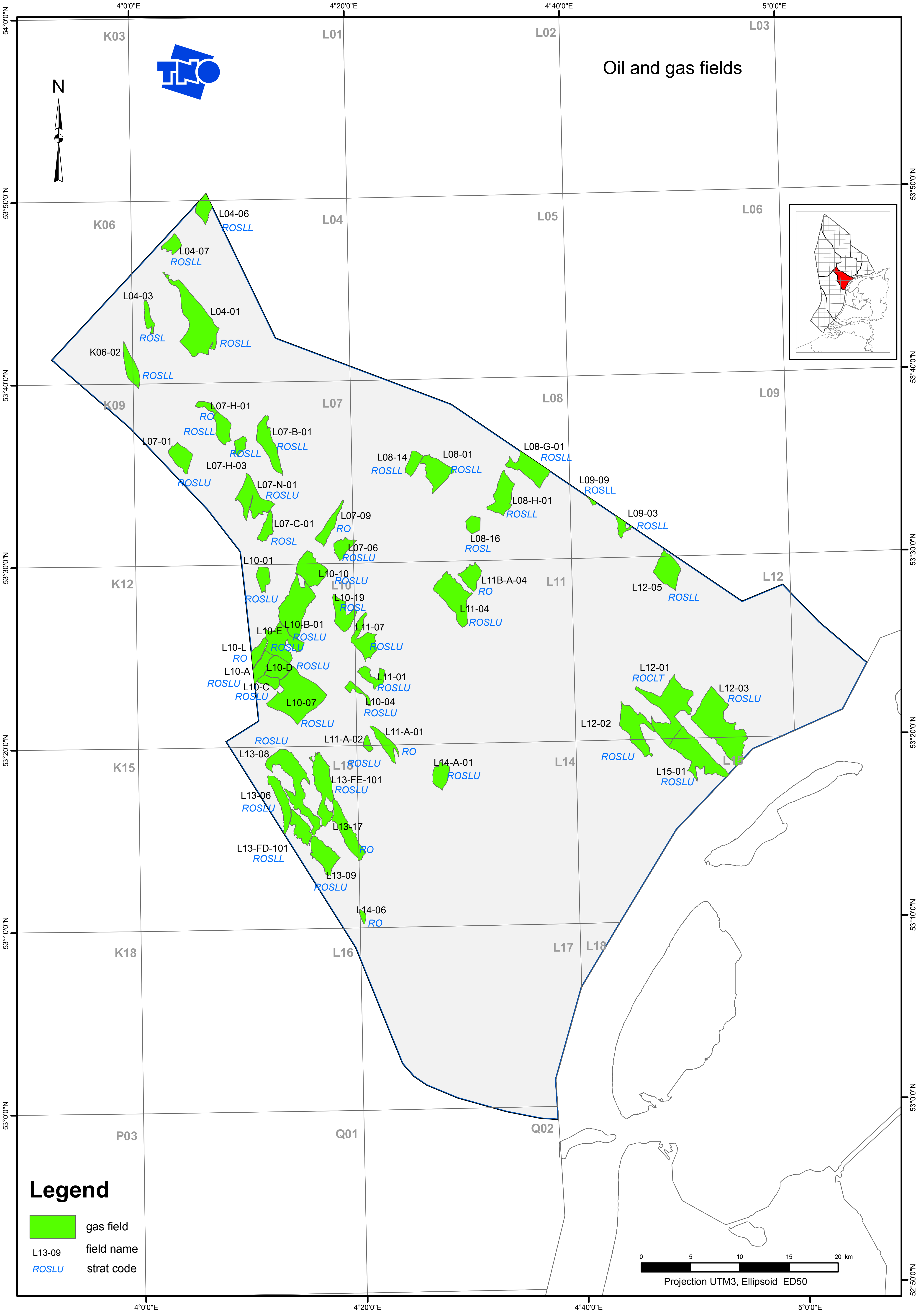

Oil and gas fields
N
4°0'0"E
4°20'0"E
4°40'0"E
5°0'0"E
54°0'0"N
53°50'0"N
53°40'0"N
53°30'0"N
53°20'0"N
53°10'0"N
53°0'0"N
52°50'0"N
K03
L01
L02
L03
K06
L04
L05
L06
K09
L07
L08
L09
K12
L10
L11
L12
K15
L13
L14
L15
K18
L16
L17
L18
P03
Q01
Q02
L04-06
ROSLL
L04-07
ROSLL
L04-03
ROSL
L04-01
ROSLL
K06-02
ROSLL
L07-H-01
RO
ROSLL
L07-B-01
ROSLL
L07-01
ROSLL
L07-H-03
ROSLU
L07-N-01
ROSLU
L07-C-01
ROSL
L07-09
RO
L07-06
ROSLU
L08-14
ROSLL
L08-01
ROSLL
L08-G-01
ROSLL
L08-H-01
ROSLL
L08-16
ROSL
L09-09
ROSLL
L09-03
ROSLL
L10-01
ROSLU
L10-10
ROSLU
L10-19
ROSL
L10-B-01
ROSLU
L10-E
ROSLU
L10-L
RO
L10-A
ROSLU
L10-D
ROSLU
L10-C
ROSLU
L10-07
ROSLU
L11-07
ROSLU
L11-01
ROSLU
L10-04
ROSLU
L11B-A-04
RO
L11-04
ROSLU
L12-05
ROSLL
L12-01
ROCLT
L12-03
ROSLU
L12-02
ROSLU
L15-01
ROSLU
L11-A-02
ROSLU
L11-A-01
RO
L13-08
ROSLU
L13-FE-101
ROSLU
L13-06
ROSLU
L13-17
RO
L13-FD-101
ROSLL
L13-09
ROSLU
L14-A-01
ROSLU
L14-06
RO
Legend
gas field
L13-09
field name
ROSLU
strat code
0
5
10
15
20 km
Projection UTM3, Ellipsoid ED50